A ^{17}O NUCLEAR MAGNETIC RESONANCE STUDY OF HIGH TEMPERATURE SUPERCONDUCTORS.

Andrew Paul Howes

A thesis submitted to the University of Warwick for admission to the degree of Doctor of Philosophy.

Department of Physics

March 1992

This thesis is dedicated to my family.

List of Contents.

List of Tables.

List of Figures.

Acknowledgments.

I would like to thank the SERC and National Power PLc. for their financial assistance during this study. 'A man can not serve two masters' is an old saying, I had three supervisors, Prof. Ray Dupree, Dr. Donald McKenzie Paul both of the Physics Dept. and Dr. Stewart Male of National Power. Fortunately Ray did most of the talking with Don adding further suggestions on HiT_c. I would like to thank Stewart for giving me the Bismuth sample and Dr. R. S. Lui of the IRC at Cambridge for supplying the Thallium sample.

Dr. A. T. Boothroyd and I would occasionally discuss superconductivity. I would also like to thank Andrew for letting me live in his house for the last two years.

A number of people have kept my social life in tact over the last three years. The NMR coffee club was always an enjoyable excuse for a break and I would like to thank all its members past and present including GAS, MES, ZPH, PD, AG, LC, TK, DK, JR, DG, MPS and GB. The 'Solid State Boys' were always a great source of amusement, especially RE and SD. Other people in the lab I would like to acknowledge include OP, SC, NF, SY and EW.

I would especially like to thank 'Twinny' and Dr. Simon Kohn, they have both offered me plenty of advice on matters not concerned with NMR or superconductivity.

I escaped from Coventry for plenty of weekends away, either to visit family or to go to the hills. I am grateful to all those I have had good fortune to climb with including PN, JK, IR, DL, ML and MC. I am especially grateful to my long term climbing partner and friend Julian Terry not only for our friendship but also for his having stopped me from falling 300ft one occassion. I would not have finished this study if it were not for his quick actions.

Declaration.

The work for this thesis was carried out in the Department of Physics at the University of Warwick from October 1988 to September 1991. This thesis is the result of my own independent research except where referenced and has not been previously submitted for any other degree.

Some parts of this thesis have been published or accepted for publication,

1) "^{17}O NMR characterisation of the oxygen sites in the $Bi_2Sr_2Ca_{n-1}Cu_nO_{4+2n}$ (n=1,2,3) high temperature superconductors."

R. Dupree, Z. P. Han, A. P. Howes, D. McK. Paul, M. E. Smith and S. Male (Physica C 175 (1991) 269).

2) "^{17}O NMR of the $Bi_2Sr_2Ca_2Cu_3O_{10}$ high temperature superconductor."

A. P. Howes, R. Dupree, D. McK. Paul and S. Male (Physica C 185-189 (1991) 1137).

3) "An ^{17}O NMR study of the Cu-O planes of $Bi_2Sr_2Ca_2Cu_3O_{10}$."

A. P. Howes, R. Dupree, D. McK. Paul and S. Male (Physica C, accepted to be published).

It is anticipated that other parts of this thesis will be submitted for publication in the future.

A. P. Howes.

Additional papers written in the period October 1988 to September 1991,

1) "NMR studies of $Nd_{2-x}Ce_xCuO_4$."

S. M. Doyle, R. Dupree, A. P. Howes, D. McK. Paul and M. E. Smith (Bull. Mat. Sci 14 (1991) 619).

2) "A ^{89}Y NMR study of Pr and Nd doped $YBa_2Cu_3O_7$."

Z. P. Han, R. Dupree, D. McK. Paul, A. P. Howes and L. W. J. Caves. (Physica C 181 (1991) 335).

Abstract.

^{17}O Nuclear magnetic resonance is an ideal probe of the high temperature superconductors as it can sample both the static and dynamic electronic susceptibilities of the Cu-O planes of these materials. The ^{17}O NMR site assignments and the temperature dependence of the shift and spin-lattice relaxation has been investigated for the n = 1 and 3 phases of $Bi_2Sr_2Ca_{n-1}Cu_nO_{4+2n}$ and the n = 3 phase of $Tl_2Ba_2Ca_{n-1}Cu_nO_{4+2n}$.

The shift of the ^{17}O resonance associated with the Cu-O plane of the non-superconducting $Bi_2Sr_2CuO_6$ is temperature independent from room temperature to 5K. This is not the situation for $Bi_2Sr_2Ca_2Cu_3O_{10}$ and $Tl_2Ba_2Ca_2Cu_3O_{10}$.

For the $Bi_2Sr_2Ca_2Cu_3O_{10}$ superconductor ($T_c \approx 107K$) both of the distinct Cu-O planes of the unit cell show a marked but different temperature dependence of the NMR shift above T_c. The shift associated with the central Cu-O plane starts to decrease below ~ 300K and the spin component of the Knight shift has dropped to ~ 1/2 of its room temperature value by T_c. The outer Cu-O plane shift is almost temperature independent until ~ 120K when it decreases sharply and the spin component of the Knight shift is ~ 2/3 of its room temperature value by T_c. The difference in these temperature dependencies suggests that a one component susceptibility model cannot describe this system.

The $Tl_2Ba_2Ca_2Cu_3O_{10}$ superconductor is structurally very similar to $Bi_2Sr_2Ca_2Cu_3O_{10}$. The ^{17}O NMR shift has been studied for this sample before an annealing process ($T_c \approx 114K$) and after ($T_c \approx 124K$). The room temperature resonances observed before and after the anneal are essentially the same. Interestingly the resonances observed for the two distinct Cu-O planes of the structure have very similar shift values and cannot be easy resolved (unlike the situation for $Bi_2Sr_2Ca_2Cu_3O_{10}$). Before and after annealing a temperature dependence of the resonance associated with the Cu-O planes is observed but in contrast to $Bi_2Sr_2Ca_2Cu_3O_{10}$ the two different plane resonances show the same temperature dependencies. Before the anneal the spin component of the shift is estimated to be ~ 2/5 of its room temperature value by T_c whereas after the anneal the shift has drooped to ~ 1/6 of its room temperature value by T_c.

For both $Bi_2Sr_2Ca_2Cu_3O_{10}$ and $Tl_2Ba_2Ca_2Cu_3O_{10}$ the relaxation behaviour of the Cu-O planes appears to be Korringa like ($K_s^2T_1T$ is constant) in the normal state despite these temperature dependent shifts. The values obtained for $K_s^2T_1T$ is similar to the theoretical value for simple s-type metals with no electron-electron or antiferromagnetic interaction. However the data does not completely rule out any other relaxation behaviour.

Chapter 1. Introduction.

1.1. Superconductivity.

Superconductivity is an electronically ordered state that occurs in certain materials below a particular temperature referred to as the superconducting transition temperature (T_c). Superconductivity is in fact a common phenomenon and over one third of the elements are superconductors.

Superconductivity was first observed in 1911 by H. Kamerlingh Onnes while studying the D.C. resistivity of mercury at low temperatures[1]. He observed that below a temperature near 4.2K the resistivity of the sample disappeared. The discovery of other superconducting elements soon followed as well as the discovery that above a certain critical current density (J_c) the superconductivity was quenched.

In 1933 Meissner and Ochsenfeld found that when a material went into the superconducting state all magnetic flux was expelled from its interior and this effect became known as the Meissner effect[2]. Not only was a superconductor a perfect conductor but it was also a perfect diamagnet. It was later shown that the superconducting state was an equilibrium state with no sample history dependence. In addition to the Meissner effect it was found that if a magnetic field was applied with the sample already below T_c no flux would enter.

Since the superconducting state is an equilibrium state Gorter and Casimir developed a thermodynamical model which was in reasonable agreement with experiment[3]. These arguments explain the temperature dependence of the critical field (H_c) which had been discovered earlier[4] (One of the first applications for these materials was the production of magnetic fields by superconducting

solenoids. It was discovered that the maximum field that could be achieved with available materials was very small, due to this critical field).

These superconductors are now referred to as the type I superconductors. The magnetic field dependence of Type II superconductors is described by two critical fields. Magnetic flux penetrates at fields above H_{c1} and penetration is complete with superconductivity destroyed by H_{c2} (see figures 1.1 and 1.2). It was found that it was possible to achieve high magnetic fields with these type II superconductors.

Early attempts to produce a theory of superconductivity failed but the phenomenological London equations[5] described how a magnetic field behaved in a superconductor. This introduced the London penetration depth (λ_L), a characteristic decay length of the field entering the superconductor. Fröhlich[6] in 1950 proposed that an electron-phonon interaction could produce an attractive force between electrons. From this model he suggested that the interaction would produce an electron ground state of lower energy than that of 'normal' conduction electrons. However, calculation of this new ground state by perturbation theory failed. It was not until 1957 that Bardeen, Cooper and Schriefer[7] proposed the BCS theory which explained all of the existing experimental results.

A full description of the BCS theory and many other aspects of superconductivity can be found in Parks[8]. The essential first step of the BCS theory was Cooper's study of an electron-phonon-electron interaction. From this he proposed that an attractive force could exist between two electrons in the superconducting state, forming a bound stable state[9]. The two electrons of this Cooper pair with wave vectors $\underline{k}$ and $-\underline{k}$ and total momentum zero pass through the

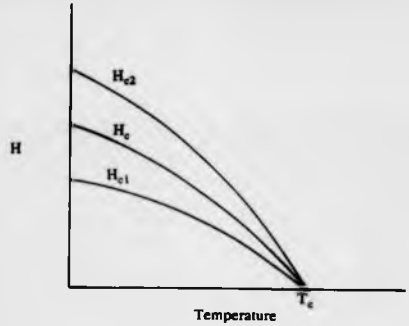

Figure 1.1. Temperature dependence of the critical field for Type I (H_c) and Type II (H_{c1} and H_{c2}) superconductors.

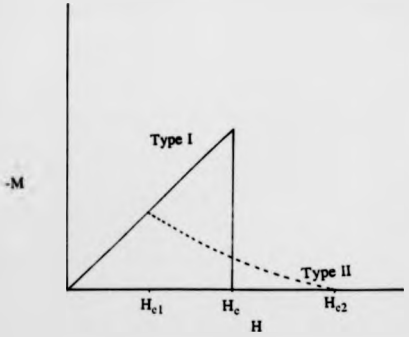

Figure 1.2. Magnetization curves for Type I and Type II superconductors.

lattice without interacting with it. Bardeen, Cooper and Schriefer then argued that each bound pair restricts allowed electron wave vectors (from the exclusion principle). From this they constructed a ground state in which all electrons form bound pairs at T=0, despite the weakness of the attractive force. This microscopic theory proposed by Bardeen, Cooper and Schriefer gave good agreement with all known experimental results. It was a variational method that involved taking a trial wave function describing the Cooper pairs and minimising the expectation value of the energy associated with the parameters that control the wave function.

In the ground state Cooper pairs occupy all the region near the Fermi surface. To break up a pair requires a finite amount of energy corresponding to the binding energy of a pair. At T=0 all electrons are paired whereas at a finite temperature but below T_c some electrons will be excited to a higher energy state and will not be in a bound pair. Since a finite energy is associated with the binding there will be a gap (the superconducting energy gap) centred on the Fermi energy level in the electronic spectrum of occupancy. In BCS superconductors the distance between the two electrons of a pair can be large ($\sim$ 1000nm) and so many pairs will overlap and interact with each other (in fact this overlapping is essential to the stability of the superconducting state). The energy gap will depend on the density of the pairs and as this density is temperature dependent so too is the energy gap. At the transition temperature the thermal energy will be just great enough to break up the binding ($k_B T_c \sim E_g(T_c)$).

By 1986 many elements and alloys had been found to be superconductors. However, the highest known transition temperature was only 23K for Nb_3Ge and

the current theories suggested that very much higher T_c's were not likely. Late in 1986 the first of many reports of high temperature (HiT_c) superconductivity was published by Bednorz and Müller. They had been studying a range of perovskite structures and found that La_2CuO_4 doped with 8% Barium on the Lanthanum site had a T_c of $\sim 35K$[10]. It was also found that Strontium could be used instead of Barium as a dopant. Interestingly these particular perovskites containing copper and oxygen had been studied before but their resistivity had only been studied down to liquid nitrogen temperatures.

In early 1987, soon after Bednorz and Müller's discovery, a group led by Chu announced the discovery of the superconductor $Y_1Ba_2Cu_3O_{7-\delta}$[11] later called yttrium 123 or YBCO with a T_c of $\sim 90K$. It was later found that the yttrium could be replaced with almost any rare earth[12,13] even gadolinium[14] despite the fact that local magnetic moments were known to quench superconductivity. Another interesting aspect was that to a certain extent the T_c of a sample of $Y_1Ba_2Cu_3O_{7-\delta}$ could be controlled by varying the oxygen stoichiometry[15]. This material was considered a breakthrough since it had a T_c of $\sim 90K$ well above the boiling point of liquid nitrogen and a large proportion of subsequent research on HiT_c has gone into studying yttrium 123 and associated compounds. Other discoveries followed, most of which were copper-oxide based superconductors. However, above 20K superconductivity was also found in $BaBiO_3$ based systems[16]. At present the highest T_c material is $Tl_2Ba_2Ca_2Cu_3O_{10}$ with a T_c of 125K[17,18].

The new materials are in some ways very similar to conventional metallic superconductors. At room temperature they show an electrical resistivity which

decreases with temperature and below a specific temperature the thermal fluctuations become too small to prevent pairing. The material then exhibits all the properties of a superconductor. However, there are a number anomalous features in the normal state behaviour of these materials. The most obvious of these is the linear temperature dependence of the normal state resistivity. This is in contrast to the resistivity observed for transition metal superconductors or other oxide superconductors[19]. Other anomalies include the temperature dependent Hall coefficient[20] (in metals these are normally temperature independent) and normal state tunnelling measurements[21].

High temperature superconductivity is a constantly changing and enlarging field and there have been over thirty thousand papers published in the first five years since 1986. There is still no single theory which is able to explain all the different experimental data as satisfactorily as the BCS theory (with some modification) has for conventional superconductors. A full review of experimental results and theory would be very large and out of date very quickly. The fundamental interactions which give rise to superconductivity in the HiT_c materials are still not understood. However, it is possible to identify the molecular and structural features which are common to most of the HiT_c materials.

Most HiT_c materials contain planes of copper and oxygen atoms between layers of other atoms. They are typically very two dimensional with c lattice spacing (perpendicular to the Cu-O plane) much larger than a or b (which have similar values). In the superconducting state it is the conduction band associated with the Cu-O planes where superconductivity occurs. The layers in between the Cu-O planes are the doping sources that act as reservoirs of charge which

contribute to this conduction band. This conduction band is common for a number of materials containing copper and oxygen and explains the reasonably low room temperature resistance associated with the HiT_c materials.

Most of the materials so far studied have a structural distortion due to the Jahn-Teller effect where it is energetically favourable for some crystal symmetry to be lost or the crystal lattice is orthorhombic. This is thought to be important for superconductivity[18].

There also appears to be a trade off between antiferromagnetism and superconductivity in these systems. An example of this is the Lanthanum system. Undoped La_2CuO_4 is antiferromagnetic at room temperature, whereas a small amount of doping i.e. substitution of Lanthanum by Barium or Strontium destroys this (see figure 1.3). This system is also a good example of what is meant by a charge reservoir since if Barium is substituted for Lanthanum forming $La_{2-x}Ba_xCuO_4$ one copper atom will go from a 2+ state to a 3+ state for every Barium atom added, to maintain charge neutrality. These extra electrons are not localised and contribute to the conduction band. The copper atoms can be thought of as having an average valence value, above a valence of +2.2 antiferromagnetism disappears and the material is superconducting[18,22].

In the Yttrium based materials doping is not required as the extra charge is controlled by the oxygen concentration. The average copper valence in $Y_1Ba_2Cu_3O_6$ is +1.7 and the material is antiferromagnetic, whereas the average copper valence in $Y_1Ba_2Cu_3O_7$ is +2.3 and the material is superconducting. The $Y_1Ba_2Cu_3O_{7-\delta}$ system has a similar phase diagram to the Lanthanum cuprate system with regions of antiferromagnetic, metallic, insulating and superconducting

regions.

A number of the HiT$_c$ materials have a variable number of Cu-O planes per unit cell such as $Y_1Ba_2Cu_{3+n/2}O_{7+n/2}$ with n=0,1,2 and 4[18,23-25], $Bi_2Sr_2Ca_{n-1}Cu_nO_{2n+4}$ with n=1,2 or 3[18,26,27], $Tl_2Ba_2Ca_{n-1}Cu_nO_{2n+4}$ with n=1 to 6[17,18,26-30] and $TlBa_2Ca_{n-1}Cu_nO_{2n+3}$ with n=1 to 5[18,31]. The last two are of some interest since they agree with the thought that T_c will increase with the number of planes per unit cell (n for the Bismuth and Thallium materials) until there are three planes (n=3) and then decrease. This idea was based on considering the average valence of the Cu^{2+} ion. Single phase samples of Yttrium n=3 or 5 or Bismuth n=4 have not yet been fabricated.

A number of experiments have now been performed on the HiT$_c$ materials that demonstrate that flux is quantised,[32-35] with the flux quantum of h/2e, the same as for conventional superconductors. Therefore in the superconducting state pairing occurs and most experimental results of the superconducting state can be explained by a modified BCS theory involving strong correlations of electrons[36,37]. There is still a lot of uncertainty about the source of this pairing mechanism. Early suggestions included the Jahn-Teller effect[38,39] or a pairing associated with magnetic ordering or fluctuations[40] because of the strong relationship between antiferromagnetism and superconductivity in these systems. However at present it is not known whether the mechanism for superconductivity is due to phonons (such as for simple metal superconductors) or spin fluctuations (the pairing mechanism for superfluid helium-3) or something more exotic.

The source of the attractive interaction is important for a theoretical model (i.e. what is happening in the normal state). Once the normal state is theoretically

understood then the pairing mechanism should be explainable. There are many different and conflicting theories of the normal state[41], which is not surprising since it is a very diverse problem with the phase diagram showing regions of antiferromagnetic, semiconductive, superconductive and metallic behaviour for different doping. Fermi liquid theory will not adequately describe the normal state and current work can be divided loosely into two categories, those that retain a Fermi liquid like description and those that do not. The antiferromagnetic Fermi liquid theory[42] and the marginal Fermi liquid theory[43] are both experimentally based. However there are arguments that suggest abandoning Fermi liquid theory all together[44]. The non-Fermi liquid theory that Anderson[45,46] proposes is that the system can be described as a Luttinger liquid[47] (which is like a one-dimensional Fermi liquid). The consequence of this approach is that spin and charge are separated. The t-J model[48,49] also includes a separation of spin and charge with different velocities associated with the spin and charge ($V_s \neq V_c$). Another approach studies the interplay between antiferromagnetism and superconductivity. Schrieffer[50-52] argues that antiferromagnetic fluctuations cause regions of reduced spin or charge wave density. These regions referred to as 'spin-bags' lead to an attractive interaction between electrons. It would appear that the antiferromagnetic insulating phases are theoretically well understood[53-55] but do the copper spin interactions produce the pairing mechanism or compete with it ?[56,57]. Some workers still propose a BCS like mechanism, or a modified gapless BCS type mechanism with a gap opening up well below T_c[58]. Anisotropic pairing produced by an exchange of spin-fluctuations that was proposed for organic and heavy fermion superconductors[36,37] has also been suggested for the HiT_c

systems. However there are still other approaches suggesting that a strong correlation between electrons is the important factor[40,59].

1.2. Nuclear Magnetic Resonance.

The basis of Nuclear Magnetic Resonance (NMR) Spectroscopy is the measurement of the energy separation of the ground state nuclear spin energy levels in an applied magnetic field. Nuclear Magnetic Resonance was first observed by two groups headed by Purcell[60] and Bloch[61] working independently in 1945. However, Gorter[62] in 1942 was the first to look for a resonance but failed due to the sample he had chosen.

Very soon after the initial experiments it was discovered that for the same value of the applied magnetic field the NMR frequency of a particular nucleus varies slightly from the Larmor frequency expected from the Zeeman interaction. This is due to variations of local electronic environment for nuclei in different systems. This was first observed in 1949 in metals where the effect is largest and is called the Knight shift after its discoverer[63]. The Knight shift is caused by the spin susceptibility of conduction electrons altering the magnetic field at the nucleus. A shift in resonant frequency was later observed for other materials[64,65] where the effect is due to non-conduction electrons. These electrons shield the nucleus from the magnetic field (diamagnetic term) as well as there being a simultaneous interaction of an electron with the nucleus and with the applied magnetic field (Van Vleck). The Van Vleck term arises from the ground state of an electron being altered by the applied magnetic field causing higher electron states to be mixed in with the ground state. The Van Vleck term is hard or impossible to calculate since it involves not just the electron ground state but also

higher electron states. The non-conduction electron shift is referred to as the chemical shift.

Generally the shifts observed for a particular nucleus are quoted as a parts per million (ppm) or a percentage shift relative to the frequency of the same nucleus but in a sample where the shift in frequency is small compared with the resonant frequency of a 'bare' nuclei (i.e. the Larmor frequency). An increase in resonant frequency is termed a positive shift.

NMR quickly became important in the study of metals, where the shifts are large and in the solution state where, despite the relatively small shifts involved, the widths of resonances observed are comparatively small. This is because of the rapid tumbling of molecules averaging away anisotropic interactions, this results in comparatively narrow lines. In the solid state there are a number of interactions (e.g. the dipole-dipole interaction and in polycrystaline samples Knight shift anisotropy and quadrupole interactions) which broaden the NMR lineshape. In some situations this broadening can be used to obtain information. In other situations it is desirable to reduce this broadening and it was suggested that these anisotropic interactions could be averaged away by physical motion of the sample. This was demonstrated in 1958[66] and the most common technique in use today is Magic Angle Spinning (MAS)[67]. Great improvements in experimental techniques for solid state NMR have been made since then, including cross polarization[68], decoupling[69], dynamic angle spinning[70], double angle rotation[70] and a combination of these techniques.

The energy associated with each nuclear spin in an applied magnetic field is one of the Zeeman energy levels, which is modified slightly by the energy of

internal interactions. The distribution of these spins (classically) is governed by Boltzmann statistics. This results in a small population difference which is seen as a macroscopic magnetization, generally in the same direction as the magnetic field. An NMR experiment perturbs this spin system by applying an alternating magnetic field B_1 orthogonal to the static field B_0. The perturbed system then re-achieves equilibrium by spins 'flipping' from one state to another giving up energy equal to the difference in energy between the different energy levels. This energy is detected by the electromagnetic device that initially drives the transition of states. The probability of spontaneous 'flipping' with the emission of energy in a system in equilibrium is low.

This re-achieving of equilibrium leads to the second useful concept in NMR, that of relaxation whereby spins having been perturbed relax back into thermal equilibrium with each other and with their surroundings (the lattice).

A single time constant may not adequately describe the relaxation of the spins to equilibrium with the lattice but, at least, gives some idea of the time scale involved and is referred to as the spin-lattice or longitudinal relaxation time T_1. A similar time constant associated with achieving equilibrium within the spin system is referred to as the spin-spin or transverse relaxation time T_2. In some solids T_1 may be very long ($\sim$ hours) although in metals it may be comparatively short ($\sim$ ms) at room temperature. This is because of different relaxation mechanisms being dominant in different systems. T_2 in solids is often very much less than T_1.

The concept of relaxation can be thought of in a classical sense where a 'classical' nuclear spin aligns itself with B_0. The spin is then perturbed by B_1 and

then relaxes back to its original alignment. This idea is the basis of the phenomenological Bloch equations[71] which describe the relaxation.

In metals spin-lattice relaxation is achieved via simultaneous spin-flips of nuclear spin and conduction electron spin. The measurement of T_1 can give information on magnetic fluctuations and conduction electrons. The spin-spin correlation function $\chi(\underline{q},\omega) = \chi'(\underline{q},\omega) + i\chi''(\underline{q},\omega)$ with wave vector $\underline{q}$ and frequency ω describes the electronic susceptibility of a system. The static spin susceptibility $\chi'(0,0) = \chi_0$ is related to the electron spin contribution to the Knight shift K_s by,

$$K_s = A_{hf}\,\chi_0 \qquad (1.1)$$

where A_{hf} is termed the hyperfine interaction which describes the coupling of the nuclear and electronic spins. Thus the observation of the Knight shift can give a direct measure of the electronic susceptibility of a system if A_{hf} is known.

There are a number of other mechanisms for spin-lattice relaxation including electron orbital effects and quadrupole relaxation. However, the most important is the above contact interaction and for this the Knight shift and the spin-lattice relaxation are related by,

$$\frac{1}{T_1 T} \propto K_s^2 \qquad (1.2)$$

where T_1 is the spin-lattice relaxation time, T is temperature and K is the Knight shift. This is termed the Korringa relationship after its discoverer[72].

1.3. NMR and the Study of Superconductivity.

Both the normal and superconducting states are worth studying to determine the mechanisms for superconductivity since how a sample behaves in the normal state has some bearing on the reason why it becomes superconducting. Performing a NMR experiment in the superconducting state may seem difficult since a magnetic field will only penetrate a distance of the order of the penetration depth λ_L. Since this distance is small and of the order of 10nm for metals[73] but 100nm for the high temperature superconductors[74] NMR only samples the surface unless the sample (or sample grain size) is smaller than λ_L. Interestingly, experiments performed on small metal samples give almost the same results as those performed on bulk metal samples[73].

Experiments performed on Type II superconductors below H_{c1} will be the same as those performed on Type I superconductors below H_c. However there is a region of interest between H_{c1} and H_{c2}. Between these two critical fields there are two regions, one of normal state material and one in the superconducting state. This is referred to as a mixed state where there is an inhomogeneous field within the superconductor which will broaden the NMR lineshape. Regions of normal state material increase as H_{c2} is approached. The vortex structure of the mixed state can be studied by observing the broadening and lineshape of the NMR spectra caused by the distribution of the inhomogeneous field in the material.

Solid state phenomena are unaffected by NMR since the energy associated with nuclear spin interactions are small in comparison with electron and phonon energies. Therefore, soon after the discovery of NMR it was used to study the normal and superconducting properties of the conventional BCS superconductors.

The first study of a material in the superconducting state was made by Reif on mercury[75]. Knight also performed a similar study slightly later [76]. The non-zero Knight shift at T=0, once field inhomogeneity and diamagnetic shift (caused by the partial expulsion of flux) had been taken in to account, contradicted what was expected from the BCS theory developed after these experiments. For a simple metal the normal state spin susceptibility is independent of temperature and therefore so is the Knight shift. The pairing up of electron spins reduces this spin susceptibility and at T=0 the spin susceptibility should be zero and therefore so should the observed Knight shift. Two contributions were later included to resolve this discrepancy, the orbital shift and spin-orbit coupling[77,78]. Spin-orbit coupling is the result of the interaction between the spin of an electron and its' orbital motion if the electron is moving in an electric field. Spin-orbit coupling is capable of mixing electron states both in the normal and superconducting states. The result of this is that for some electron pairs BCS pairing is no longer maintained and this gives rise to a spin susceptibility below T_c.

In 1958 using the BCS theory Yosida theoretically calculated the spin susceptibility as a function of temperature in the superconducting state[79]. The Yosida function was found to fit well with the data obtained for Aluminium[80] where the effects of spin-orbit coupling are small (see figure 1.4).

One consequence of the BCS theory was the prediction of the build up of the density of states near to T_c (the coherence factor). In 1957 Hebel and Slichter measured the spin-lattice relaxation time in superconducting Aluminium[81] and found that the results were in complete agreement with the BCS theory including the observation of the coherence factor as a peak in the relaxation rate ($1/T_1$) just

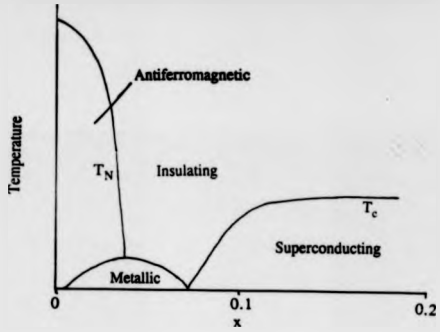

Figure 1.3. Phase diagram of $La_{2-x}Ba_xCuO_4$

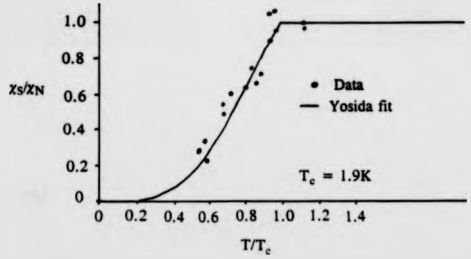

Figure 1.4. The Yosida function applied to ^{27}Al NMR data[63].

below T_c. Further experiments performed on BCS superconductors verified a gap opening up[81,82] and the observation of the field distribution due to the flux line lattice (vortex lattice) below the transition temperature[83].

All NMR results on the conventional superconductors were in fact in agreement with the models of superconductivity which expanded from the BCS theory. Since NMR had proved to be such a excellent probe of the conventional superconductors studies immediately began after the discovery of the HiT_c materials since they contain many nuclei susceptible to NMR, such as ^{63,65}Cu, ^{89}Y, ^{205}Tl, ^{139}La and, if isotope exchanged, ^{17}O. These experiments probe the static and dynamic electronic structure at different sites in the superconductor.

Over 500 NMR papers have been published in the first five years since the discovery of HiT_c materials and as for all other aspects of these materials there are many differences in results, conclusions and theories with many conflicting views. NMR results can be divided into different topics for each nucleus such as, room temperature spectra and site assignment, room temperature magnetic field dependencies to find information on any electric field gradient, variable temperature shift and spin lattice relaxation measurements in the normal and superconducting states and the study of flux vortices in the superconducting state. In the superconducting state one noticeable feature in all NMR data is the lack of a coherence peak in the spin-lattice relaxation. However, it has been shown that if the electron pairs are strongly bound this will not be observed[58]. Another common feature of the results was the observation of temperature dependent shifts in the normal state, for ^{89}Y, ^{63}Cu and ^{17}O in oxygen depleted yttrium 123 and for ^{63}Cu and ^{17}O in the Lanthanum system. This contrasts with simple metal systems

where the Knight shift is constant above T_c and with ^{89}Y, ^{63}Cu and ^{17}O in fully oxygenated $Y_1Ba_2Cu_3O_7$ where a decrease in Knight shift is only observed below T_c[84-98]. Early work on fully oxygenated $Y_1Ba_2Cu_3O_7$ studying the Knight shift below T_c tried to determine whether s or d electron pairing was involved since the Yosida function is different for the two cases. Unfortunately the data could be fitted to both functions since there was uncertainty in the value to be used for the orbital shift[99]. The normal state spin-lattice relaxation also proved interesting with some systems such as the fully oxygenated $Y_1Ba_2Cu_3O_7$ showing Korringa like behaviour in the normal state although the ^{63}Cu relaxation is influenced by electron-electron interactions and other systems such as the oxygen depleted $Y_1Ba_2Cu_3O_{7-\delta}$ showing non-Korringa like relaxation[100-107].

Early attempts to explain these normal state NMR shifts, normal state relaxation and the lack of a coherence peak involved spin fluctuations which make the superconducting state gapless[37]. A more thorough approach to explain these results is a phenomenologically based antiferromagnetic Fermi liquid theory proposed by Monien, Miles and Pines[41,108,109]. This involves temperature dependent antiferromagnetic correlations in the normal state and is also consistent with the NMR results for fully oxygenated $Y_1Ba_2Cu_3O_7$ (but of course in this case no shift is seen above T_c). A more detailed review of work relevant to this study will be given in chapter 6.

1.4. An Oxygen-17 Approach.

There are very good reasons for an ^{17}O study of HiT_c superconductors which may be summarized as follows,

1) All the HiT_c materials are oxides with one or more Cu-O planes in their structure.

2) Superconductivity is somehow inextricably linked with these Cu-O planes.

3) There are more non-equivalent oxygen sites than any other including copper for ^{17}O NMR to probe.

4) ^{17}O has a much smaller Quadrupole moment than ^{63}Cu or ^{65}Cu providing better resolution in aligned powders.

5) Hybridization of the Cu 3d state and the O 2p state will mean that information obtained from ^{17}O NMR will be related to the Cu site[110,111].

6) There are lower T_c materials which are copper free but contain oxygen where a comparison of results may prove useful.

Unfortunately ^{17}O has a low natural abundance, but ^{17}O exchange has proved to be relatively straightforward and the correct oxygen stoichiometry can be achieved without adverse affects to the sample. The two samples of main interest in this study were the n=3 phases of $Bi_2Sr_2Cu_nO_{2n+4}$ and $Tl_2Ba_2Cu_nO_{2n+4}$. These two materials are of interest since they have the two highest, reliably reported, superconducting transition temperatures (110K and 125K respectively).

Chapter 1. References.

1. H. Kamerlingh Onnes: Commun Phys. Lab. Univ. Leiden No. 120b, 122b, 124c (1911).
2. W. Meissner and R. Ochsenfeld: Naturwissenshaften 21 (1933) 787.
3. G. J. Gorter and H.B.G. Casimir, Phys. Z. 35 (1934) 963.
4. H. Kamerlingh Onnes and W. Tuyn: Commun Phys. Lab. Univ. Leiden No. 160a, 160b, 167a (1923).
5. 'An Introduction to the Theory of Superconductivity': C. G. Kuper (Oxford University Press 1968).
6. H. Fröhlich: Phys. Rev. 79 (1950) 845.
7. J. Bardeen, L. N. Cooper and J. R. Schrieffer: Phys. Rev 108 (1957) 1175.
8. 'Superconductivity': R. D. Parks (Ed) (Dekker 1969).
9. L. N. Cooper, Phys. Rev. 104 (1956) 1189.
10. J. G. Berdnorz and K. A. Müller: Z. Phys. 64 (1986) 189.
11. M. K. Wu, J. R. Ashburn, C. J. Torng, P. H. Han, R. L. Meng, L. Gao, Z. J. Huang, Y. Q. Wang and C-W. Chu: Phys. Rev. Lett 58 (1987) 908.
12. D. W. Murphy, S. Sushine, R. B. Van Dane, R. J. Cava, B. Batlogg, S. M. Zahuak and L.F. Schneeneger: Phys. Rev. Lett. 58 (1987) 1888.
13. P. H. Han, R. L. Meng, Y. Q. Wang, L. Gao, Z. J. Huang and C-W. Chu: Phys. Rev. Lett 58 (1987) 1891.
14. Z. Fisk, J. P. Thompson, E. Zirngiebl, J. L. Smith and S-W. Cheong: Solid State Comm. 62 (1987) 743.
15. R. J. Cava, B. Batlogg, K. M. Rabe, E. A. Rietman, P. Gallagher and L. W. Rupp: Physica C 156 (1988) 523.
16. L. F. Mattheiss, E. M. Gyorgy and D. W. Johnson: Phys. Rev. B. 37 (1988) 3745.
17. C. C. Toradi, M. A. Subramarian, J. C. Calabrese, J. Gopalakrihnan, K. J. Morriesey, T. R. Askew, R. B. Flippen, U. Chowdry and A. W. Sleight: Science 240 (1988) 631.
18. R. J. Cava: Scientific American 263 (1990) 24.
19. K. Kitazawa, H. Takagi, K. Kisho, T. Hasegawa, S. Uchida, S. Tajima, S. Tanaka and K. Fueki: Physica C 153-155 (1989) 9.
20. N. P. Ong, T. W. Jing, T. R. Chien, Z. Z. Wang, T. V. Ramakrishnan, J. M. Tarascon and K. Remschnig: Physica C 185-189 (1991) 34.
21. J. R. Schrieffer: Conference Summary of Materials and Mechanisms of Superconductivity, High Temperature Superconductors III, Physica C 162-164 (1989).
22. 'Superconductivity': A. Kitazawa 45 (Springer 1990).
23. H. W. Zandbergen, R. Gronski, K. Wang and G. Thomas: Nature 331 (1988) 596.
24. P. Bordet, C. Chaillout, J. Chenavas, J. L. Hoden, M. Marezio, J. Karpinski and E. Kalidid: Nature 334 (1988) 596.
25. J. Karpinski, E. Kaldis, E. Jilek, S. Rusiecki and B. Bucher: Nature 336 (1988) 660.
26. J. M. Tarascon, W. R. McKinnon, P. Barboux, D. M. Hwang, B. G. Bagley, L. h. Greene, G. W. Hull, Y. LePage, N. Stoffel and M. Giroirel: Phys. Rev. B38 (1988) 8885.

27. M. A. Subramarian, C. C. Toradi, J. C. Calabrese, J. Gopalakrihnan, K. J. Morriesey, T. R. Askew, R. B. Flippen, U. Chowdry and A. W. Sleight: Science 239 (1988) 1015
28. M. Kikuchi, S. Nakajima, Y. Syono, K. Hiraga, T. Oku, P. Shindo, N. Kobayashi, H. Iwaski and Y. Muto: Physica C 158 (1989) 79.
29. J. P. Shang, D. J. Li, H. Shiahara and L. D. Marks: Supercond. Sci. Tech 1 (1988) 132.
30. M. Werwerft, G. V. Teneloooand S. Amelink: Physica C 156 (1988) 607.
31. H. Ihara, R. Sugise, M. Hirabagashi, N. Terada, M. Jo, K. Hayashi, A. Negishi, M. Tokumoto, Y. Kimura and T. Shimomura: Nature 334 (1988) 510.
32. P. L. Gammel, D. J. Bishop, G.J. Dolan, J. R. Kwo, C. A. Murray, L. F. Schneemeyer and J. V. Waszcak: Phys. Rev. Lett. 59 (1987) 2592.
33. W. R. McCrath, H. K. Olsson, T. Claeson, S. Eriksson and L.G. Johansson: E. Phys. Lett 4 (1987) 357.
34. R. H. Koch, C. P. Umbach, C. J. Clark, P. Chaudhai and R. B. Laibowitz: App. Phys. Lett. 51 (1987) 200.
35. C. E. Gough, M. S. Colclough, E. M. Forgan, R. G. Johnston, M. Keene, C. M. Muirhead, A. I. M. Roe, N. Thomas, J. S. Abell and S. Sutton: Nature 326,855 (1987).
36. M. Sigrist and K. Ueda: Rev. Mod. Phys. 63,2 (1991) 239.
37. T. Koyama and M. Tachiki: Phys. Rev. B 39 (1989) 2279.
38. H. Kamimura: Jap. J. Appl. Phys 26 (1987) 1092.
39. G.M. Vujicic, V. L. Aksenov, N. M. Plakida and S. Stomenkovic: Phys. Lett A 73 (1989) 439.
40. P. Lulde: Physica C 153-155 (1989) 1769.
41. See 'Proceedings of the Int. Con. of Superconductivity High Temperature Superconductors III', Physica C 185-189 (1991).
42. A. J. Millis, H. Monien and D. Pines: Phys. Rev. B 42 (1990) 167.
43. C. M. Varma, P. B. Littlewood, S. Schmitt-Rink, E. Abrahams and A. E. Ruckenstein: Phys. Rev. Lett. 63 (1989) 1996.
44. P. W. Anderson and R. Schrieffer: Physics Today, June (1991) 61.
45. P. W. Anderson: Phys. Rev. Lett 64 (1990) 1839.
46. P. W. Anderson: Phys. Rev. B.42 (1990) 2624.
47. F. D. M. Haldane: J. Phys C. (1981) 2585.
48. B. S. Shastry: Phys. Rev. Lett. 63 (1989) 1288
49. F. Mila and T. M. Rice: Physica C 157 (1989) 561.
50. J. R. Schrieffer, X. G. Wen and S. C. Zheng: Phys. Rev. B. 39 (1989) 11663.
51. A. Kampf and J. R. Schrieffer: Phys. Rev. B. 41 (1990) 6399.
52. J. R. Schrieffer, X. G. Wen and S. C. Zheng: Phys. Rev. Lett. 60 (1988) 944.
53. R. R. P. Singh, M. P. Gelfand and D. A. Huse: Phys. Rev. Lett 61 (1988) 2484.
54. S. Chakravarty, B. I. Halperin and D. R. Nelson: Phys. Rev. B. 39 (1989) 2344.
55. P. Littlewood, C. M. Varma and E. Abrahams: Phys. Rev. Lett 63 (1989) 2602.
56. V. J. Emery and G. Reiter, Phys. Rev. B 38 (1989) 11938.

57. Y. Kitaoka: Physica C 162-164 (1989) 195.
58. X. Su, J. Shen, L. Zhang and C. Chen: Physica C 165 (1990) 8.
59. P. W. Anderson, G. Baskaran, Z. Zou and T. Hsu: Phys. Rev. Lett 58 (1987) 2790.
60. E. M. Purcell, H. C. Torrey and R. V. Pound: Phys. Rev. 69 (1946) 37.
61. F. Bloch, W. W. Hansen and M. E. Packard: Phys. Rev. 69 (1946) 127.
62. C. J. Gorter and L. J. F. Broer: Physica 9 (1942) 591.
63. W. D. Knight: Phys. Rev. 76 (1949) 1259.
64. W. G. Procter and F. C. Yu: Phys. Rev 77 (1950) 717.
65. W. C. Dickinson: Phys. Rev 77 (1950) 736.
66. E. R. Andrew, A. Bradbury and R. G. Eades: Nature 182 (1958) 1659.
67. E. R. Andrew: Inter. Rev. Phys. Chem. 1 (1981) 195.
68. A. Pines, M. G. Gibby and J. S. Waugh: J. Chem. Phys. 59 (1979) 569.
69. M. Mehring, A. Pines, W. K. Rhim and J. S. Waugh: J. Chem. Phys. 54 (1971) 3234.
70. B. F. Chmelka, K. T. Mueller, A. Pines, J. Stebbins, Y. Wu and J. W. Zwanziger: Nature 339 (1989) 42.
71. R. K. Harris, 'Nuclear Magnetic Resonance Spectroscopy',Longman (1986).
72. J. Korringa Physica 16 (1950) 601.
73. D. E. MacLaughin: Sol. State Phys. 31 (1976) 1.
74. B. Batlogg: Physica B (1991) 7.
75. F. Reif: Phys. Rev. 102 (1956) 1417.
76. W. D. Knight, G. M. Androes and R. H. Hammond, Phys. Rev. 104 (1956) 852.
77. Z. Ferrell: Phys. Rev. Lett 3 (1959) 262
78. P. W. Anderson: Phys. Rev Lett. 3 (1959) 325.
79. K. Yosida, Phys. Rev. 110 (1958) 769.
80. H. L. Fine, M. Lipsicas and M. Strongin: Phys. Lett. 29A (1969) 366.
81. L. C. Hebel and C. P. Slichter: Phys. Rev. 113 (1957) 1175.
82. Y. Masuda and A. G.Redfield: Phys. Rev. 125 (1962) 159.
83. A. G. Redfield: Phys. Rev. 162 (1967) 367.
84. J. T. Markert, T. W. Noh, S. E. Russek and R. M. Cotts: Sol. State. Comm 63 (1987) 847.
85. Lutgemeier and M. W. Pieper: Sol. State. Comm. 64 (1987) 267.
86. W. W. Warren, R. E. Walstedt, G. F. Brennert, G. P. Espinosa, J. P. Remeika: Phys. Rev. Lett. 59 (1987) 1860.
87. M. Mali, D. Brinkmann, l. Pauli, J. Roos, H. Zimmerman and J. Haliger: Phys. Lett A 124 (1987) 112.
88. Y. Kitaoka, S. Hiramatsu, T. Kondo, K. Asayama: J. Phys. Soc. Jpn 57 (1988) 30.
89. C. H. Pennington, D. J. Durand, D. B. Zax, C. P. Slichter, J. P. Rice and D. M. Ginsberg: Phys. Rev. B 37 (1988) 7944.
90. M. Takigawa, P. C. Hammel, R. Heffner, Z. Fisk: Phys. Rev. B 39 (1989) 7371.
91. G. Balakrishan, R. Dupree, I. Farnan, D. McK. Paul and M. E. Smith: J. Phys. C 21 (1988) L847.
92. H. Alloul, T. Ohno and P. Mendels: Phys. Rev Lett 63 (1989) 1700
93. A. J. Vega, W. E. Garneth, E. M. McCarron and R. K. Bordia: Phys. Rev.

B 39 (1989) 2322.
94. Y. Kitaoka, K. Ishida, F. Fijiwara, T. Kondo, K. Asayama, M. Horvatic, Y. Berthier, P. Butaud, P. Segrransan, C. Berthier, H. Katayama-Yosida, Y. Okabe and 95. T. Takahasashi 'Strong Correlation and Superconductivity (Springer 1989).
96. G. J. Kramer, H. B. Brom, J. Van den Berg, P. H. Kes, D. J. W. Ijdo: Sol. State Comm 64 (1987) 705.
97. P. Butand, M. Horvatic, Y. Berthier, Segansan, Y. Kitaoka: Physica C 166 (1990) 301.
98. Y. Kitaoka, Y. Berthier, P. Butand, M. Horvatic, P. Segransan and C. Berthier: Physica C 162-164 (1989) 195.
99. D. J. Durand, S. E. Barrett, C. H. Penningto, C. P. Slichter, E. D. Bukowski, T. A. Freidmann, J. P. Rice and D. M. Ginsberg: 244 'Strong Correlations and Superconductivity (Springer 1889).
100. P. C. Hammel, M. Takigawa, R. Heffner, Z. Fisk and K. C. Ott: Phys. Rev. Lett. 63 (1989) 1992.
101.T. Ohno, T. Kanashiro and K. Mizuno: J. Phys. Soc. Jpn. 60 (1991) 2040.
102. H. Alloul, T. Ohno and P. Mendels: Phys. Rev. Lett 63 (1989) 1700.
103. M. Takigawa, A. P. Reyes, P. C. Hammel, J. D. Thompson, R. Heffner, Z. Fisk and K. C. Ott: Phys. Rev. B 43 (1991) 247.
104. P. Butaud, M. Horvatic, Y. Berthier, P. Segransan, Y. Kitaoka, C. Berthier: Physica C 166 (1990) 301.
105. Y. Yoshinari, H. Yasuoka, Y. Ueda, K. Koga and K. Kosuge: J. Phys. Soc. Jpn. 59 (1990) 3698.
106. H. Monien, D. Pines and M. Takigawa: Phys. Rev. B 43 (1991) 258.
107. R. E. Walstedt and W. W. Warren: Science 248 (1990) 1082.
108. H. Monien, P. Monthoux and D. Pines: Phys. Rev. B 43 (1991) 275.
109. H. Monien, D. Pines and M. Takigawa: Phys. Rev. B 43 (1991) 258.
110. M. Takigawa, A. P. Reyes, P. C. Hammel, J. D. Thompson, R. H. Heffner, Z. Fisk and K. C. Ott: Phys. Rev. B 43 (1991) 247.
111. F. C. Zhang and T. M. Rice: Phys. Rev. B 37 (1988) 3759.

Chapter 2. Theoretical Background.

2.1 Introduction.

NMR and superconductivity are two vast subjects and it is not intended here to discuss the theory behind them in depth but rather to describe the more important aspects which are related to this study. It is important to remember that although the theoretical background of NMR and BCS like superconductors is well understood, this not true of the HiT$_c$ materials where theory is far from being fully understood.

NMR probes the ($\underline{q}$,ω) dependence of the spin susceptibility χ_{spin} ($\underline{q}$,ω) with ω at the Larmor frequency (ω_N). The NMR relaxation rate ($1/T_1$) is a measure of the summation of χ''_{spin} ($\underline{q}$,ω_N) over $\underline{q}$.

2.2 The Nuclear Spin Hamiltonian.

The energy associated with a nucleus of non zero spin ($I \neq 0$) can be expressed in terms of the Hamiltonian,

$$H_{tot} = H_z + H_{rf} + H_d + H_q + H_{hf} + \cdots \qquad (2.1)$$

Each term will be briefly considered here, further details can be found in the books by Abragam[1], Poole and Farach[2], Slichter[3], and Winter[4].

If a nucleus has a nuclear spin ($I \neq 0$) then it possesses spin angular momentum $\hbar\underline{I}$ which gives rise to a magnetic moment.

$$\underline{\mu}_N = \gamma_N \hbar \underline{I} \qquad (2.2)$$

where γ_N is the nuclear gyromagnetic ratio.

The interaction of this magnetic moment with an externally applied

magnetic field (B_0) gives rise to the Zeeman splitting term H_z,

$$H_z = -\underline{\mu}_N \cdot \underline{B}_0 \qquad (2.3)$$

If the direction of B_0 defines the z direction then,

$$H_z = \gamma_N \hbar B_0 m \qquad (2.4)$$

where m is the z direction component of $\underline{I}$ and has values I,I-1,I-2,..,-I. Therefore for a spin system I there will be 2I+1 energy levels with a separation of $\gamma_N \hbar B_0$. Since $\gamma_N \hbar B_0$ is an energy term it can be described in terms of a frequency ω_N the Larmor frequency,

$$\gamma_N \hbar B_0 = \hbar \omega_N \qquad (2.5)$$

In thermal equilibrium the populations of the different energy levels are described by Boltzman statistics.

H_{rf} represents a radiofrequency magnetic field B_1. In a simple NMR experiment this is applied orthogonal to B_0 and induces transitions between the Zeeman energy levels but only when the frequency of oscillation of B_1 is close to the Larmor frequency. It can be represented by a raising and a lowering operator,

$$H_{rf} = \frac{-\gamma_N \hbar B_1}{2} \left(I_+ e^{-i\omega t} + I_- e^{i\omega t} \right) \qquad (2.6)$$

Both H_z and H_{rf} are externally imposed Hamiltonians, the other Hamiltonians to be considered are internal and can provide valuable information

about a nuclei's local electronic environment via their affect on the Zeeman energy levels. If the contribution of these Hamiltonians to the total energy is small compared with the Zeeman term then standard perturbation theory[1,5] can be used to determine their influence. For high values of B_0 this situation is generally true, but the quadrupole interaction (H_q) can still be appreciably large[1,6].

Using Perturbation theory the total energy of the m^{th} level is given by,

$$E_m = E_m^{(0)} + E_m^{(1)} + E_m^{(2)} + \cdots \qquad (2.7)$$

where,

$$E_m^{(0)} = \langle m|H_z|m\rangle = -\hbar\omega_0 m \qquad (2.8a)$$

and,

$$E_m^{(1)} = \langle m|H_I|m\rangle \qquad (2.8b)$$

and,

$$E_m^{(2)} = \sum_{m \neq m'} \frac{\langle m'|H_I|m\rangle\langle m|H_I|m'\rangle}{E_m^{(0)} - E_{m'}^{(0)}} \qquad (2.8c)$$

H_I is the Hamiltonian of the interaction under consideration.

These internal interactions can be described as second rank tensors. An interaction $\underline{P}_{xyz}$ can be simplified by a transformation $\underline{R}$ so that only the diagonal elements are non-zero $\underline{R}^{-1}\underline{P}_{xyz}\underline{R} = \underline{P}_{diag}$ The new coordinate system is referred

to as the principal axis system (PAS). It is usual to characterise the interaction in terms of (i) an isotropic value $P_{iso} = 1/3(P_{11} + P_{22} + P_{33})$ if the tensor is not traceless, which is observed as a shift in the Larmor frequency, (ii) an anisotropy $\delta = P_{33}-P_{11}$ and (iii) an asymmetry $\eta = P_{22}-P_{11}/P_{33}$.

The magnetic interactions of nuclear spins coupling to conduction electrons are referred to as hyperfine interactions after the proposal that magnetic coupling could explain the hyperfine structure in optical spectra. An example of a hyperfine interaction is the Knight shift observed in metals. The coupling of electrons with nuclei (with $I \neq 0$) in a metal is very different from that in a non-metal due to the nature of conduction electrons, (although the same interaction can be used to describe both situations). Since the conduction electrons are not localised a nuclear spin will be subjected to all the magnetic fields produced by all the conduction electrons at the same time. With no externally applied magnetic field there is no preferential orientation for the electron spins and the magnetic coupling to the nuclei averages to zero. However a static field B_0 will polarise the electrons resulting in a non-zero average s type electron coupling (s-type, since they are the only electrons to have a non-zero wave function amplitude at the nucleus). This coupling is described by an interaction $\underline{\Delta}$ such that,

$$H_K = \sum_i \underline{s} \cdot \underline{\Delta}_i \cdot \underline{I}_i \qquad (2.9)$$

Where H_K is the hyperfine hamiltonian for the Knight shift interaction and $\underline{s}$ is the electron spin. The summation is required because one electron spin couples

with a number of nuclear spins. This interaction results in a change in the magnetic field 'seen' by a nucleus in the same direction as B_0.

Since non s-type electron wavefunctions are zero at the nucleus the only interaction between these electrons and the nucleus may occur via an exchange interaction with the s-type electrons. This occurs in transition metals (d-type) and is termed core-polarization. The resulting contact field produced is a small change in magnetic field at the nucleus compared with that from the s-type electrons and is often opposite in direction to the applied field.

The observed Knight shift is proportional to applied magnetic field since the degree of electron spin polarization is proportional to the applied field and is defined as a fractional shift $\Delta B/B_0$. This may be written as,

$$\frac{\Delta B}{B_0} = \frac{8\pi}{3} \langle |U_k(0)|^2 \rangle_{E_F} \chi_e^s \qquad (2.10)$$

where $\langle |U_k(0)|^2 \rangle_{E_F}$ is the average of the conduction electron probability density evaluated at the Fermi energy level and χ_e^s is the total electron spin susceptibility. As the polarisation of s-type electrons (which produces χ_e^s) and $\langle |U_k(0)|^2 \rangle_{E_F}$ are independent of temperature in simple metals, the Knight shift is also temperature independent.

There is a shift due to the orbital angular momentum of the electrons. The corresponding hamiltonian can be written as,

$$H_{orb} = \underline{B} \cdot \underline{Q} \cdot \underline{I} \qquad (2.11)$$

Where $\underline{Q}$ is the orbital shift interaction.

There is also a contribution to the magnetic field at the nucleus that arises from the interaction of the inner core electrons and the applied static magnetic field, the chemical shift. This is made up of two contributions. The diamagnetic term, from these inner core electrons setting up a magnetic field that opposes B_0 (Lenz's Law). The second term arises from B_0 modifying the ground-state electron wavefunctions by the mixing in of some excited states. This is termed the paramagnetic or Van Vleck contribution and is dependent on the symmetry of the local electronic environment. These inner core interactions may be large but of opposite sign resulting in the orbital shift being small compared to that from the s-state interaction. In non-metals where there are no conduction electrons the chemical shift is dominant.

The nuclear charge distribution for $I > 1/2$ is not spherical and it has a nuclear quadrupole moment. This moment interacts with the electric field gradient which may be present in a sample. As an example of tensor analysis the quadrupole interaction will be described in more detail. The quadrupole hamiltonian may be written as,

$$H_q = \underline{I} \cdot \underline{Q} \cdot \underline{I} \qquad (2.12)$$

Where $\underline{Q}$ is the quadrupole energy tensor. Using the fact that this tensor is symmetric and traceless and that $I(I+1) = I_x^2 + I_y^2 + I_z^2$ (the eigenvalue of the operator I^2) the Hamiltonian can be simplified to,

$$H_q = \frac{1}{2} C [\, 3I_z^2 - I(I+1) + \eta (I_x^2 - I_y^2)\,] \qquad (2.13)$$

with x,y and z as the principal axis system, C as a constant and $|Q_{xx}| \leq |Q_{yy}| \leq |Q_{zz}|$ and where Q_{ii} are the three diagonal components of $\underline{Q}$ (remembering that in the PAS all other components are zero). η is defined as,

$$\eta = \frac{Q_{xx}-Q_{yy}}{Q_{zz}} \qquad (2.14)$$

and,

$$Q_{xx} = -\tfrac{1}{2}C(1-\eta), \quad Q_{yy} = -\tfrac{1}{2}C(1+\eta), \quad Q_{zz} = C \qquad (2.15)$$

Classically the scalar quadrupole moment Q is defined by,

$$eQ = \int \rho(r)\,(3\cos^2\theta-1)\,d\tau \qquad (2.16)$$

where e is the electronic charge, $\rho(r)$ is the nuclear charge density over which the integral is carried out and θ is the angle made by $\underline{r}$ and the internuclear axis. The electric field gradient V_{ij} is defined as,

$$V_{ij} = -\frac{\partial E_i}{\partial x_i} = \frac{\partial^2 V}{\partial x_i \partial x_j} \qquad (2.17)$$

Q_{ij} and V_{ij} are related by,

$$Q_{ij} = \frac{eQ}{2I(2I-1)} V_{ij} \qquad (2.18)$$

V_{zz} is referred to as the electric field gradient eq (with q being the field gradient). Notice that C of equations (2.13) and (2.14) is proportional to e^2qQ. It can now be seen why the quadrupole energy tensor is traceless since the e.f.g obeys the Laplace equation,

$$\nabla^2 V = V_{xx} + V_{yy} + V_{zz} = 0 \qquad (2.19)$$

The quadrupole coupling constant is defined as $C_q = e^2qQ/h$.

C_q, η and the six Eulerian angles describing the orientations of the crystallographic and principal axis system are all that is required to describe the field gradient tensor. The second term for the quadrupole hamiltonian ($E_m^{(1)}$) from perturbation theory has a $3\cos^2\Theta$-1 variation where Θ is an angle from the z-axis of the PAS and B_0.

The nuclear dipolar hamiltonian can be described as the interaction between two classical magnetic dipoles . It is a traceless and axially symmetric tensor and has a simple $3\cos^2\Theta$-1 angular variation. Θ is again the angle from the z-axis of the PAS and B_0. However, it is not necessary for two interactions to have a common PAS.

If the resulting complete Hamiltonian H_{tot} is anisotropic then the powder pattern obtained results from the randomly orientated crystallites each having its' own PAS. The lineshape obtained for single crystals or aligned samples will of course depend on orientation.

2.3. Sample Rotation.

Contributions to the (frequency) lineshape of a randomly orientated powder can be divided into two types. A homogeneous lineshape where all the nuclei contribute to it or an inhomogeneous lineshape where isolated spins contribute to different parts of it. In the inhomogeneous case the width associated with one spin is narrower than the total linewidth. This may arise either from differently orientated crystallites in the powder or from structural defects and impurities in each crystallite.

If an interaction results in a homogeneous linewidth of $\Delta\nu$ then the spin-spin relaxation time will be of the order of $1/\Delta\nu$. Therefore for an imposed modulation to affect this interaction a causality argument would suggest that it must be of a shorter time scale than $1/\Delta\nu$. Many broadening interactions such as chemical shift anisotropy and the quadrupole interaction have a $(3\cos^2\Theta\text{-}1)$ dependence (where Θ is the angle between the z-axis of the PAS and B_0). Spinning the sample with the axis of rotation at $\Theta=\cos^{-1}(3^{-1/2})$ at a frequency $\nu_r > \Delta\nu$ will narrow the lineshape. Inhomogeneous broadening is not affected since each contribution is narrowed but overall little or no narrowing takes place. Magic angle spinning[7] NMR (MAS-NMR) can therefore be used to improve the resolution of homogeneous lineshapes and is a method of determining the major contribution to the broadening of an observed lineshape by only narrowing the homogeneous part. For a fuller discussion on MAS and its uses the reader is directed to reference 8.

2.4. Relaxation.

A nuclear spin system with excited energy states will relax back to its ground state with the transfer of energy. This relaxation involves two processes, the spin-spin (or transverse) relaxation (T_2) where the spin system establishes internal thermal equilibrium and spin-lattice (T_1) where the spin system establishes thermal equilibrium with its surroundings.

Spin-lattice relaxation is achieved via a fluctuating magnetic field that a nucleus experiences and associated with every observed shift in frequency is a corresponding fluctuating magnetic field. There are, therefore, a large number of relaxation mechanisms. In a metal the relaxation is predominately due to the coupling of the nuclei with the spin magnetic moment of the conduction electrons.

The spin-lattice relaxation time is related to the imaginary component of the spin-spin correlation function via the dynamical structure factor $S(q,\omega)$ which describes the electron dynamics of a system,

$$S(q,\omega) = \frac{1}{1-e^{-\hbar\omega/k_BT}}\chi''(q,\omega) \qquad (2.19)$$

If the hyperfine coupling is the dominant relaxation mechanism then, quite generally, the spin lattice relaxation time can be written as,

$$\frac{1}{T_1T} = \frac{\gamma_n^2 k_B}{2\mu_B^2}\sum_q |A_q^2| S(q,\omega) \qquad (2.20)$$

where A_q is the form factor which describes the nuclear spin interaction and μ_B

is the Bohr magneton. In NMR ω is at the Larmor frequency (ω_N) and is small compared with the correlation rate τ^{-1} of the rapidly fluctuating conduction electrons. Therefore quite generally, the NMR relaxation rate $1/T_1$ can be expressed in terms of the dynamical spin susceptibility[9] such that,

$$\frac{1}{T_1 T} = \frac{\gamma_N^2 k_B}{\mu_B^2} \sum_q |A_q^2| \frac{\chi''(q, \omega_N)}{\omega_N} \qquad (2.22)$$

where,

$$A_q = \sum_i A_i e^{iq r_i} \qquad (2.23)$$

A_i the hyperfine coupling between the nuclear spin and the electron spin at r_i.

The form factors are related to the hyperfine coupling constants of surrounding nuclei and are generally also q dependent. The factors that control how the summation is performed are clearly important from a theoretical view.

$\chi''(q,\omega)/\omega$ in the paramagnetic state has a Lorentzian frequency dependence with a width Γ_q and may be written as,

$$\frac{\chi''(q, \omega_N)}{\omega_N} = \frac{\pi \chi(q)}{\Gamma_q} \qquad (2.24)$$

Where $\chi(q)$ is the static wave-vector dependent spin susceptibility. For a Fermi liquid $\chi(q)$ and Γ_q are only weakly q dependent and,

$$\sum_q \chi''(q, \omega_N) / \omega_N = \pi \mu_B^2 \rho_0^2 = \pi \chi_s^2 / \mu_B^2 \qquad (2.25)$$

where ρ_0 is the density of states. For non-interacting electrons and a g independent and isotropic hyperfine interaction,

$$T_1 T K_s^2 = \frac{\hbar}{4\pi k_B} \frac{\gamma_e^2}{\gamma_n^2} \qquad (2.26)$$

This is the Korringa relationship[10] and relates the Knight shift to the spin-lattice relaxation time if the relaxation due to the hyperfine interaction is the dominant relaxation process.

The Korringa relationship only involves one relaxation mechanism. However in reality other mechanisms may also contribute to the relaxation such as the orbital electron or quadrupole interaction. This would decrease the observed relaxation time from that suggested from equation 2.26. Even in simple systems the relationship is not strictly correct due to electron-electron[11,12] interactions or antiferromagnetic correlations[13-15].

2.5. Relaxation In A Spin > 1/2 System.

In a spin system (I) there will be 2I+1 energy levels, therefore for I > 1/2, other transitions will occur than just the +1/2⇔ -1/2 transition. For this reason the recovery of magnetization in an NMR experiment where I > 1/2 cannot be simply described by an exponential function used to describe the recovery of a spin=1/2 system, which is of the form,

$$M_0 = M_z(1-2e^{-t/T_1}) \qquad (2.27)$$

To describe the +1/2 ⇔ -1/2 relaxation behaviour in a spin > 1/2 system

is reasonably straight forward and assuming that the energy separation of levels is unequal so that simultaneous spin-flips are forbidden by energy conservation it can be shown that for a spin = 5/2 system (i.e. ^{17}O)[16,17],

$$M(t) = M(0)\left[1-a_1 e^{-t/T_1} - a_2 e^{-6t/T_1} - a_3 e^{-15t/T_1}\right] \quad (2.28)$$

Where a_1, a_2 and a_3 are set by the initial populations of the energy levels. Figure 2.1 shows this recovery assuming that only the 1/2 and -1/2 energy levels have been perturbed in which case a_1 = 27/105, a_2 = 28/105 and a_3 = 50/105. After a time $t = 0.5T_1$ the sum of the $-6t/T_1$ and $-15t/T_1$ terms are less than 10% of that of the t/T_1 term and the relaxation can be adequately described a single exponential and a characteristic time T_1.

2.6. NMR and Superconductors.

Before discussing the new HiT$_c$ superconductors it is worth giving a short overview concerning the BCS like superconductors, further details may be found in a review by MacLaughlin[18] and in the references listed at the beginning of the chapter.

NMR of the normal state for BCS superconductors can be adequately described as that for a metal (since all BCS superconductors are metals). In the normal state the conduction electron susceptibility can be divided into three contributions,

$$\chi_{tot} = \chi_s + \chi_{orb} + \chi_d \quad (2.29)$$

Where χ_s is the s-type spin susceptibility, χ_{orb} is the orbital susceptibility and χ_d is the spin susceptibility of non s-type electrons (for transition metals the d-type

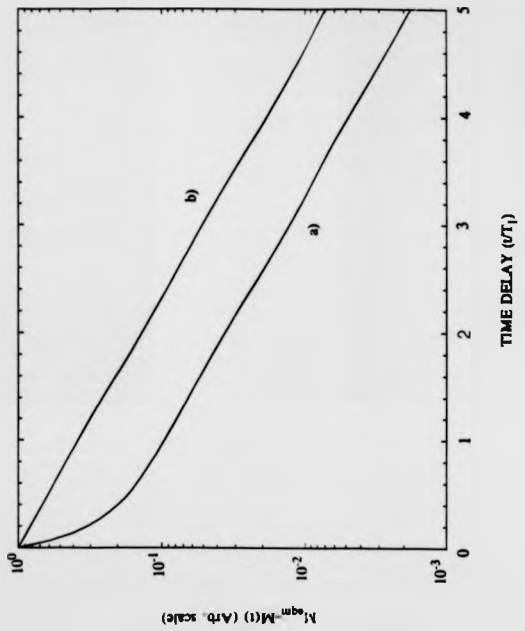

Figure 2.1. Relaxation of magnetization as a function of time for a) a spin = 5/2 system with only the ½ ⇔ - ½ transition initially disturbed and b) a spin = 1/2 system.

electrons will be important).

Each susceptibility contributes to the Knight shift,

$$K_{tot} = K_s + K_{orb} + K_d = a\chi_s + b\chi_{orb} + c\chi_d \qquad (2.30)$$

K_s, K_{orb} and K_d in the normal state have already been discussed. The coefficient c (of equation 2.30) is often negative resulting from the contact field produced between the s and non s type wavefunctions being opposite in direction from the applied field. It is assumed that the dipolar contribution to the spin susceptibility is unimportant.

In s-type superconductors the Knight shift is proportional to χ_s and $\langle |U_k(0)|^2 \rangle_{E_F}$. In the normal state the Knight shift can be approximately calculated (e.g. for aluminium or mercury)[1,2,4,18]. Yosida[19] calculated χ_s in the superconducting state described by the BCS theory[20]. As expected the Yosida function predicts a zero χ_s at T=0. The non-zero Knight shift observed in some cases can be explained by spin-orbit coupling and the orbital shift contribution[18,19,21,22]. If d-type electrons form Cooper pairs in the superconducting state this contribution to the Knight shift should also disappear.

The orbital contribution is independent of spin-susceptibility of the electron and is not changed by spin pairing and so K_{orb} is the same in the normal and superconducting state and will contribute to the observed shift at T=0.

In the superconducting state diamagnetic supercurrents will be set up to oppose B_0. The local fields caused by these currents will affect the magnitude of the Knight shift; because of this Knight shift data of the superconducting state can not be directly extrapolated to zero to measure the temperature independent

orbital shift.

2.7. Spin-lattice Relaxation in BCS Superconductors.

The normal state spin-lattice relaxation in the normal state of BCS like superconductors has already been described in section 2.4. In the superconducting state as the electrons pair they can no longer contribute to the relaxation mechanism. The spin-lattice relaxation in the superconducting state can be described very well by the BCS theory and was first derived by Hebel and Slichter[23]. This theory includes contributions to the relaxation from the orbital and core-polarisation interactions. Near the transition temperature there is a decrease in T_1 due to the increase in the density of states at the Fermi level as the superconducting gap opens up. This is termed the coherence peak that is observed in experiments on conventional BCS superconductors. Below T_c the spin-lattice relaxation time increases approximately exponentially.

2.8. NMR in High Temperature Superconductors.

The Hyperfine Hamiltonian for the Cu-O planes of a HiT$_c$ superconductor maybe written as[24],

$$H_{hf} = \sum_{i,\alpha} {}^{63}I_{i,\alpha}A_{\alpha\alpha}S_{i,\alpha} + \sum_{i,j,\alpha} {}^{63}I_{i,\alpha}BS_{j,\alpha} + \sum_{\langle ij\rangle,\alpha} {}^{17}I_{i,\alpha}CS_{j,\alpha} \quad (3.31)$$

Where the ^{63}Cu nuclear spins are coupled to an electron spin at the same site S_i (one per unit cell) by a hyperfine coupling tensor $A_{\alpha\alpha}$ and to the electron spins

at the four nearest neighbour sites by a hyperfine coupling constant B. The ^{17}O nuclear spins couple via a transferred hyperfine coupling constant C to the two nearest neighbour spins S_j.

The thermal average of the ^{17}O interaction will give the isotropic spin component of the Knight shift,

$$\langle {}^{17}H_{hf} \rangle = \sum_{\langle jj' \rangle, \alpha} {}^{17}I_{i,\alpha} C \langle S_{j,\alpha} \rangle \qquad (2.32)$$

With $\langle -\gamma_n \hbar S_{j,z} \rangle = \chi_0 B_0$ and $\langle H_{hf} \rangle = \langle -\chi_n \hbar \Delta B S_{j,z} \rangle$ then,

$$\frac{\Delta B}{B_0} = {}^{17}K_{iso} = \frac{2C\chi_0}{{}^{17}\gamma_n \gamma_e \hbar^2} \qquad (2.33)$$

The spin component of the ^{17}O Knight shift is proportional to the spin susceptibility at the two adjacent Cu sites.

In 1990 Monien, Monthoux and Pines proposed a phenomenological antiferromagnetic theory to explain the results of NMR studies of the Yttrium and Lanthanum superconductors[13-15]. Here this will be applied to the oxygen sites in the Cu-O planes. The general expression for spin-lattice relaxation times is given in equation 2.22 Performing the sum when antiferromagnetic correlations are involved can be difficult. With short range correlations both $\chi(q)$ and $1/\Gamma_q$ will peak at $q = Q_{AF} = (\pi/a, \pi/a)$, (where a is the lattice constant). These correlations will, in general, decrease the value of $T_1TK_s^2$. The MMP model assumes a dynamical susceptibility of the form,

$$\frac{\chi''(q,\omega_N)}{\omega_N} = \frac{\pi\chi(0)}{\Gamma} + \frac{\pi\chi_{AF}(q)}{\Gamma_{AF,q}} \qquad (3.34)$$

The first term is the q-independent contribution (Fermi like term) and the second is the contribution for the antiferromagnetic spin fluctuations (which have a characteristic length ξ). For an oxygen nucleus coupled to two nearest neighbour Cu spins the form factor can be written as $A_q = A[1+\exp(iqa)]$[9]. This goes to zero at $q = Q_{AF}$ and so the antiferromagnetic correlations are not seen at the oxygen site (if they are small). Therefore on performing the sum over q the only important term would be the Fermi liquid like term and a normal Korringa like behaviour would be expected for the oxygen sites. This is not true at other sites as the form factor would be different and in some cases more q dependent. On performing the sum over q it is assumed that a=b for the lattice spacings a and b and the sum is performed by integration.

If the antiferromagnetic correlations are stronger so that $(\xi/a) > 1$ the MMP model suggests that,

$$\frac{1}{T_1 T} \propto \chi(0) \qquad (2.35)$$

i.e that the Korringa relation no longer holds and T_1TK_s is constant.

Chapter 2. References.

1. A. Abragam, 'Principles of Nuclear Magnetism' (OUP 1961).
2. C. P. Slichter, 'Principles of Magnetic Resonance, (Springer-Verlag 1990).
3. C. P. Poole and H. A. Farach, 'Theory of Magnetic Resonance' (Wiley 1987).
4. J. Winter, 'Magnetic Resonance in Metals' (OUP 1971).
5. M. Cohen and F. Reif: Solid State Phys. 5 (1957) 321.
6. R. K. Harris, 'Nuclear Magnetic Resonance Spectroscopy' (Longman 1987).
7. E. R. Andrew: Inter. Rev. Phys. Chem. 1 (1981) 195.
8. M. E. Smith, 'A High Resolution Multinuclear Resonance Study of Ceramic Phases' (Ph.D Thesis University of Warwick 1987).
9. M. Takigawa, A. P. Reyes, P. C. Hammel, J. D. Thompson, R. Heffner, Z. Fisk and K. C. Ott: Phys. Rev. B 43 (1991) 247.
10. J. Korringa Physica 16 (1950) 601.
11. D. Pines: Sol. State Phys. 1 (1955)
12. R. E. Walstedt and W. W. Warren: Science 248 (1990) 1082.
13. H. Monien, P. Monthoux and D. Pines: Phys. Rev. B 43 (1991) 275.
14. H. Monien, D. Pines and M. Takigawa: Phys. Rev. B 43 (1991) 258.
15. A. J. Millis, H. Monien and D. Pines: Phys. Rev. B 42 (1990) 167.
16. E. R. Andrew and D. P. Tunstall: Proc. Phys. Soc. 78 (1961) 1.
17. A. Narath: Phys. Rev. 162 (1967) 320.
18. D. E. MacLaughlin: Solid. State Phys. 31 (1976) 1.
19. K. Yosida, Phys. Rev. 110 (1958) 769.
20. J. Bardeen, L. N. Cooperr and J. R. Schrieffer: Phys. Rev 108 (1957) 1175.
21. Z. Ferrell: Phys. Rev. Lett 3 (1959) 262
22. P. W. Anderson: Phys. Rev Lett. 3 (1959) 325.
23. L. C. Hebel and C. P. Slichter: Phys. Rev. 113 (1957) 1175.
24. F. Mila, T. M. Rice: Physica C 157 (1989) 561.

Chapter 3. Experimental Methods and Techniques.

3.1. Pulsed Fourier Transform NMR.

In 1950 Hahn[1] demonstrated that it was possible to perform NMR spectroscopy using a pulsed technique rather than the continuous wave method. One of the advantages demonstrated was the direct measurements of relaxation behaviour. Later Lowe and Norberg[2] showed that, apart from at very low temperatures, the resulting free induction decay from the spin system reacting to the RF pulse is the Fourier transform corresponding to the steady-state (CW) resonance. Therefore the FID contains the same information in the time domain as the CW resonance does in the frequency domain. This was demonstrated by Clark[3] by sweeping the field and using a box-car integrator and by Ernst and Anderson[4] who performed a Fourier transform of the FID using a computer.

Modern NMR spectroscopy involves radiofrequency measurements as a consequence of the large static magnetic fields used (1-15 Tesla and $\omega_N = \gamma_N B_0$). A schematic diagram of a modern NMR spectrometer is shown in figure 3.1. Superconducting cryomagnets are ideal magnets to use with an NMR system as the magnetic field used must be homogeneous over the sample and remain constant during the experiment. A spectrometer consists of a stable continuous wave generator capable of producing the radio frequencies, linked to a pulse programmer via a gate to produce pulses of the required length. The pulse programmer should be capable of generating long and complex pulse programmes for sophisticated experiments. These pulses are used to drive an RF transmitter which is capable of producing rectangular pulses which are typically 1-20μs in length. Normally the output of the transmitter is terminated to 50Ω and has a

Figure 3.1. Schematic diagram of a modern NMR spectrometer.

pulsed power rating of a few Kilowatts. The pulses from the transmitter are then fed into the NMR probe inside the bore or pole pieces of the magnet. The probe consists of an electrical circuit (Figure 3.2) with a coil (the NMR coil) that is normally positioned orthogonal to the direction of B_0. The circuit is tunable to the required frequency and matched to 50Ω for coupling to the transmitter using variable capacitors and inductances.

The NMR coil, which contains the sample under investigation, converts the RF pulse into the oscillating magnetic field (B_1, which is of the order of mT) discussed in Chapter 2. The magnetisation will be tipped into the transverse direction by an angle θ from the direction of B_0 such that,

$$\theta = \gamma_n B_1 T \qquad (3.1)$$

Where T is the duration of B_1. B_1 is dependent on the quality factor of the coil, (i.e. the design of the tunable circuit) and the power supplied by the transmitter.

The resulting transverse resonant signal caused by B_1 induces a small voltage in the coil which is amplified by the preamplifier before going to the receiver via a number of filters. The induced voltage in the coil is of the order of a few microvolts and this is generated immediately after the tunable circuit has been subjected to the large voltage of the pulse. It is therefore necessary to design the electronics so that the transmitter and receiver are both coupled to the probe circuit but not to each other.

As the induced voltage is at its largest immediately after the RF pulse it is important that the receiver can recover quickly from any overload produced by the transmitter pulse leaking into it. The first part of the FID can also be corrupted

by ringdown (the decay of the RF pulse) and mechanical oscillations of the probe induced by the RF pulse[5]. The time immediately after the pulse where the signal is corrupted by these effects is referred to as the deadtime (or ringdown time) of the probe. The signal is only sent to the receiver at a time comparable with the deadtime after the pulse to protect the receiver. The overall FID can be severely altered by the coil electrically breaking down due to too high a power being used for the RF pulse and arcing occurring between the coil windings.

Broad lines in frequency space have short FIDs (a function of Fourier transforms) therefore all the information may be lost in the deadtime of the probe. To overcome this problem it may be necessary to use a spin-echo pulse program which will be discussed later in this chapter.

Quadrature phase sensitive detection using two PSDs[5] is commonly used to observe the signal. This has the advantage of distinguishing higher and lower frequencies than the irradiation frequency, by observing the in phase and out of phase components of the signal and an improvement of signal to noise (by $2^{1/2}$) over that using a single PSD. The resulting signal is then digitised and stored for later manipulation by computer. This digitisation is one of the limiting factors of the data acquisition as the spectral width observed is dependent on the sampling rate of the digitisation.

The Fourier transform of a sine wave of frequency ν_0 in a rectangular envelope of duration T shows that the irradiation as a function of frequency is related to ν_0 and T by,

$$F = sinc\ (\pi(\nu-\nu_0)T) \qquad (3.2)$$

(See figure 3.3). It is advantageous to work within a spectral range such that the region of interest is irradiated uniformly (i.e. close to the centre of the sinc-function) as by 1/T from the centre of resonance the amplitude of the sinc-function has decreased to zero. This is the case for high resolution work where spectral widths are $\leq 10^4$Hz, however, a width of the order of 10^5Hz wide would require a pulse width of less than $\sim 20\mu s$ just to observe the line. Since the length of the pulse (in the time domain) is also one of the governing factors in the tip angle (equation 3.1) there is a need in solid state NMR for short but intense RF pulses.

A large number of factors need to be taken in account in performing even a simple NMR experiment, first to detect a signal and then to improve the signal to noise.

a) To improve S/N the FIDs resulting from successive pulses may be added together with a subsequent improvement of $n^{1/2}$ in the S/N over one FID (where n is the number of FIDs). There are two limiting considerations that need to be taken into account for improvement. If the repetition time is much shorter than T_1 then the magnetization tipped into the transverse direction will not have time to recover back into the B_0 direction but will remain in one direction, this is saturation. Conversely if the repetition time is much longer than T_1, time will be wasted after the magnetisation has fully relaxed back into the B_0 direction. Generally for quantitative spectra the repetition period has to be longer than $3T_1$ however this does not optimise S/N of the pulses which is an important consideration for experiments which require a large amount of time, if the signal is small and T_1 long[6,7,8].

b) As stated earlier there is a trade off between the range of frequencies

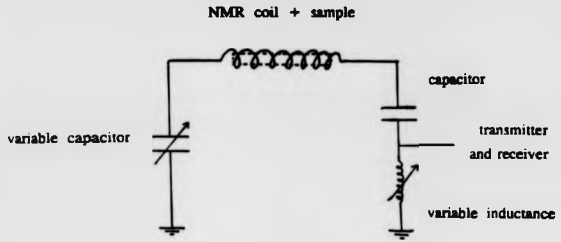

Figure 3.2. Tunable circuit with NMR coil used on the helium probe.

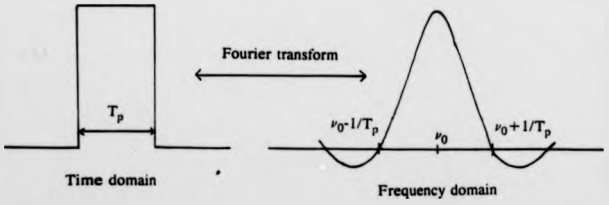

Figure 3.3. Frequency and time domains of an RF pulse of frequency ν_0 and duration T_p.

irradiated and the tip angle. The width may not be a problem in some circumstances as long as some check is made of whether the whole spectrum is being irradiated. A pulse program that tips all the magnetization into the transverse direction (a 90° pulse) and with a repetition rate that allows the magnetization to completely equilibrate in the B_0 direction will not give the optimum S/N.[6,7,8] It may be best to have a shorter pulse that irradiates a larger width and also allows the magnetization to return to equilibrium in the B_0 direction more quickly so that a faster repetition rate can be used[6].

c) The sampling rate of the digitiser is an important consideration as this sets the limit to the spectral width observed and consequently the S/N. Nyquist's theorem states that a sampling frequency of f will result in a highest measured frequency of f/2. Quadrature phase detection has the advantage of separating frequencies above and below the frequency of the pulse by sampling the in-phase and out of phase components of the signal compared with the pulse frequency. For quadrature phase sensitive detection simultaneous rather than sequential detection of the in phase and out of phase magnetisation is better since then all the phase at a particular time is known.

d) Modern NMR transmitters are easy tunable to the required frequency and in most cases resonance can be found by selecting the frequency from tables then using a broad frequency sweep width and observing the resonance and then changing the frequency if necessary. However, there are occasions when the resonance of a particular nuclei in a system may be very different from that suggested by tables (e.g ^{205}Pb in some lead compounds), in this case an educated guess and luck are required.

3.2 The Bruker MSL-360 NMR Spectrometer.

All NMR experiments were performed using a commercially built Bruker MSL 360 spectrometer together with an 8.45T Oxford Instruments wide bore (~85mm) superconducting cryomagnet. The spectrometer is capable of operation over a continuous range of frequencies from 4 to 150MHz (low frequency) and at 360MHz (proton frequency at 8.45T). The spectrometer is managed by the Aspect-3000 computer which allows simultaneous data acquisition and data manipulation using the DISMSL program. Operation of the spectrometer and the change of parameters (such as spectrometer frequency and sweep width) are accomplished via the keyboard normally by short (2 to 4 letter) instructions.

The transmitters and receivers of the spectrometer are run by the system process controller (SPC) of the Aspect-3000. The SPC is programmed by the operator to perform the pulse program, this may be a very simple single pulse experiment or a multi-pulse complex pulse sequence using both the low frequency transmitter and the proton frequency transmitter. This is all achieved using a highly structured programming language common to MSL spectrometers[9].

Continuous low frequencies (1 to 200MHz) are generated by a frequency synthesizer with a resolution of 1Hz. Pulses are then produced by the SPC via an RF interface. These pulses are of the order of 1 V in amplitude and are fed through a broadband (20 W) amplifier which drives the two available transmitters. The low power (~200W) broadband transmitter is built entirely from solid state electronics and is housed within the main spectrometer and is perfectly adequate for some solid state NMR work. One disadvantage of this transmitter is that the power output is only controllable using plug-in attenuators. The high power

transmitter (-1 KW) is an addition to the spectrometer (commercially available from Bruker) and is tunable from 10 to 150MHz using plug-in units for different frequency ranges. The final stage of this transmitter uses valves and the output power is continuously variable.

The induced voltage from the coil (the NMR signal) passes through the preamplifier where the first amplification of the signal occurs (50 dB). The preamplifier is tunable to different frequency ranges using plug-in units and also contains RF filters. The signal is then passed to the broadband receiver which can use both single and quadrature phase sensitive detection. For quadrature phase sensitive detection the data points are taken sequentially from each phase. The receiver gain and the phase of the receiver channels are controllable from the SPC. The receiver uses both electronic and computer controlled filters. The signal is then sent to one of two digitisers for analog to digital conversion. If the dwell time is $\leq 4\mu s$ the 9-bit digitiser is used, for longer dwell times the slower (but with better resolution) 12-bit digitiser replaces it.

Field homogeneity of the cryomagnet is not a problem with the comparatively wide NMR lines observed in this study. Field homogeneity is achieved by using internal superconducting shim coils of the magnet as well as room temperature shimcoils inserted in the bore of the magnet. Linewidths of ~ 30Hz for protons in water can be achieved with a field drift of $\leq$ 20Hz per week.

Further details of spectrometer operation and magnet design can be found in the Bruker reference manual[10] and in the Oxford Instruments manual[11].

3.3. The NMR probes.

Two different NMR probes were used for the variable temperature measurements. Both of these were of the similar design, consisting of a solenoid coil and a simple tuneable circuit. Samples in the original probe were cooled by passing gas over the coil. This gas was first cooled by passing it through a heat exchanger containing liquid nitrogen the temperature of the gas was then regulated using a series of heaters before the gas was in contact with the coil. This system was very simple to operate but was limited to a minimum temperature of 100K.

The second low temperature probe was a more sophisticated system. A simple solenoid coil was again used but this was inserted into an constant flow helium cryostat (Oxford instruments CF1200). This cryostat was then inserted into the bore of the magnet. The temperature was regulated using either an Oxford Instruments or a Thor temperature controller. Despite being upside down from its normal mode of operation the cryostat performed adequately with a base temperature of 5K using liquid helium and 80K using liquid nitrogen.

Two different sized solenoid coils were used with the constant flow cryostat. A 10mm diameter coil was originally used with a 90° pulse length for ^{17}O in water of 20μs with 500 volts produced by the transmitter, this would only irradiate a width of $\sim 10^5$Hz but had the advantage of not electrically breaking down when using helium gas. A shorter pulse length was therefore used to increase the observable spectral width which resulted in a poorer signal to noise. To overcome these problems a 6mm coil was made for which the 90° pulse (on water) was found to be 6μs with 500 volts applied to the probe. In a liquid all energy levels are irradiated. The 90° pulse for a solid sample will be $1/(I+\frac{1}{2})$ of

that for the liquid if only the ½ ⇔ - ½ transition is irradiated in the solid[12]. Therefore the solid 90° pulse for ^{17}O will be 1/3 of that for a liquid. However, it is not necessary to use a 90° pulse in a simple NMR experiment but this will give the maximum signal for one pulse.

Both coils were potted in epoxy resin for electrical insulation. Despite containing much less sample than the original 10mm coil a much better signal to noise was achieved using the 6mm coil. The only disadvantage found with this coil was that it would electrically break down with helium gas if more than ~ 100 volts applied to the probe, however no problems were encountered using nitrogen. The dead time for all the probes used was less than 5μs. Further details of probe and cryostat operation can be found in the respective Bruker and Oxford Instruments manuals[13-17].

For spinning experiments a Doty high speed spinning probe was used with a ~ 5mm coil. The maximum spinning speed achieved was 14KHz. No variable temperature spinning measurements were performed. For setting the stator of the Doty probe to the magic angle the reader is referred to reference 6, Further details of the operation of the Doty probe can be found in the Doty manuals[18].

3.4. Pulse Programs.

Two different types of pulse program were employed to obtain NMR spectra, one a simple single pulse sequence with a delay after the pulse and before acquisition to protect the receiver and the other a simple spin-echo pulse sequence. In both cases quadrature phase sensitive detection was used. Extended phase cycling was used to reduce the effect of 'ringdown' and other unwanted artifacts such as baseline errors[19]. The spin echo pulse sequence was of the form 90° -

τ - 180° - τ' - Acquire, rather than the quadrupole echo sequence of the form 90° - τ - 90° - τ' - Acquire, as this is more suitable for the inhomogeneous spectra observed in this study[12,20,21] (see figure 3.4.).

Two pulse programs were used to measure the spin-lattice relaxation time. The inversion-recovery pulse program first tips the magnetization into the -z direction (z being defined by the direction of B_0). A time τ later the magnetization is sampled using a spin-echo. A number of these experiments would be performed on a sample with different τ delays. T_1 is measured from the change in amplitude and/or area of the resulting frequency domain spectra obtained from the FIDs at each τ delay experiment.

The second pulse program used saturation recovery. The first part of this pulse sequence is a saturating 'comb' of 90° pulses (or something close to 90°) with a spacing of the order of T_2. The number of pulses varies and may be very long. The intention of using this comb is to reduce the magnetization of the sample to zero. After a time delay τ the magnetization is sampled with a spin-echo. Successive experiments are performed with different τ delays and T_1 calculated as for the inversion recovery pulse program[12,19,20] (see figure 3.5).

3.5. Data Acquisition.

Most of the NMR spectra observed were of broad lines. The resulting FID from a one pulse experiment would be very short with much signal being lost in the deadtime from the probe. In general, to overcome this problem a spin-echo pulse sequence was used together with extended phase cycling. A typical pulse sequence would be a 90° pulse of 2μs followed by a delay of 50μs then a 180° pulse of 4μs. The resulting echo would then be acquired. Successive echoes

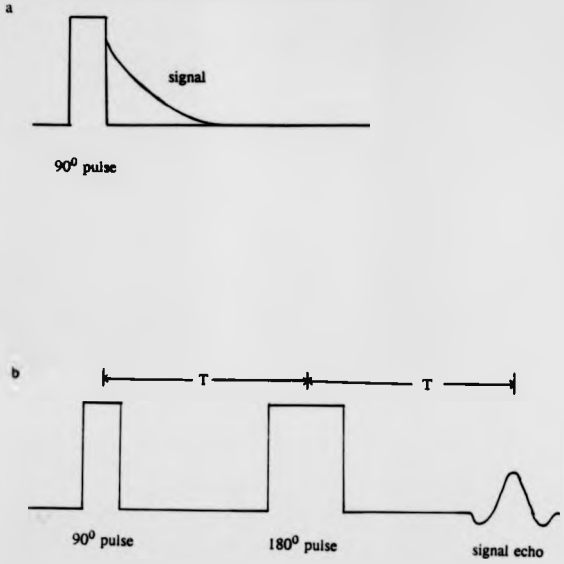

Figure 3.4. Simple one pulse (a) and spin-echo (b) pulse sequences in time domain.

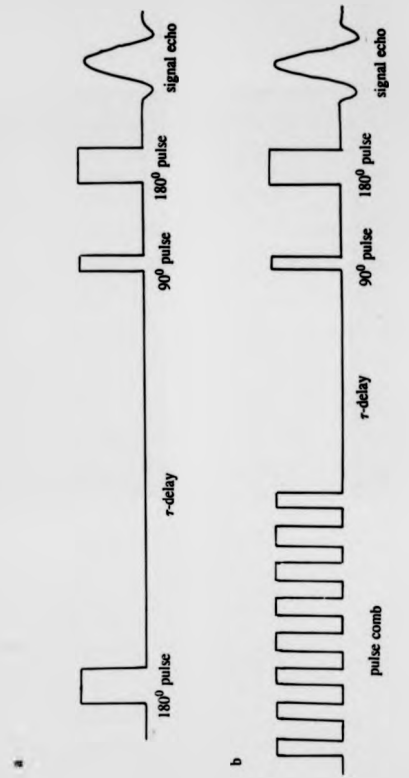

Figure 3.5. Inversion recovery (a) and saturating comb (b) pulse sequences to measure T_1.

would be averaged for sufficient signal to noise and the last half of the echo Fourier transformed to produce the frequency spectrum. Typical repetition periods for the pulse sequence were of the order of 100ms. The spin-spin relaxation time (T_2) was sufficiently long as to not be a problem in acquiring data in this manner.

It was not possible to measure the spin-lattice relaxation time (T_1) of the ^{17}O nuclei by using an inversion pulse with the two pulses of the spin-echo to sample the magnetization. This was probably due to the limitations of the spectrometer and the smallness of the $T_1/15$ exponential term of the recovery of the magnetization (see chapter 2) which is of the order of 1ms in these systems at room temperature.

T_1 was finally measured using a saturating comb of 80 true 90° pulses with a spacing of 2ms between pulses. This was followed by a two pulse spin-echo to sample the magnetization after a delay (τ). As the spacing between pulses in the comb is of the order of $T_1/15$ for the samples at room temperature, the first component in the recovery of the magnetization was never reduced to zero. By $3T_1$ the first term ($T_1/15$) in the recovery of the magnetization has reached its equilibrium value (within the limitations of the spectrometer and signal to noise), the second term ($T_1/6$) 90% of its equilibrium value and the third term (T_1) 50% of its equilibrium value. The spin-lattice relaxation time was measured by observing the final recovery of the magnetization where the T_1 term was dominant.

3.6. Data Manipulation.

Once the FID has been digitised, or successive FIDs digitised and added together, the time domain signal is processed to be in the form of a frequency

domain spectrum. Operations are all performed using the software of the spectrometer's computer. Manipulations include Fourier transformation, smoothing of the spectra, phase correction and baseline correction. Care has to be taken with all these operations to ensure that the resulting spectrum is a true representation of the time domain signal in frequency space.

Typical processing would be of the form,

1) Selection of the point at which to start the Fourier transform. For a single pulse experiment the first few points of the digitised FID may be corrupted because of probe deadtime or the pulse leaking through from the transmitter to the receiver. For a spin-echo the point with the largest amplitude is generally taken as the middle of the echo and the point from which to perform the Fourier transform. This point is not normally the point found from calculation[20] using the delay between the 90^0 and 180^0 pules, presumably due to a time delay inherent in the spectrometer.

2) The FID is then smoothed by multiplying by an exponential function that enhances signal at short times. This is to improve signal to noise and is termed linebroadening since the line is broadened by this process[5]. Incorrect use of linebroadening results in a corruption of the lineshape and incorrect interpretation of the data. It is therefore best to use either no linebroadening or as little as possible[22].

3) The time domain signal then undergoes a Fourier transform to give the frequency domain spectrum.

4) First and second order phase correction is then applied to the spectra. This involves the mixing of the signals from the two phases of the PSDs to obtain

the pure absorption spectra. It is mainly carried out by eye by observing peak symmetry and the baseline so for broad lines is rather subjective.

5) The baseline may be distorted because of probe deadtime; if this is the case baseline correction can be applied to correct it.

3.7. Oxygen-17 Exchange.

Oxygen-17 exchange was performed on the manufactured samples using oxygen gas supplied by MSD Isotopes Ltd. and Icon Ltd. Figure 3.7 illustrates the furnace set up. The volume of the furnace was 200ml and 100ml glass flasks of oxygen at a pressure of one atmosphere containing 40% oxygen-17 were used. The amount of material used in each exchange was such that approximately 10% .of the oxygen in the sample would be oxygen-17 if the distribution was even throughout all the sites in the material. The exchange procedure was the same for both the thallium sample and the bismuth sample. The furnace would be sealed with an atmosphere of air in it. The temperature would be increased at a rate of 100°C/hr until 500°C for the bismuth sample and 400°C for the thallium sample. The seal to the oxygen flask would then be broken by a steel weight dropped using a magnet and the furnace left at the exchange temperature for 12 hours. The furnace was then cooled at 50°C/hr to room temperature. These slow rates of cooling were for two purposes, 1) so as not to thermally shock the glassware of the furnace and 2) to allow the sample and gas to come in to equilibrium if the setpoint temperature was too high.

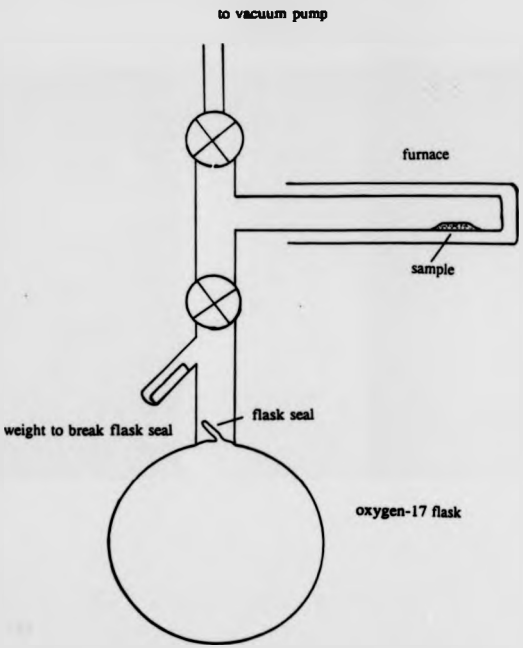

Figure 3.6. The oxygen-exchange furnace.

Chapter 3. References.

1. E. L. Hahn: Phys. Rev. 80 (1950) 580.
2. I. J. Lowe and R. E. Norberg: Phys. Rev 107 (1957) 46.
3. W. G. Clark: Rev. Sci. Inst. 35 (1964) 316.
4. R. R. Ernst and W. A. Anderson: Rev. Sci. Inst. 37 (1966) 93.
5. 'Experimental Pulse NMR', E. Fukushima and S. B. W. Roeder (Addison-Wesley 1981).
6. M. E. Smith, 'A High Resolution Multinuclear Resonance Study of Ceramic Phases' (Ph.D Thesis University of Warwick 1987).
7. J. S. Waugh: J. Mol. Spec. 35 (1970) 298.
8. K. A. Christensen, D. M. Grant, E. M. Shulman and C. Walling: J. Phys. Chem 78 (1974) 1971.
9. 'Aspect 3000 MSL Software manual', Bruker manual 1986.
10. 'MSL System Description' ,Bruker 1986.
11. 'Superconducting Magnet for NMR Operating Instructions', Oxford Instruments 1984.
12. 'Principles of Nuclear Magnetism', A. Abragam (Oxford 1985)
13. 'Operating Manual for Static probe', Bruker (Probe head group) 1984.
14. 'Operating Manual for H.P. L.T. 50 probe', Bruker (Probe head group) 1989.
15. 'Instruction Manual for Continuous Flow Cryostat CF1200', Oxford Instruments 1988.
16. 'Temperature Controller Model ITC 4 Operating Manual', Oxford Instruments 1987.
17. 'D-VT 1000 Variable Temperature Unit', Bruker 1984.
18. 'User's Manual for Solid State NMR probes' Doty Scientific Inc. 1987.
19. 'A Handbook of Nuclear Magnetic Resonance', Freeman (Longman 1988).
20. 'Principles of Magnetic Resonance', C. P. Slichter (Springer-Verlag 1990).
21. T. Rega: J. Phys. Con. Matt. 3 (1991) 1871.
22. L.F. Gladden, T. A. Carpenter, J. Klinowski and S. R. Elliot: J. Mag. Resn. 66 (1986) 93.

Chapter 4. The Bismuth Superconductors.

4.1 Introduction.

The Bismuth superconductors with the general formula $Bi_2Sr_2Ca_{n-1}Cu_nO_{4+2n}$ were discovered in 1988[1,2]. The superconducting transition temperature increases with n. Early work led to the observation that a higher proportion of single phase n=3 material could be made with the substitution of lead for some of the bismuth (<10%)[3,4,5]. So far only the n=1,2 and 3 phases have been made as single phase materials. Pure undoped n=1 phase is either not superconducting or has a low T_c (6-10K) depending on sample preparation. Doping with a small amount of La for Sr (5-10%) increases T_c up to 32K[6-8]. For the n=2 and 3 phases T_c is 85K and 110K respectively[6,8-11].

The unit cell of $Bi_2Sr_2Ca_{n-1}Cu_nO_{4+2n}$ is made up of two Bi-O and two Sr-O planes with Cu-O planes in between them. The Cu-O planes of the n=2 and n=3 phases are separated by Ca planes (see figure 4.1). It is easiest to designate the Bi-O plane oxygens and the Sr-O plane oxygens as O(1) and O(2) respectively using the same notation as Carillo-Cabera et al.[12].

The n=1 phase has only one Cu-O plane, which has two non-equivalent oxygen sites O(3) and O(4). The n=2 phase has two equivalent Cu-O planes but each with two non-equivalent Cu-O distances (as in the n=1 phase). These two planes are separated by a Ca plane. The n=3 phase again contains two equivalent Cu-O planes as in the n=1 and n=2 phase (Cu-O(3,4) and a central Cu-O plane separated by a Ca plane on each side. This central plane is flat (all other Cu-O planes in the n=1,2 and 3 phases are buckled) with four equal Cu-O distances. This is designated the Cu(1)-O(5) plane and all other Cu sites in the three phases as

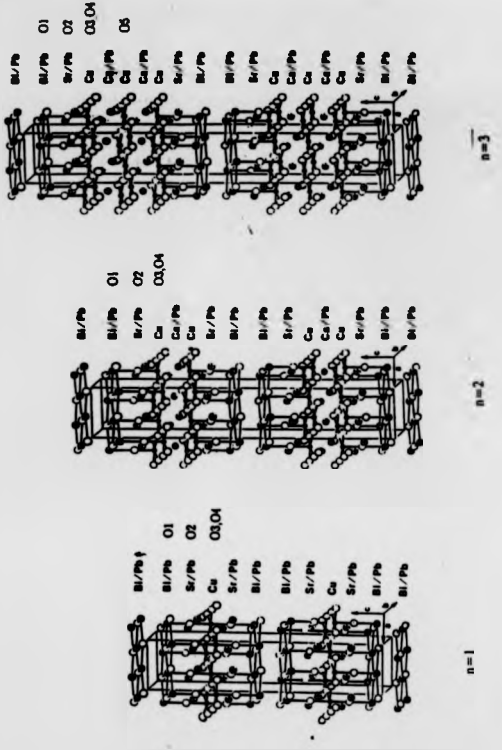

Figure 4.1. The structure of the n=1,2 and 3 phases of $Bi_2Sr_2Ca_{n-1}Cu_nO_{4+2n}$.

Cu(2).

The Cu(2)-O(3) and Cu(2)-O(4) distances are similar. The O(3) and O(4) sites are therefore expected to be very similar, so that for a randomly orientated powder sample the ^{17}O NMR resonance observed will not discriminate between the slightly different sites in the same plane.

As mentioned previously Pb is substituted in to the material to promote single phase growth for the n=3 phase. It is likely that the Pb would be substituted at the Sr sites as well as the Bi sites, which would lead to more sample inhomogeneity. It has been observed that the n=2 and 3 phases are incommensurately distorted so that the Bi-O(1) distance is modulated[13,14].

In this work an extensive ^{17}O NMR study has been made of the n=1 (doped and undoped) and n=3 phases. No work was done on the n=2 phase as other groups have undertaken ^{17}O NMR studies of this phase[15-19].

Two n=1 phases were prepared at Warwick by Z. P. Han, one with no doping and one that was doped with La. The n=1 pure phase was prepared by solid state reaction in air. Bi_2O_3, $SrCO_3$ and CuO of high purity (>99.9%) were mixed together in the correct stoichiometric proportions (together with La_2O_3 for the doped sample) and calcined at temperatures between 790°C and 810°C with one intermediate grinding for 16 hours. The powder was then reground and made into pellets using a hydraulic press. These pellets were then heat treated at 840°C for one hour. This process did not involve the introduction of Pb to aid single phase growth. X-ray diffraction showed that the material is mainly the n=1 phase with traces of unreacted CuO and $SrCO_3$. AC susceptibility measurements showed that the sample was not superconducting above 5K. The doped sample was prepared in

a similar manner but with the addition La_2O_3 so that the ideal stoichiometric composition would have been $Bi_2Sr_{1.7}La_{0.3}CuO_y$. X-ray diffraction showed vary little second phase contamination and the transition temperature was found to be 10K by AC susceptibility.

The n=3 phase material used was manufactured at the Technology and Environmental Centre of National Power PLC (then the Central Electrical Research Laboratories of the CEGB). Bi_2O_3, $SrCO_3$ and CuO together with Pb_3O_4 were mixed together in the correct stoichiometric ratios to produce a compound with the cation ratio $(Bi_{0.8}Pb_{0.2})_2Sr_2Ca_{2.5}Cu_{3.5}$. The mixed powder was calcined in air at 800°C for 16 hours, reground and formed into pellets. The pellets were then annealed at 845°C for 270 hours with a cold intermediate regrinding after 150 hours, after which the powder was re-pelletised. X-ray diffraction on the resulting material indicated that the sample was 85% n=3 phase with a secondary phase of Ca_2CuO_y. Wave length dispersive analysis showed that the n=3 phase had a composition of $(Bi_{0.93}Pb_{0.07})_{2.1}Sr_{1.87}Ca_{2.0}Cu_{3.02}O_{9.97}$. AC susceptibility measurements gave a transition temperature of 107K[17].

All samples were enriched with ^{17}O by the method described in Chapter 3. Approximately 5g of each sample was enriched and a simple calculation of the volumes of oxygen in the furnace and in the sample suggests that 10% of the oxygen was replaced by ^{17}O. Although the oxygen content of the Bismuth superconductors influences the transition temperature, T_c was not affected by the ^{17}O enrichment (shown by AC susceptibility).

4.2. ^{17}O NMR Results.

4.2.1. Room Temperature Results.

Figure 4.2 shows the static ^{17}O NMR spectra for the unaligned n=1,2 and n=3 phases obtained using a spin-echo pulse program (the n=1 phase sample is the undoped material and the n=2 spectra is from ref 17). All shifts are relative to the ^{17}O resonance of tap water (defined as 0ppm). All spectra have a relatively narrow line at ~275ppm which is ~400ppm wide. In addition to this there is a much broader resonance at 1500-1900ppm which is narrower in the n=2 and n=3 phases. The n=3 phase has an additional peak at ~1300ppm. There appears to be no differences between the room temperature spectrum obtained for the pure n=1 sample and the doped n=1 sample.

The ~275ppm line in the n=1 and 2 phases can be fitted to a single quadrupole lineshape and is within the region typical for ^{17}O shifts of copper free materials[15]. It would be reasonable to assign this line to the oxygens in either the Sr-O or Bi-O planes. It is most likely that this resonance is from the Sr-O plane since structural models of the incommensurate modulation suggest a wide variety of environments for the Bi-O plane oxygens[21]. This modulation would cause this resonance to be very broad and unobservable, (in fact there is no ^{17}O NMR data for any material whose structure is incommensurately modulated). The spectrum obtained with the sample spinning at 12kHz (figure 4.3) gives further evidence for there being only one line at ~275ppm as this line narrows to a width of ~150ppm but still shows only one resonance. It would be very unlikely that the resonances from the two distinct planes would be identical. This spectrum was obtained using a spin echo with a delay of 83μs between the centres of the two pulses (the same as

Figure 4.2. The ^{17}O NMR spectra of the n=1, 2 and 3 phases of $Bi_2Sr_2Ca_{n-1}Cu_nO_{4+2n}$ at room temperature (n=2 spectra from ref. 17).

the period of rotation).

The broader resonances lie outside the region of typical orbital shifts and are greater than shifts observed for Cu-O free systems[17]. These resonances are therefore from the Cu-O planes. The n=1 phase has only one Cu-O plane and the n=2 phase has two equivalent Cu-O planes in their respective unit cells. Therefore, as expected, only one resonance is observed in the Cu-O plane ^{17}O NMR region for each of the two phases. The n=3 material has three Cu-O planes per unit cell however, the two outer planes are identical. The ~1300ppm line is very symmetrical and is assigned to the central Cu-O plane oxygens (O(5)) and the ~1900ppm resonance to the oxygens of the two equivalent Cu-O planes (O(3,4). This assignment also explains why the ~1900ppm resonance has a higher intensity since there are twice as many O(3,4) oxygens as O(5) oxygens. The n=3 phase Cu-O planes resonances are not narrowed by spinning. This suggests that one of the broadening mechanisms at the Cu-O plane oxygen sites is sample inhomogeneity.

These assignments are consistent with those for other HiT$_c$ ^{17}O NMR studies including the n=3 phase of $Tl_2Sr_2Ca_{n-1}Cu_nO_{4+2n}$ material to be discussed in Chapter 5 and are further justified by variable field measurements of this phase[22].

The parameters used to fit the room temperature static spectrum of the n=3 phase are shown in Table 4.1 and the simulation together with the experimental data is shown in figure 4.4. Only second order quadrupole and shift broadenings have been considered. This fitting gives further evidence for the correct assignment of the two distinct Cu-O planes. The central plane ^{17}O resonance can be fitted to a Gaussian lineshape with no electric field gradient, this is reasonable as the central plane is in a symmetric environment where only a small electric field gradient (or

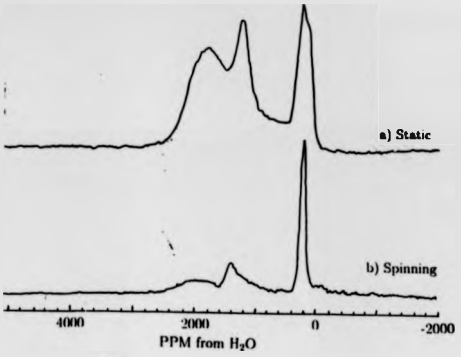

Figure 4.3. The ^{17}O NMR spectra observed for the n=3 phase a) static b) spinning.

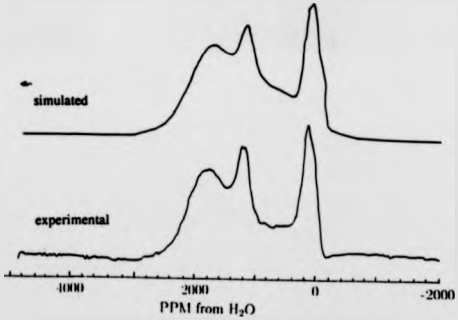

Figure 4.4. The simulated and experimental ^{17}O NMR spectra of the n=3 phase.

none at all) would be expected. To simulate the 1900ppm resonance both an electric field gradient (C_q=2.8MHz) and an axial shift are needed. This would be expected if this ^{17}O resonance was associated with the outer Cu-O planes. This modelling together with the spinning spectrum also show that there must be a large amount of inhomogeneity at the Cu-O plane sites as these resonances are very broad and are not narrowed by spinning whereas the major contribution to the width of the Sr-O plane resonance is a quadrupole interaction. It is not possible to find one unique set of parameters using data measured at a single magnetic field, however these parameters are in agreement with those obtained using measurements at a number of different magnetic fields[22].

Peak Posn. (ppm)	Model	Shift (ppm)	C_q (MHz)	ΔK (ppm)	η_q	Broadening (Hz)
275	Quad.	275	4.6	-	0.6	4000
1300	Gauss.	1300	-	-	-	8000
1900	Shift+Quad	1560	2.8	1200	0	20000

Table 4.1 Simulation parameters for the n=3 phase at room temperature.

The ½ ⇔ -½ transition is unaffected by first order quadrupole effects. An approximation to the quadrupole static quadrupole linewidth ($\Delta\nu_{st}$) can be derived from the second order term. With η=0, $\Delta\nu_{st}$ can be written as[23],

$$\Delta\nu_{st} = \frac{225}{576}\frac{C_q^2}{\nu_L}\frac{[I(I+1)-3/4]}{I^2(2I-1)^2} \qquad (4.1)$$

Where ν_L is the Larmor frequency. A C_q value of 2.8MHz at a Larmor frequency of 48.8MHz would result in a quadrupole width of 20kHz for a spin =5/2 system.

Since the outer Cu-O plane is of the order of 100kHz wide the dominant broadening mechanism is not quadrupole but the axial contribution ($\sim$ 60kHz)[22]. There is also a broadening due to the inhomogeneity of the sample at the Cu-O plane oxygen sites ($\sim$ 20kHz).

Changing the delay between the pulses in the spin-echo pulse sequence is an effective way of measuring the spin-spin lattice relaxation time. Figure 4.5 shows the ^{17}O spectra for the n=3 phase for delays of 50μs and 500μs. The change of lineshape of the Cu-O planes resonance also suggests an inhomogeneity of the structure since different regions of the resonance have different T_2 values.

4.2.2. Variable Temperature Shift Measurements.

Using, initially, the Bruker static probe and then later the more sophisticated Bruker low temperature probe and Oxford instruments cryostat measurements were taken between 400K and 5K. Figure 4.6 shows the observed spectra at room 293K, 120K, 60K and 5K for the undoped n=1 and the n=3 phase. All spectra were obtained using a spin-echo pulse sequence but at low temperatures (<50K) the lineshapes for the n=3 phase were similar to those obtained using a single pulse experiment. This is because the FIDs of the low temperature data are of the order of $\sim$ 10μs long and are not corrupted by the ringdown of the probe, unlike the shorter FIDs ($\sim$5μs) obtained at higher temperatures.

The position of the resonance of the Cu(1)-O(3,4) oxygens changes only slightly with temperature (if at all) for pure n=1 phase. However, the line width increases with decreasing temperature and changes from 2500ppm (FWHM) at room temperature to 3500ppm (FWHM) at 5K. The doped n=1 sample showed the same temperature dependence as the undoped n=1 sample. In both cases the line at

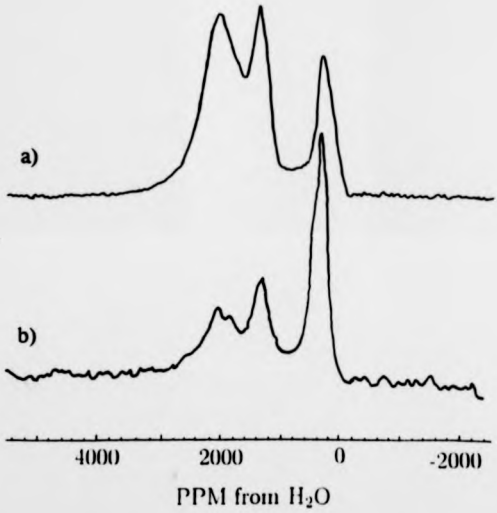

Figure 4.5. ^{17}O NMR spectra for a) 50μs and b) 500μs for the n=3 phase.

Figure 4.6. The ^{17}O NMR spectra for the n=1 and 3 phases at 293K, 120K, 60K and 5K.

~275ppm did not move or change width with temperature.

To locate the peak position of the ^{17}O resonance of the two Cu-O planes of the n=3 phase at each temperature a fitting program was used that fitted the data only to a Gaussian/Lorenztian lineshape. This does not fit the lineshape exactly but it does give the peak position accurately. Figure 4.7 is a plot of peak position for the ^{17}O resonance at the two Cu-O plane sites as a function of temperature for the n=3 phase. The position of the ^{17}O resonance associated with the Sr-O plane was found to be independent of temperature apart from demagnetisation effects (with a value of ~275ppm). At 85K all the lines have merged into one and it is not possible to resolve separate lines below this temperature.

For the central Cu-O plane this peak position is the isotropic shift whereas this is not true for the outer Cu-O plane where a large shift anisotropy (~1200ppm at room temperature) contributes to the linewidth. These measurements clearly show a strong temperature dependence of the ^{17}O resonances of the two distinct Cu-O planes above the superconducting transition temperature. T_c of the sample was found to be 96K, at the magnetic field of the NMR measurements (8.45T), as observed by a large change in the Q of the NMR coil. These results are quite startling in themselves but it would be useful to have some estimate of the spin component of the Knight shift (K_s) for the outer Cu-O plane as this is the only temperature dependent contribution to the observed shift.

If S_{peak} (the peak position of the resonance) is assumed to be equal to the parallel component of the measured shift (which is true for an axial lineshape) and ignoring quadrupole effects then,

$$S_{iso} = S_{peak}(T) - \tfrac{1}{2}\Delta K \qquad (4.2)$$

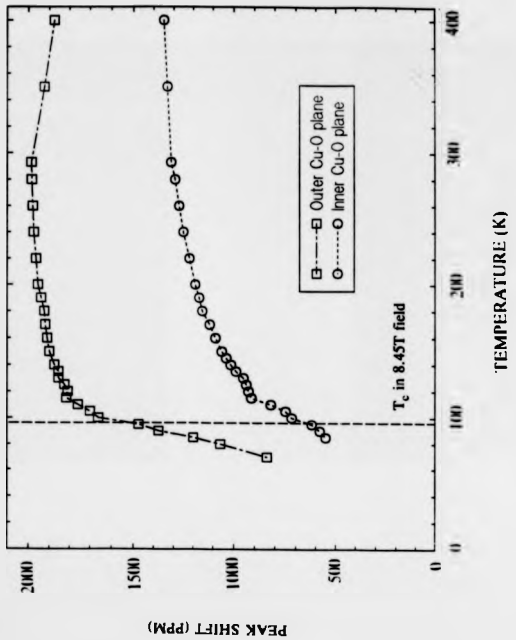

Figure 4.7. Peak position of the two Cu-O plane ^{17}O resonances for the n=3 phase as a function of temperature.

Where S_{iso} is the isotropic shift and ΔK is the axial contribution to the shift at room temperature. In this case ΔK is taken to be -1200ppm. Therefore the isotropic shift at room temperature is -400ppm less than the peak position. To calculate S_{iso} as a function of temperature it has been assumed that the axial contribution to the shift varies proportionally to S_{iso}, (this is known to be true for $YBa_2Cu_3O_{7-\delta}$[24]) so that,

$$S_{iso}(T) = S_{peak}(T) - \tfrac{1}{3}\Delta K \frac{S_{peak}(T)}{S_{peak}(RT)} \qquad (4.3)$$

Although this may not be strictly true it is a reasonable approximation since there will be some uncertainty in determining the temperature independent contribution (K_{orb}) to S_{iso}. S_{iso} as a function of temperature for the two Cu-O plane ^{17}O plane resonances is shown as figure 4.8. The isotropic shift is essentially the same as the peak position but with -400ppm subtracted at room temperature and -200ppm subtracted at 70K. No account of a temperature dependent electric field gradient has been made, since the quadrupole contribution to the broadening is small it has been assumed that any temperature dependence will also be comparatively small.

This isotropic shift is the sum of two components, the temperature dependent spin contribution to the Knight shift (K_s) and the temperature independent orbital contribution (K_{orb}). The temperature independent contribution to the shift cannot be determined by extrapolation to T=0, since demagnetisation effects due to the induced diamagnetic supercurrents need to be taken into account. In fact the resonance at 5K (which is just one broad line including the Sr-O plane oxygens) is at -280ppm indicating a diamagnetic shift of ~ 500ppm. Estimates of the

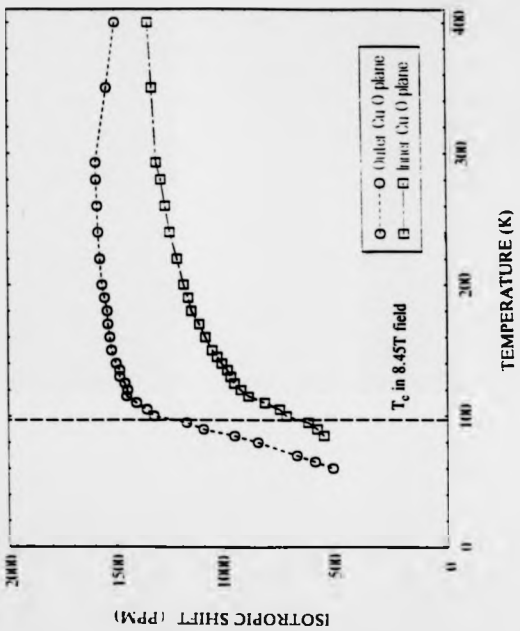

Figure 4.8. Isotropic position of the two Cu-O plane ^{17}O resonances for the n=3 phase as a function of temperature.

temperature independent contributions for the ^{17}O resonances of the Cu-O planes will be discussed in Chapter 6.

The temperature dependence of the ^{17}O spin component of the Knight shift associated with the two Cu-O planes is very different from NMR results observed for conventional superconductors. The central plane position slowly decreases from 300K with the decrease becoming quicker below 120K, by T_c the value of K_s is $\sim 1/2$ of its room temperature value. The temperature dependence of the outer Cu-O plane shows a different trend. The shift is almost temperature independent until 120K and then starts to drop rapidly and is $\sim 2/3$ of its room temperature value by T_c. The temperature dependencies of the shifts give no indication of the superconducting transition temperature. It is interesting that the two planes do not appear to be strongly coupled as the temperature dependencies of the shifts are rather different.

The Gaussian/Lorentzian lineshape fitting program does not model the lineshape exactly but it does give a measure of the line width. It was observed that this width for both planes followed the same trend with the width slowly increasing as the temperature decreases, reaching a maximum $\sim$ 115K and then starts to decrease (see figure 4.9). The mechanism for this increasing width is unknown but the decrease below 115K can be explained by the inhomogeneous contribution to the lineshape. The width would decrease if the shift of higher frequency (higher ppm) decreased more rapidly with temperature than shifts with lower frequency. Interestingly, the ratio of the width of one line divided by the width of the other is reasonably constant with temperature. This implies that the width changes of the outer Cu-O plane resonance are not due to changes in the axial contribution to the

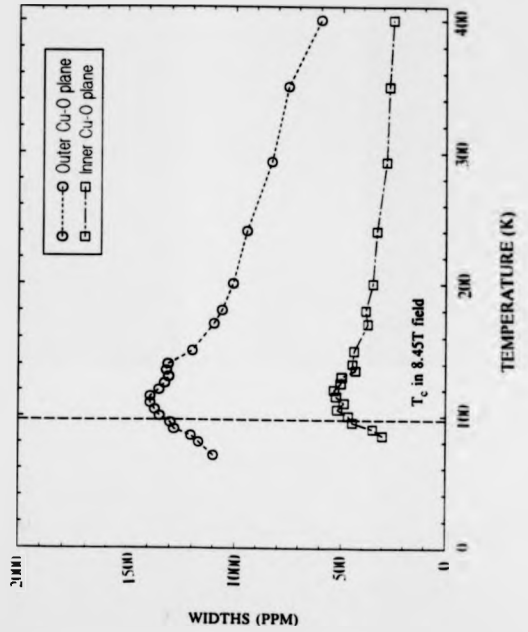

Figure 4.9. Approximate widths of the two Cu-O plane ^{17}O resonances for the n=3 phase as a function of temperature.

shift.

4.2.3. Variable Temperature Spin-lattice Relaxation Measurements.

All spin-lattice relaxation times were measured using a saturating comb of pulses as described in the Chapter 3. If the transmitter output is 500V (into 50Ω) and there are 80 pulses of 2μs each in the comb, then the amount of energy applied to the coil is of the order of 1 joule for each comb of pulses. This is a comparatively large amount of energy to put into the system. However, this does not cause sample heating. At 100K the rate of change of shift is 20ppm/K this gives a temperature scale resolution of $\sim$2K. Observation of the spectra during T_1 measurements at all temperatures revealed no change in peak positions, showing that heating effects must be negligible.

Tables 4.2 and 4.3 show the relaxation times measured at different temperatures. One experiment to sample the magnetization at a particular τ delay takes approximately one hour. Normally a guess would be made at the value of T_1 and the values for the τ delays set. Typically a T_1 measurement would consist of 7 different τ delays each run twice in a random order in an attempt to reduce errors due to the drift in gain of the amplifiers. To further decrease the error in these measurements, (which are mainly due to S/N), would require very much longer times which, when considering the possible drift in gain of the amplifiers, was not considered to be practical. Figure 4.10 shows the recovery of magnetisation as a function of τ delay for the 1900ppm line at room temperature. As the temperature decreased S/N improved, despite the increase in the relaxation times, due to the larger magnetisation produced at lower temperatures.

As can be seen from figure 4.11 $[T_1T]^{-1}$ varies with temperature in the

normal state (see also tables 4.2 and 4.3). This is not the case for the relaxation behaviour of the n=2 phase[18,19] or for the ^{17}O relaxation of the higher T_c HiT_c materials in general[19]. However, these materials do not show such a large change with temperature of the Knight shift in the normal state (apart from a few cases including the oxygen depleted $Y_1Ba_2Cu_3O_{7-\delta}$ to be discussed later).

Temp (K) ±2K	T_1 (s) ±10%	S_p (ppm) ±10ppm	S_{iso} (ppm) ±10ppm	T_1T (sK) ±10%
RT	0.021	1950	1590	6.15
200	0.036	1900	1560	7.20
140	0.055	1850	1500	7.70
110	0.080	1750	1410	8.80
100	0.10	1650	1330	10.0

Table 4.2 ^{17}O Shift and Relaxation data for the outer Cu-O plane.

Temp (K) ±2K	T_1 (s) ±10%	S_{peak} (ppm) ±10ppm	T_1T (sK) ±10%
RT	0.035	1300	10.26
200	0.067	1150	13.40
140	0.12	1020	16.80
110	0.26	820	28.60
100	0.40	700	40.0

Table 4.3 ^{17}O Shift and Relaxation data for the inner Cu-O plane.

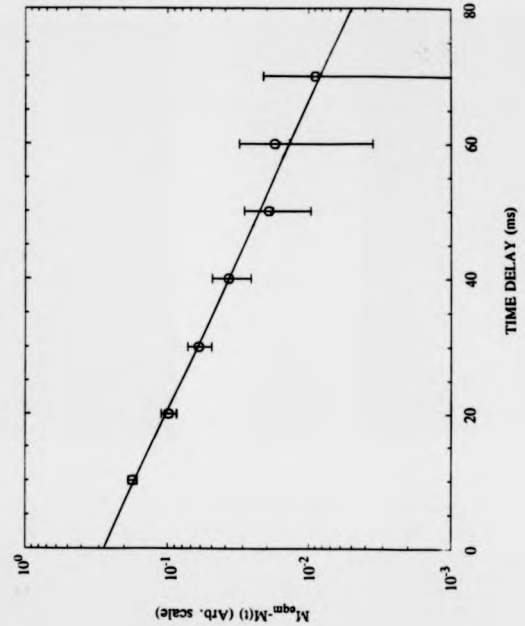

Figure 4.10. Relaxation data for the 1900ppm line of the n=3 phase at room temperature.

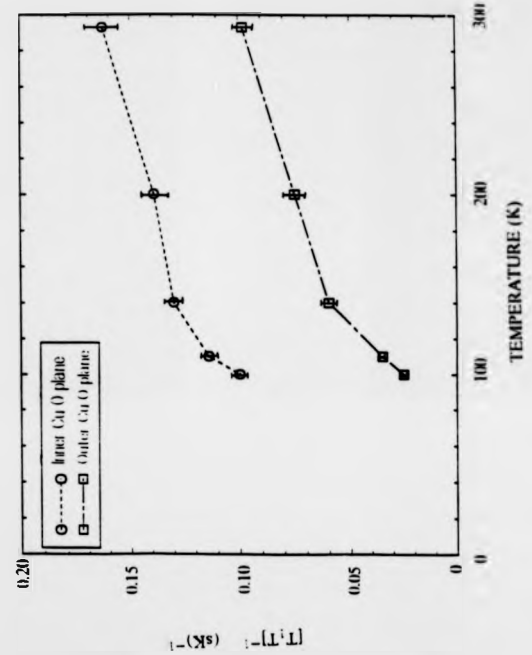

Figure 4.11. ^{17}O $[T_1T]^{-1}$ data as a function of temperature for the two Cu-O plane resonances of the $n=3$ phase.

T_1 in the superconducting state was not measured. No spin-lattice relaxation measurements were made for the Sr-O line (which has a very much longer T_1 estimated when analyzing the Cu-O plane data), or for the doped or undoped n=1 phases.

4.3. Discussion.

If the conduction electrons behave as a free electron gas the Korringa relationship would be valid ($K_s^2T_1T$ is constant). However the phenomenological application of an antiferromagnetic Fermi liquid theory to the lanthanum and yttrium superconductors by Millis, Monien and Pines[25-27] suggests that if antiferromagnetic correlations are large enough K_sT_1T is constant. One problem with testing both models is that K_{orb}, the temperature independent part of the shift is unknown. However, plots of $[T_1T]^{-1}$ and $[T_1T]^{-½}$ as a function of shift will give the orbital contribution for both models and the Korringa constant for the $[T_1T]^{-½}$ plot. To test both cases figures 4.12 and 4.13 show $[T_1T]^{-½}$ and $[T_1T]^{-1}$ respectively as a function of S_{iso} for the two planes of the n=3 phase. Despite the fact that K_s varies significantly with temperature above T_c both plots give reasonable fits to the data. For the Korringa plot the data for the outer and inner planes can be fitted reasonably well to a single line indicating that they both have similar values for the Korringa constant ($K_s^2T_1T$) and for K_{orb}. The values obtained are tabulated in table 4.4. The value of $K_s^2T_1T$ obtained for the two planes is $[1.50\pm0.08]*10^{-5}$ sK. This value is very close to the theoretical value of $1.43*10^{-5}$ sK for simple S type metals with no or little electron-electron interaction. It is also interesting to note the rather large values of K_{orb} obtained assuming a K_sT_1T relationship (see Chapter 6).

Figure 4.12. $[T_1T]^{-1/2}$ as a function of isotropic shift for the two Cu-O planes of the n=3 phase.

Figure 4.13. $[T_1T]^{-1}$ as a function of isotropic shift for the two Cu-O planes of the n = 3 phase.

Cu-O plane site	Value of $K_s^2T_1T$ [$*10^{-5}$ sK]	K_{orb} (ppm)	Value of K_sT_1T [$*10^{-4}$ sK]	K_{orb} (ppm)
Inner Plane O(5)	1.50±0.08	90±20	8.2±0.4	520±25
Outer plane O(3,4)			4.3±0.8	930±100

Table 4.4 $K_s^2T_1T$ and K_sT_1T data for ^{17}O in the Cu-O of the n=3 phase.

Trokiner et al[28] have also studied the ^{17}O NMR for the n=3 phase and they also report a temperature dependence of the shift above T_c (but do not report the any relaxation data). The temperature dependence of the peak position for the outer Cu-O plane oxygen site is similar in the two sets of data. However, the temperature dependence of the shift measured here for the central plane is different from their reported temperature dependence, showing no sharp decrease at 120K but a smoother decrease. It is worth noting that their work was carried out at a lower field (7.0T) and they report the peak position rather than the isotropic value. This slightly lower field is enough to lose resolution between the two Cu-O plane sites making determination of the peak positions difficult.

There are no other reports of spin-lattice relaxation measurements of the n=3 phase but the temperature dependence and spin-lattice relaxation times have been studied for the ^{17}O NMR resonance of the n=1 and 2 phases of the Bismuth superconductor[15]. In both cases the oxygen sites in the Cu-O planes have T_1T constant and a value of the Korringa constant close to the theoretical value (i.e. Korringa like behaviour in the normal state) however no large change in K_s is observed above T_c and so the data would also fit a K_sT_1T model.

Since there are similarities in the data obtained for the n=3 phases $Bi_2Sr_2Ca_2Cu_3O_{10}$ and $Tl_2Ba_2Ca_2Cu_3O_{10}$ further discussion of these results may be found in Chapter 6.

Chapter 4. References.

1. M. A. Subramarian, C. C. Toradi, J. C. Calabrese, J. Gopalakrihnan, K. J. Morrieaey, T. R. Askew, R. B. Flippen, U. Chowdry and A. W. Sleight: Science 239 (1988) 1015
2. J. M. Tarascon, W. R. McKinnon, P. Barboux, D. M. Hwang, B. G. Bagley, L. h. Greene, G. W. Hull, Y. LePage, N. Stoffel and M. Giroirel: Phys. Rev. B38 (1988) 8885.
3. M. Takano, J. Takada, K. Oda, H. Kitaguchi, Y. Miura, Y. Ikeda, Y. Tomii and H. Mazaki: Jap. J. App. Phys. 27 (1988) L1041.
4. M. Mizuno, H. Endo, J. Tsuchiya, N. Kijima, A. Sumiyama and Y. Oguri: Jap. J. App. Phys. 27 (1988) L1225.
5. S. A. Sunshine, T. Siemist, L. F. Schneemeyer, D. W. Murphy, R. J. Cava, B. Batlogg, R. B. van Dane, R. M. Fleeming, S. H. Glarum, S. Nakahara, R. Farrow, J. J. Krajewski, S. M. Zahurak, J. V. Waszczak, J. H. Marshall, P. Marsh, L. W. Rupp and W. F. Peck: Phys. Rev. B. 38 (1988) 893.
6. J. B. Shi, B. S. Chiou and H. C. Ku: Phys. Rev. B. 43 (1991) 13001.
7. J. Akimitsu, A. Yamazaki, H. Sawa and H. Fuijki: Jpn. J. Appl. Phys. 26 (1987) L2080.
H. Meda, Y. Tanaka, M. Fukitomi and T. Asano: Jpn. J. Appl. Phys. 27 (1988) L209.
8. R. J. Cava: Scientific American August (1990) 24.
9. R. M. Hazen, C. T. Prewitt, R. J. Angel, N. I. Ross, L. W. Finger, C. G. Hadidiacos, D. R. Veblen, P.J. Heaney, P. H. Hor, R. L. Meng, Y. Y. Sun, Y. Q. Wang, Y. Y. Xue, Z. J. Huang, L. Gao, J. Bechtold and C-W. Chu: Phys. Rev. Lett 60 (1988) 1174.
10. M. A. Subramanian, C. C. Torardi, J. C. Calabrese, J. Gopalakrishnan,K. J. Morrissey, T. R. Askew, R. B. Flippen, U. Chowdhry and A. W. Sleight: Science 239 (1988) 1015.
11. G. S. Grader, E. M. Gyorgy, P. K. Gallagher, H. M. O'Bryan, D. W. Johnson, S. Sunshine, S. M. Zahurak, S. Jin and R. C. Sherwood: Phys. Rev. B. 38 (1988) 757.
12. W. Carrilo-Cabera and W. Gopel: Physica C. 161 (1989) 373.
13. Y. Gao, P. Lee, P. Coppens, M. A. Subramanian and A. W. Sleight: Science 24 (1989) 954.
14. W. M. Stobbs, S. B. Newcomb, R. E. Dunin-Borkowski and S. E. Male: Superconductor Sci. and Tech. 3 (1990) 414.
15. L. Reven, J. Shore, S. Yang, T. Duncun, D. Schwartz, J. Chung and E. Oldfield: Phys.Rev.B 43 (1991) 10466.
16. A. Trokiner, L. LeNoc, J. Schneck, A. M. Pouguet R. Mellet, J. Primot, H. Savary, Y. M. Gao and S. Aubry: Phys.Rev.B 44 (1991) 2426.
17. E. Oldfield, C. Coretsopoulos, S. Yang, L. Reven, H. C. Lee, J. Shore, O. H. Han and E. Ramli: Phys. Rev. B. 40 (1989) 6832.
18. Y. Kitaoka, Y. Berthier, P. Butaud, M. Horvatic, P. Segransan and C. Berthier: Physica C 162 (1989) 195.
19. P. C. Hammel, M. Takigawa, R. M. Heffner, Z. Fisk, K. C. Ott and J. D. Thompson: Phys.Rev.Lett. 63 (1989) 1992.
20. J. R. Laverty, A. D. Caplin and S. E. Male: Physica C 162-164 (1989) 1165.

21. Y. LePage, W. H. McKinnon, J. M. Tarascon and P. Barboux: Phys. Rev. B 40 (1989) 6810.
22. R. Dupree, Z. P. Han, A. P. Howes, D. McK. Paul, M. E. Smith and S. Male: Physica C 175 (1991) 269.
23. 'Principles of Nuclear Magnetism', A. Abragam (Oxford 1985)
24. M. Takigawa, A. P. Reyes, P. C. Hammel, J. D. Thompson, R. M. Heffner, Z. Fisk and K. C. Ott: Phys.Rev.B. 43 (1991) 247.
25. H. Monien, P. Monthoux and D. Pines: Phys. Rev. B 43 (1991) 275.
26. H. Monien, D. Pines and M. Takigawa: Phys. Rev. B 43 (1991) 258.
27. A. J. Millis, H. Monien and D. Pines: Phys. Rev. B 42 (1990) 167.
28. A. Trokiner, L. LeNoc, J. Schneck, A. M. Pouguet R. Mellet, J. Primot, H. Savary, Y. M. Gao and S. Aubry: Phys.Rev.B 44 (1991) 2426.

Chapter 5. The n=3 Phase of the Thallium Superconductor $Tl_2Ba_2Ca_{n-1}Cu_nO_{4+2n}$.

5.1. Introduction.

Many high temperature superconductors have been fabricated containing thallium since the initial discovery of a Tl-Ba-Ca-Cu-O system with a transition temperature of 110K[1-5]. Four of these thallium based superconductors form a family with the general formula $Tl_2Ba_2Ca_{n-1}Cu_nO_{4+2n}$ with n=1 to 4. These can all be made as single phase compounds. T_c increases with n to n=3 and then decreases (T_c of 85k, 110K, 125K, and 112K for n=1,2,3 and 4 respectively[6]). The n=3 phase was first discovered in 1988[7] and the superconducting properties were later improved by Parkin et al[8], who increased the superconducting transition temperature to 125K. The unit cell of the n=3 phase is orthorhombic and comprises of two thallium-oxygen (Tl-O(1)), two barium-oxygen (Ba-O(2)) planes and three copper-oxygen (Cu-O(3) and Cu-O(4,5)) planes with two calcium planes between them. This is very similar to the structure of the $Bi_2Sr_2Ca_2Cu_3O_{10}$ material but with no modulation of the Tl-O distance and with the Cu-O(3,4) plane less buckled (See figure 5.1).

There have been a large number of NMR and NQR studies of all three phases of $Tl_2Ba_2Ca_{n-1}Cu_nO_{4+2n}$ since ^{205}Tl[9-13] as well as $^{63,65}Cu$[14] and ^{17}O[14-16] are accessible to NMR. ^{205}Tl and $^{63,65}Cu$ NMR and NQR studies have been carried out on the n=1,2 and 3 phases but the only ^{17}O NMR work reported has been on the n=1 and 2 phases.

Since there are structural similarities between the n=3 phases of the $Tl_2Ba_2Ca_{n-1}Cu_nO_{4+2n}$[17] and the $Bi_2Sr_2Ca_{n-1}Cu_nO_{4+2n}$[18] an ^{17}O NMR study of

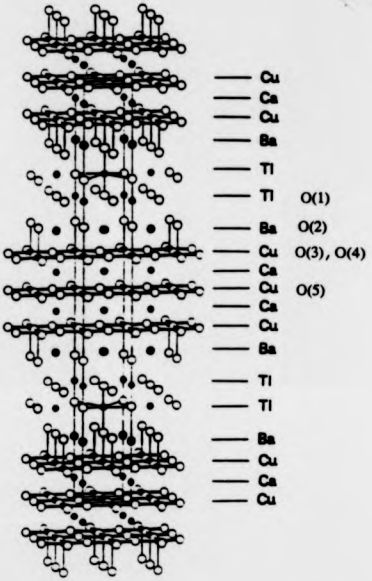

Figure 5.1. The structure of $Tl_2Ba_2Ca_2Cu_3O_{10}$ (ref 17).

the n=3 phase of the Thallium superconductor was thought to be worthwhile to compare with the data obtained for the n=3 phase of Bismuth superconductor.

The n=3 phase sample used in this study was made at the IRC for Superconductivity at the University of Cambridge by R.S. Liu and P.P. Edwards. The sample was prepared for a study of materials with the composition $Tl_{2-x}Ba_2Ca_{2+x}Cu_3O_{10}$ as it had been suggested that Ca could be substituted for Tl[19]. The sample was made by mixing Tl_2O_3, BaO_2, CaO and CuO in the correct stoichiometric proportions and then pressed into pellets. The pellets were then wrapped in silver foil to prevent the loss of thallium and were oxygen annealed in a furnace at 910°C for 3 hours and then cooled back to room temperature[20]. The sample chosen for the experiments had a composition of $Tl_{1.8}Ba_2Ca_{2.2}Cu_3O_{10}$ and a superconducting transition temperature of 117K measured by A.C susceptibility (the highest T_c for all the samples manufactured). X-ray diffraction showed no sign of a minority phase however A.C. susceptibility measurements of the sample after ^{17}O enrichment suggest that a small fraction of the n=2 phase is present.

^{17}O enrichment was carried out as described in Chapter 3 on approximately 15g of material at a temperature of 450°C for 16 hours and then slowly cooled to room temperature. A calculation of oxygen volumes in the furnace and sample implies that if the ^{17}O is distributed uniformly then approximately 8% of the oxygen in the sample would be ^{17}O. A.C. susceptibility measurements showed that the transition temperature had decreased by 3K to 114K presumably due to a slight oxygen deficiency, excess or inhomogeneity.

After initial ^{17}O NMR measurements had been completed it was discovered (by R.S. Liu) that a vacuum anneal at a temperature of 750°C for 10 days

increased the superconducting transition temperature of the n=3 phase[22]. The sample was returned to the IRC for this anneal. After this the transition temperature had increased to 124K and no evidence of the n=2 phase could be observed by A.C. susceptibility measurements (see figure 5.2). Fortunately during this anneal little or no ^{17}O was removed from the sample as was shown by the S/N of later NMR experiments.

5.2. ^{17}O NMR Results.

5.2.1. Room Temperature Results and Site Assignment.

The room temperature ^{17}O NMR spectra obtained using a spin-echo pulse sequence were made on an unaligned powdered sample of the n=3 phase of the Thallium superconductor before and after the vacuum anneal (these spectra are shown in figure 5.3). The spectra show the same trends as for other high temperature superconductors with a peak at ~280ppm (within the region for diamagnetic oxides) and another peak at ~1400ppm (within the region of Cu-O planes). There is very little difference between the before and after anneal results apart from a slight narrowing of the Cu-O plane resonance by ~35ppm however the centre of the resonances are at the same position (± ~10ppm). This slight narrowing is probably caused by structural ordering and the removal of some dislocations and impurities during the anneal as this would increase the homogeneity of the sample. The difference in relative amplitudes of the 280ppm and 1400ppm resonance is most likely caused again by this reorganisation of the oxygen distribution.

^{17}O NMR data at different magnetic fields has shown that the line observed at 280ppm in the Thallium n=2 phase can be fitted to two resonances one from

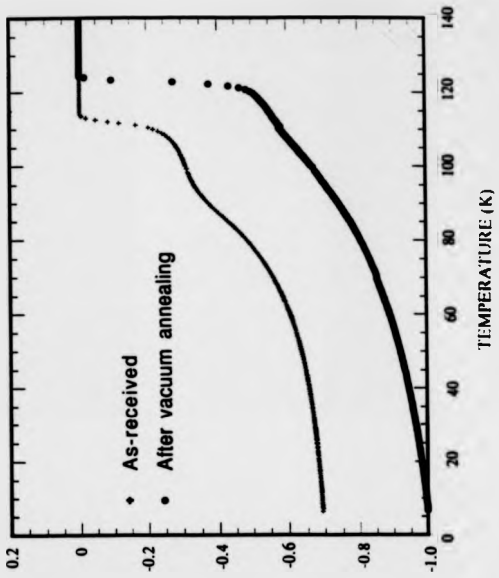

Figure 5.2. The A.C. Susceptibility of the Thallium sample before and after the vacuum anneal. (Measured by R. S. Lui at the IRC, Cambridge).

the Tl-O plane and the other from the Ba-O plane[16]. It would be reasonable to suppose that this is also true for the n=3 phase as it is possible to describe this lineshape at 280ppm using the same parameters as used for the n=2 phase[16] (see table 5.1 for parameters used). Two resonances were expected in the region of Cu-O plane ^{17}O shifts, as was found for the $Bi_2Sr_2Ca_2Cu_3O_{10}$ sample. The line at 1400ppm could be composed of two resonances as there is a slight shoulder on the low frequency (right side) of the lineshape. The lineshape does not alter apart from in the amplitude observed during a T_1 measurement. This implies that all of the lineshape has the same value of T_1. Changing the delay in the normal spin-echo experiment reveals that the line at higher frequency (higher ppm) has a slightly shorter spin-spin relaxation time (T_2). This can be seen in figure 5.4 where delays of 30μs and 500μs have been used for the τ-delay between pulses in the spin-echo.

The data cannot be fitted to one unique set of parameters and ideally data from a range of magnetic fields is required. However, a reasonable fit can be obtained using a small electric field gradient, a small shift anisotropy and a large dipolar broadening value for one of the planes and a Gaussian line shape for the other plane. Figure 5.5 shows the experimental data and the simulation of the 1400ppm and 280ppm resonances and Table 5.1 presents the fitting parameters.

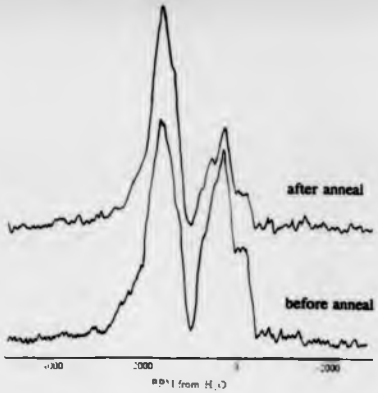

Figure 5.3. The ^{17}O NMR Resonance of the Thallium sample at room temperature.

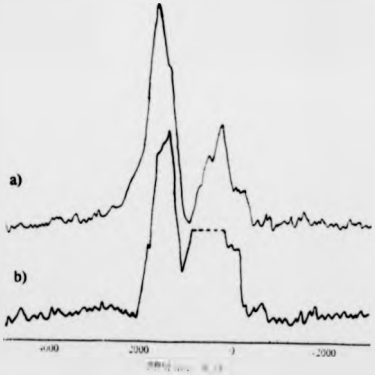

Figure 5.4. Comparison of the ^{17}O NMR resonance for the Thallium sample using a spin-echo with a) 50μs and b) 500μs delay between pulses.

Peak Posn. (ppm)	Model	Shift (ppm)	C_q (MHz)	ΔK (ppm)	η_q	Broadening (Hz)
280	Quad.	300	4	-	0.1	4000
280	Quad.	350	5.5	-	0.3	4000
1400	Gauss.	1200	-	-	0	10000
1400	Shift+ Quad	1400	>2	400	0	10000

Table 5.1 Simulation parameters for the room temperature spectrum of the Thallium n=3 phase.

The Gaussian and anisotropic lines are assigned to the central Cu-O(3) plane and to the outer Cu-O(4,5) plane respectively. This assignment is based upon what is known about the crystal structure of the phase (i.e. one symmetrical environment and one not), the similarities to the Bismuth n=3 phase and that the simulation requires the anisotropic lineshape to have approximately twice the area of the Gaussian lineshape (there are twice as many outer planes as central planes).

As is the case for the n=3 phase of the Bismuth superconductor, it would appear that their is a contribution to broadening of the Cu-O resonance from sample inhomogeneity in the Cu-O planes. The spectra obtained by spinning at 10-14kHz and using a spin-echo pulse sequence with the spacing between the echo pulses equal to the period of rotation showed no sign of narrowing any of the resonances (figure 5.6). The Tl-O and Ba-O plane resonances are also unaffected by spinning unlike the Sr-O plane of the n=3 phase of the Bismuth material (Chapter 4).

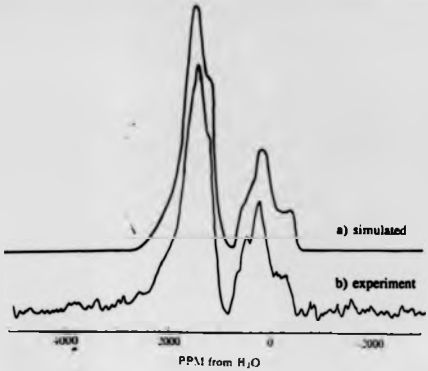

Figure 5.5. Simulated data for the Thallium sample (a) with the experimental data (b) at room temperature.

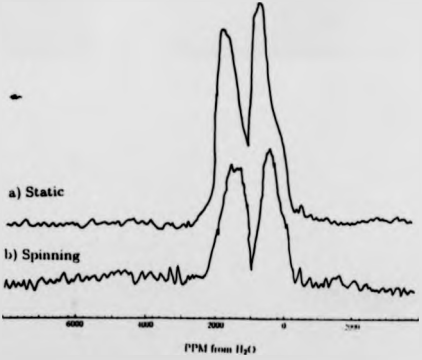

Figure 5.6. Static a) and spinning b) ^{17}O NMR resonances of the Thallium sample at room temperature (spinning at 14KHz).

5.2.2. Variable Temperature Shift Measurements.

The Bruker probe and Oxford instruments cryostat were used for all experiments. Liquid nitrogen and the 6mm coil were used down to a temperature of 80K and liquid helium and the 10mm coil were used below this temperature to avoid the problems of electrical breakdown of the 6mm coil when using helium. The use of different cryogens does not appear to affect the data as measurements up to 120K using either nitrogen or helium gave the same results.

For the sample before and after the vacuum anneal the Tl-O and Ba-O resonances showed no temperature dependence apart from demagnetisation effects at low temperatures.

Spectra recorded at room temperature (293K), 200K, 80K and 5K are shown for the sample before annealing in figure 5.7. The Tl-O and Ba-O resonances are partially saturated due to the repetition period used (100ms) for all experiments. Figure 5.8a shows the temperature dependence of the peak position of the Cu-O plane resonance as a function of temperature for the sample before the vacuum anneal. The resonance starts to decrease smoothly in frequency just below room temperature. There appears to be no anomalous behaviour in the temperature dependence near T_c where the value of the shift is approximately 2/5th of its room temperature value. By ~ 120K the Cu-O, Tl-O and Ba-O resonances have all merged into one. Since the Tl-O and Ba-O resonances do not start to move until below ~ 100K demagnetization effects due to induced supercurrents do not occur above this temperature. The 5K spectrum is at ~ -200ppm and is ~ 2000ppm wide. The width presumably is due to the diamagnetic shielding supercurrents.

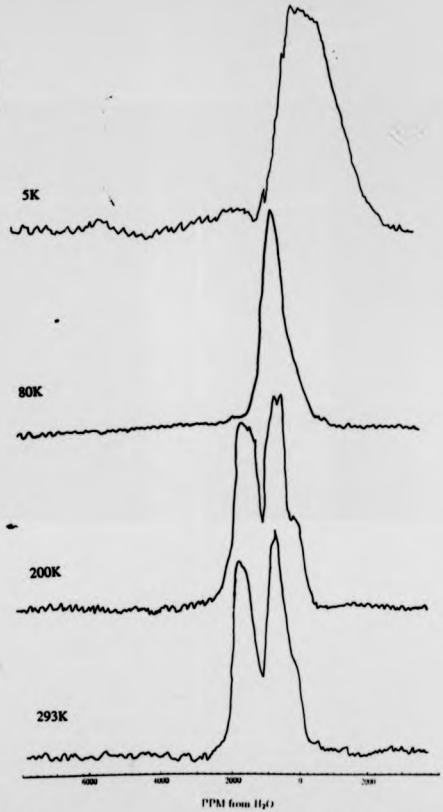

Figure 5.7. The Thallium sample ^{17}O spectra at 293K, 200K, 80K, and 5K.

Figure 5.8b shows the temperature dependence of the Cu-O plane peak position two days after the vacuum anneal. Again the value of the position of the resonance starts to decrease just below room temperature but the decrease is much quicker than for the sample before vacuum annealing and the shift is only 1/10th of its room temperature value by T_c (in zero field). Again the dependence is smooth with the rate of decrease of shift increasing at ~ 180K and then decreasing at ~ 90K. There is no indication of T_c. All resonances have merged together by ~ 120K and the Tl-O and Ba-O resonances do not move until below ~ 100K.

Figure 5.9a is the temperature dependence of the peak position of the Cu-O planes of the sample taken 14 days after the results of figure 5.8b which are shown again for comparison as figure 5.9b. Both temperature dependencies are vary similar down to ~ 130K (just a few degrees above T_c), however, there is some difference below this temperature. At T_c the position of the shift is 1/5th of its room temperature value. The resonances merge together at 120K and the Tl-O and Ba-O resonances do not start to move above ~ 100K.

It is difficult to explain the difference between the two sets of data for the same sample after the vacuum anneal. It takes a long time for the sample to come into equilibrium after the probe has been cooled. In fact it was found that once the cryostat had been cooled to 100K, which takes approximately one hour, the sample does not come in to equilibrium for another 30 minutes as was shown by the Q of the coil still changing. This was known however, and taken into account with similar waiting periods for both experiments. A more likely explanation is that some of the ordering of the oxygen atoms after the vacuum anneal has been lost or rearranged in the time between the two experiments and the sample is not

Figure 5.8. The ^{17}O MNR peak position associated with the Cu-O planes a) before the vacuum anneal and b) a few days after the anneal both as a function of temperature.

Figure 5.9. The ^{17}O MNR peak position associated with the Cu-O planes a) 14 days after the measurements made just after the vacuum anneal (shown again as b)) both as a function of temperature.

stable in oxygen stoichiometry. The sample was stored in a sealed sample container between experiments.

For all three temperature dependence experiments there appeared to be no appreciable change in the width of the Cu-O plane resonance.

5.2.3. Variable Temperature Spin-lattice Relaxation Time Measurements.

The Bruker low temperature probe with a 6mm coil and the Oxford instruments cryostat using liquid nitrogen as the cryogen were used for all spin-lattice relaxation measurements. T_1 measurements using an inversion recovery did not result in the inversion of all the magnetization (the same as for the Bismuth sample). A saturating comb pulse program was again used with 80 pulses of 2μs length with a spacing of 1ms between them. As before to measure T_1 only the last 50% of the recovery of the magnetization was observed. Heating of the sample by the saturating comb was not found to be a problem, as the Cu-O plane resonance did not change position during measurements indicating no change of temperature of the sample.

Two sets of T_1 data at different temperatures were measured, one set for the un-annealed sample (table 5.2) and one set after annealing (table 5.3), at the same time that the final set of variable temperature shift measurements were taken.

Temperature (K) ±2K	Position of Peak (ppm) ±10ppm	T_1 (ms) ±10%
293	1420	27
200	1330	45
150	1060	100
135	920	140
120	680	400
105	410	>2000

Table 5.2 ^{17}O NMR Shift and Spin lattice relaxation data for the Cu-O plane site of the un-annealed Thallium n=3 sample.

Temperature (K) ±2K	Position of Peak (ppm) ±10ppm	T_1 (ms) ±10%
293	1420	30
200	1200	65
150	960	150
130	420	1000

Table 5.3 ^{17}O NMR Shift and Spin lattice relaxation data for the Cu-O plane site of the annealed Thallium n=3 sample.

As was found with the Bismuth sample S/N improved with decreasing temperature despite the longer spin-lattice relaxation times. Typically 1-2 hours were required at each delay for sufficient S/N. $[T_1T]^{-1}$ as a function of temperature is shown as figure 5.10.

5.3. Discussion.

There appears to be no ambiguity about the site assignment for the ^{17}O NMR resonance obtained for the Thallium n=3 phase. It is interesting that the isotropic shifts of the two Cu-O planes are so close together compared with the

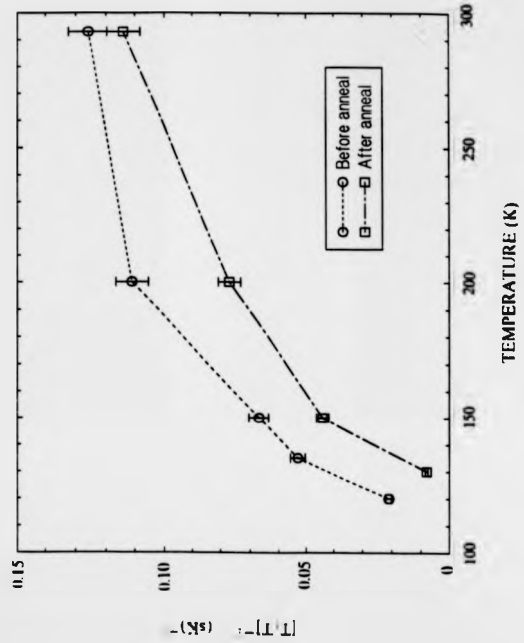

Figure 5.10. $[T_1T]^{-1}$ as a function of temperature for the ^{17}O of the Cu-O planes before and after the vacuum anneal.

results for the Bismuth n=3 sample. It is difficult to find a unique set of fitting parameters from measurements at just one magnetic field. The fit at the field used here (8.45T) suggests a much smaller electric field gradient and a smaller axial contribution to the shift for the outer Cu-O plane than for the Bismuth n=3 phase. Using ^{63}Cu NQR[23] it has been shown that the electric field gradients at the copper sites for both Cu-O planes for the n=3 phase of the Thallium phase are smaller than the electric field gradients at the copper sites for both Cu-O planes of the n=3 phase of the Bismuth phase. This, and the smaller axial shift are possibly explainable by the fact that the outer Cu-O(4,5) plane is considerably more buckled in the Bismuth n=3 phase than it is for the Cu-O(4,5) plane of the Thallium n=3 phase[7,18], this may lead to a smaller e.f.g. The Cu-O(3) central plane is flat for both materials.

The similarity of the positions may be due to some sort of coupling between the two Cu-O planes and the similarity of the planes. A difference in the temperature dependence of the two Cu-O plane oxygen sites would be seen at least by a change of width of the resonance, if not by the observation of two distinct resonances. However, there appears to be no change in width. This suggests that both planes have a common susceptibility. This would also explain why a single T_1 value can describe both planes.

Near T_c to approximately 10K below T_c (130K-110K) the S/N was found to be worse than expected. This must be caused by the sample going into the superconducting state and expelling magnetic flux. This transition however is not seen in the temperature dependence of the shift for the Cu-O plane site oxygens. The T_c of the sample in the field could not be measured by the change in Q of the

coil as no large change of Q was observed. This is strange since this measurement was possible for the Bismuth material. It is worth noting that there are no structural changes to the crystal structure at T_c[24].

As stated in Chapter 2 there are good reasons for wanting to know the relationship between the spin component of the Knight shift and the spin-lattice relaxation time. To test the Korringa relationship and the MMP suggestion, $[T_1T]^{-1/4}$ and $[T_1T]^{-1}$ have been plotted as a function of peak position of the Cu-O plane resonance for the pre-annealed and after annealed measurements (see figures 5.11, 5.12, 5.13,5.14). The deduced values of $K_s^2T_1T$ and K_sT_1T and the corresponding values of the temperature independent component of the observed shift (K_{orb}) are shown in table 5.4.

	Value of $K_s^2T_1T$ [$*10^{-5}$ sK]	K_{orb} (ppm)	Value of K_sT_1T [$*10^{-4}$ sK]	K_{orb} (ppm)
Before Vacuum Anneal	1.27 ± 0.06	141 ± 49	7.1 ± 2.9	549 ± 24
After vacuum anneal	1.54 ± 0.07	96 ± 48	9.0 ± 1.6	450 ± 120

Table 5.4 $K_s^2T_1T$ and K_sT_1T data for ^{17}O in the Thallium n=3 sample.

Apart from the vacuum annealed $[T_1T]^{-1}$ vs K_s plot (figure 5.13) all plots give reasonable good fits and there is little justification for suggesting that one type of plot gives a better fit than any other. What is interesting is that the Korringa constant obtained is close to the theoretical value if a Korringa like relationship is assumed. The values of the Korringa constant are different for the measurements before and after the anneal, suggesting a change to the relaxation process.

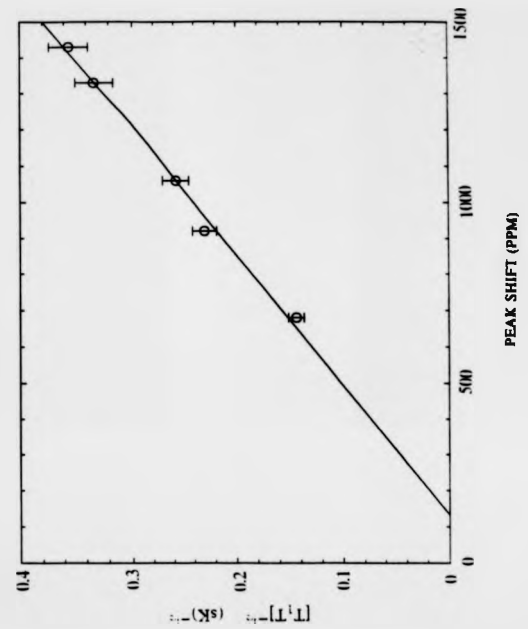

Figure 5.11. $[T_1T]^{-1/2}$ as a function of peak position shift for the ^{17}O of the Cu-O planes before the vacuum anneal.

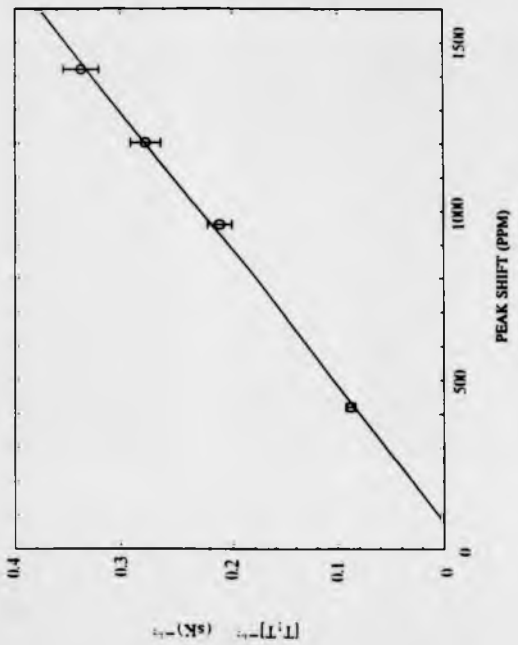

Figure 5.12. $[T_1T]^{-1/2}$ as a function of peak position shift for the ^{17}O of the Cu-O planes after the vacuum anneal.

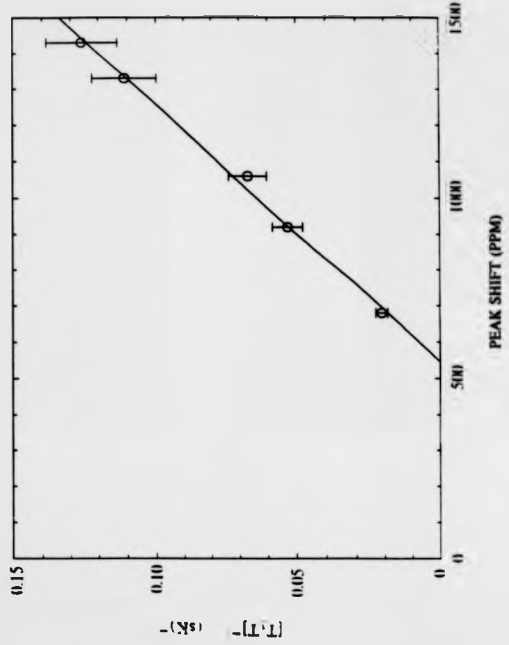

Figure 5.13. $[T_1T]^{-1}$ as a function of peak position shift for the ^{17}O of the Cu-O planes before the vacuum anneal.

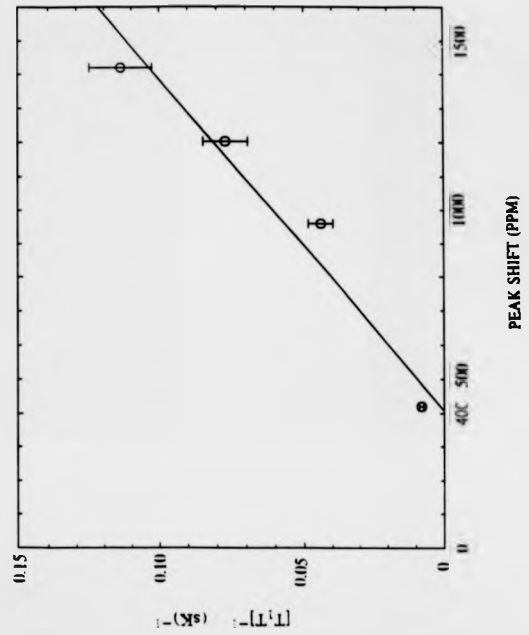

Figure 5.14. $(T_1T)^{-1}$ as a function of peak position shift for the ^{17}O of the Cu-O planes after the vacuum anneal.

Another interesting point to note is the large value of the temperature independent (K_{orb}) part of the observed shift for the $[T_1T]^{-1}$ vs K_s plot. For the sample before annealing the value of K_{orb} corresponds to the measured shift observed at a temperature of ~ 110K for the Cu-O plane ^{17}O temperature dependence. Since the Tl-O and Ba-O plane resonances do not move above a temperature of ~ 100K demagnetization effects are not important until below this temperature. It seems unlikely therefore, that the shift in position of the Cu-O plane resonance above this temperature is entirely due to demagnetisation effects. This suggests that the value of K_{orb} obtained from the K_sT_1T plot is too high. The same is true for the results obtained for the sample after vacuum anneal, since K_{orb} from the plot, assuming K_sT_1T relationship, is larger than observed shifts before demagnetization effects become important. The independent contribution to the observed shift if a $K_s^2T_1T$ relationship is assumed is a much smaller value than that assuming a K_sT_1T relationship. The values obtained are very similar to those obtained for the n=3 Bismuth sample. The Cu-O plane resonance is only at this position after demagnetization effects become important.

For the un-annealed sample T_1 measurements just below T_c were found to be difficult because of the poor S/N. However, it was possible to measure a lower limit to T_1 just below T_c as 2s. There does not appear to be any BCS like enhancement of T_1 just below T_c.

There is little temperature dependence of the shift in the thallium n=2 phase above T_c and only below T_c does the shift quickly decrease[15]. A number of ^{205}Tl studies have been carried out on the n=3 phase[9,14] and the ^{205}Tl shift is essentially temperature independent above and across the transition temperature

but the thallium is in the Tl-O planes ^{205}Tl does not sample the susceptibility of the Cu-O planes directly but only by a hyperfine interaction between the copper or oxygen nuclei and the thallium nuclei.

Since there are many similarities of these results with those obtained for the Bismuth n=3 material further discussion of these results will be made together with those of the Bismuth material in Chapter 6.

Chapter 5. References.

1. Z. Z. Sheng and A. M. Hermann: ,Nature 332 (1988) 138.
2. R. M. Hazen, L. W. Finger, R. J. Angel, C. T. Prewitt, N. L. Ross, C. G. Hadidicos, P. J. Heaney, D. R. Veblen, Z. Z. Sheng, A. El Ali and A. M. Hermann: Phys. Rev. Lett. 60 (1988) 1657.
3. H. Ihara, R. Sugise, M. Hirabagashi, N. Terada, M. Jo, K. Hayashi, A. Negishi, M. Tokumoto, Y. Kimura and T. Shimomura: Nature 324 (1988) 510.
4. C. C. Torardi, M. A. Subramanian, J. C. Calabrese, J. Gopalakrihnan, K. J. Morriesey, T. R. Askew, R. B. Flippen, U. Chowdry and A. W. Sleight: Phys. Rev. B. 38 (1988) 225.
5. L. Gao, Z. L. Huang, R. L. Meng, P. H. Hor, J. Bechtold, Y. Y. Sun, C-W. Chu, Z. Z. Sheng, A. M. Herman: 332 (1988) 623.
6. 16. R. J. Cava: Scientific American August (1990) 24.
7. C. C. Torardi, M. A. Subramanian, J. C. Calabrese, J. Gopalakrihnan, K. J. Morriesey, T. R. Askew, R. B. Flippen, U. Chowdry and A. W. Sleight: Science 240 (1988) 631.
8. S. S. Parkin, V. Y. Lee, P. T. Wu, Y. C. Chen and C. T. Chang: Jpn. J. Appl. Phys. 27 (1988) L1206.
9. A. K. Rajarajan, K. V. Gopalakrishnan, R. Vijayaraghavan and L. C. Gupta: Solid State Comm. 69 (1989) 213.
10. F. Hentsch, N. Winzek, M. Mehring, Hj. Mattausch, A. Simon and R. Kremer: Physica C 165 (1990) 485.
11. F. Hentsch, N. Winzek, M. Mehring, Hj. Mattausch, R. Kremer and A. Simon, Physica C 168 (1990) 327.
12. J. C. Jol, D. Reefman, H. B. Brom, T. Zetterer, D. Hahn, H. H. Otto and K. F. Renk: Physica C. 175 (1991) 12.
13. H. B. Brom, D. Reefman, J. C. Jol, D. M. de Leeuw, W. A. Groen: Phys. rev. B. 41 (1990) 7261.
14. S. V. Verkhovski, Y. I. Zhdanov, K. N. Mikhalyov, B. A. Aleksashin, V. I Ozhogin, A. Y. Yakubovski and L. D. Shustov: Physica B 165 (1990) 1311.
15. L. Reven, J. Shore, S. Yang, T. Duncun, D. Schwartz, J. Chung and E. Oldfield: Phys.Rev.B 43 (1991) 10466.
16. E. Oldfield, C. Coretsopoulos, S. Yang, L. Reven, H. C. Lee, J. Shore, O. H. Han and E. Ramli: Phys. Rev. B. 40 (1989) 6832.
17. B. Morosin, D. S. Ginley, E. L. Venturini, R. J. Baugham, C. P. Tiggges: Physica C. 172 (1991) 413.
18. W. Carrilo-Cabera and W. Gopel: Physica C. 161 (1989) 373.
19. K. Hiraga, D. Shindo, M. Hirabayashi, M. Kikuvhi, N. Kobayashi and Y. Syono: Jpn. J. Appl. Phys. 27 (1988) L1848.
20. R. S. Liu and P. P. Edwards: Physica C. 179 (1991) 353.
21. C. Martin, A. Maignan, J. Provost, C. Michel, M. Herview, R. Tournier and B. Raveu: Physica. C 168 (1990) 8.
22. R. S. Liu J. L. Tallon and P. P. Edwards: Physica C. 182 (1991) 119.
23. T. Oashi, K. Kumagai, H. Nakajima, M. Kikuchi, Y. Syono: Physica C 161 (1989) 367.
24. D. E. Cox, C. C. Torardi, M. A. Subramanian, J. Gopalakrishnan and A. W. Slieght: Phys. Rev. B. 38 (1988) 6624.

Chapter 6. Discussion.

6.1. Introduction.

It is intended here to discuss the results of the ^{17}O NMR experiments for the $Bi_2Sr_2Ca_2Cu_3O_{10}$ and $Tl_2Ba_2Ca_2Cu_3O_{10}$ superconductors of Chapters 4 and 5 together, as the results for the two materials are in some respects very similar. It is worth noting the interesting features of the results which need further discussion and comparison with the NMR results obtained for other HiT_c materials and nuclei. These are,

1) The temperature dependence in the normal state of the ^{17}O NMR resonances associated with the Cu-O planes of the two materials.

2) The relaxation behaviour and how it is related to the Knight shift.

3) The value of the temperature independent component of the shift (K_{orb}) for each resonance.

To avoid too much confusion each topic will be discussed (almost) separately.

6.2. The Shift Measurements.

The room temperature isotropic shifts for the two planes of the n=3 Bismuth phase are ~ 1560ppm and ~ 1300ppm and the T_c of the sample is 110K. The room temperature isotropic shifts for two Cu-O planes of the n=3 Thallium sample before and after annealing are at ~ 1400ppm and the T_c of the sample before the anneal was 114K and after 124K. The fully oxygenated $Y_1Ba_2Cu_3O_7$, the oxygen deficient $Y_1Ba_2Cu_3O_{7-\delta}$ and $La_{1.85}Sr_{0.15}CuO_4$ all have, the same value of the oxygen hyperfine coupling constant[1] (within experimental error). The Knight shift is proportional to the spin susceptibility and therefore proportional to the electronic density of states at the Fermi level (DOS)[2]. If it is supposed that

both the n=3 Thallium and Bismuth samples have the same value of oxygen hyperfine coupling constant as each other, (but not necessarily the same as for the other materials), then this implies that the DOS in the normal state is less for the Thallium sample than for the Bismuth sample. This would be in contrast to the conventional materials where higher T_c superconductors have higher DOS[3,4]. This is also true for $YBa_2Cu_3O_7$ (T_c ~ 92K) and $YBa_2Cu_4O_{10}$ (T_c ~ 80K). Band structure calculations have shown that the DOS for $YBa_2Cu_3O_7$ is larger than the DOS for $YBa_2Cu_4O_{10}$[5,6]. However, the ^{17}O shifts of the Thallium Cu-O planes did not alter with the increase of transition temperature. This suggests that either the relationship between the density of states and the transition temperature in not obvious or the hyperfine coupling constant is altered.

The most striking feature of the shift measurements for both materials is that the observed shift decreases noticeably with decreasing temperature in the normal state. This is not the case in simple metals where the Knight shift remains constant until T_c, after which it decreases as conduction electrons pair up and the susceptibility decreases[7-10]. In certain HiT_c superconductors this is not the case and a number of different nuclei, which are accessible by NMR, show some degree of temperature dependence in the normal state[10-34]. However, other HiT_c materials show no NMR shifts above T_c[32-48].

There have been a large number of NMR (and in the case of $^{63,65}Cu$ NQR) experiments performed on HiT_c materials. Superconductivity is somehow inextricably linked with the Cu-O planes and NMR experiments fall into one of two groups, $^{63,65}Cu$ and ^{17}O experiments which sample the susceptibility of the Cu-O planes directly (as well as other sites in the case of ^{17}O) and other nuclei

such as ^{89}Y and ^{205}Tl which sample the susceptibility of the Cu-O planes only indirectly via a transferred hyperfine interaction.

The Cu-O planes of the $La_{1.85}Sr_{0.15}CuO_4$ and $La_{1.85}Ca_{0.15}CuO_4$ have been studied by ^{17}O NMR[13,32], both show a temperature dependence of the shift in the normal state and for the $La_{1.85}Ca_{0.15}CuO_{4-\delta}$ material the shift has decreased to ~½ of its room temperature value by T_c. This temperature dependence is very similar to that observed for ^{89}Y, ^{63}Cu and ^{17}O NMR in oxygen deficient $Y_1Ba_2Cu_3O_{7-\delta}$ (with $\delta < 1$).

The most extensive NMR studies have been performed on $Y_1Ba_2Cu_3O_{7-\delta}$ using ^{17}O, ^{63}Cu and ^{89}Y. The variation of T_c as a function of oxygen concentration is explained by the corresponding hole doping[49]. The magnetic properties of the 60K (oxygen deficient) phase are very different from the 90K (fully oxygenated) phase. Temperature dependent NMR shifts for ^{17}O, ^{63}Cu and ^{89}Y in the normal state are observed for the 60K phase[15-25,33] but not for the 90K phase[32-43]. Using ^{63}Cu and ^{89}Y Knight shifts it was shown that this temperature dependence was associated with the spin susceptibility of the Cu-O planes[16,25]. Early experiments suggested different temperature dependencies for the ^{17}O and ^{63}Cu, further experiments[20] suggested that the ^{17}O and ^{63}Cu Knight shifts were proportional to each other (taking into account the orbital contribution to the shift). This work could be interpreted in two ways, either that, because of hybridization of the bonds between the copper and oxygen sites there was a common susceptibility in the planes, or that a one spin component model was appropriate where the Knight shifts were all proportional to a single static susceptibility χ_0, that described the whole system. Later it was shown that the ^{89}Y

spin component of the shift was also a measure of this static susceptibility giving further evidence for a one component model[50]. No conclusions could be drawn on which model was appropriate from studying fully oxygenated $Y_1Ba_2Cu_3O_7$, since no, or very little change in shifts are observed in the normal state.

As stated previously Trokiner et al[31] have performed variable temperature ^{17}O NMR experiments on the n=3 phase of the Bismuth material. The samples used contained a high proportion of the n=2 phase probably due to the high temperature used for the ^{17}O exchange, which was carried out at 800°C. Measurements were performed at 7.0T (40.4MHz) with a corresponding poorer resolution compared with the measurements reported here (8.45 T). The same site assignment conclusions are drawn and fairly similar temperature dependencies are measured. The spectrum they obtained at room temperature and the temperature dependence of the two distinct Cu-O planes are reproduced here as figures 6.1 and 6.2. The shift data for the outer Cu-O plane is essentially the same as that found in this work but there is a noticeable difference in the temperature dependence of the inner plane ^{17}O resonance. They liken the temperature dependence they observed for the inner plane to the behaviour of ^{17}O in oxygen deficient $Y_1Ba_2Cu_3O_{7-\delta}$ (with $\delta < 1$). However little or no account has been made for the fact that the resonances from the two sites overlap leading to considerable problems in determining the peak position for the inner plane.

There is only one other report of ^{17}O NMR studies on the temperature dependencies of the n=1 phase of $Bi_2Sr_2Ca_{n-1}Cu_nO_{4+2n}$[32] but there have been three for the n=2 phase[32,44,45]. Here there is no temperature dependence of the shift in the normal state although no mention is made of any changes in width.

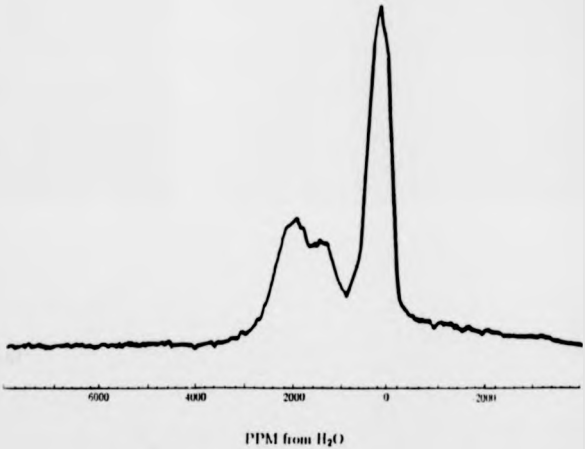

Figure 6.1. The ^{17}O NMR spectrum of the n=3 phase of $Bi_2Sr_2Ca_{n-1}Cu_nO_{4+2n}$ at room temperature measured by Trokiner etal (ref 25).

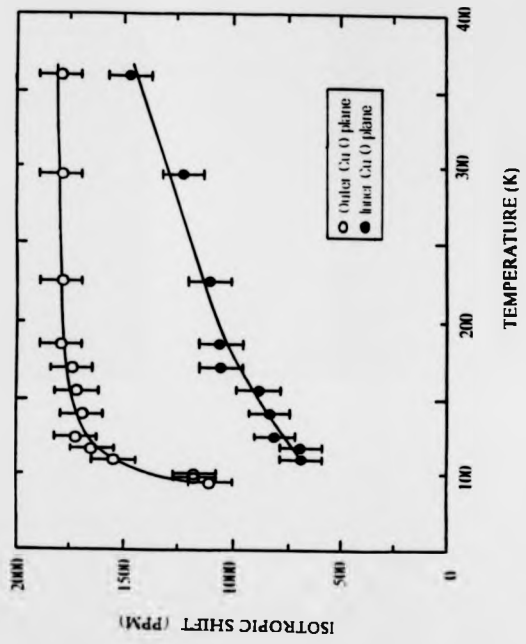

Figure 6.2 The temperature dependencies of the ^{17}O NMR peak positions associated with the two Cu-O planes of the n=3 phase of $Bi_2Sr_2Ca_{n-1}Cu_nO_{2n+4}$ measured by Trokiner etal (ref 25).

There are no reports of ^{17}O NMR in n=3 phase of $Tl_2Ba_2Ca_{n-1}Cu_nO_{4+2n}$ but two for the n=2 phase[32,48]. Only one of these[32] includes variable temperature measurements and the ^{17}O shift was found to be independent of temperature in the normal state.

^{205}Tl NMR has been performed on all phases of $Tl_2Ba_2Ca_{n-1}Cu_nO_{4+2n}$[45-48,51-53] and there is no temperature dependence of the shift in the normal state. Interestingly one piece of work noticed a defect line in an n=2 sample. This was attributed to thallium in the calcium plane next to the Cu-O plane[53]. This line followed the Curie-Weiss law reproducing the temperature dependence of the magnetic susceptibility.

There appears to be two different behaviours observed in the HiT_c materials, the NMR shift is either independent of temperature in the normal state (observed for the higher T_c HiT_c materials) or dependent as is the case for the two lower T_c materials (Lanthanum and oxygen deficient $Y_1Ba_2Cu_3O_{7-\delta}$).

A plausible explanation of these temperature dependant normal state shifts is the antiferromagnetic Fermi-liquid theory suggested by Millis,Monien and Pines[1,54,55]. Neutron scattering experiments[57-59] and Raman Spectroscopy studies[60,61] have established the existence of short range (over a few lattice spacings) antiferromagnetic spin correlations of the Cu spins in the normal state of the doped Lanthanum and oxygen deficient Yttrium superconductors. If these correlations increase with decreasing temperature then this corresponds to a decrease in the density of states as a pseudogap opens in the electronic spectrum. Since the Knight shift is proportional to the density of states, this decrease will be observed as a decrease in Knight shift. It seems strange that there is no

discontinuity at T_c for the Knight shifts but the superconductivity may in some way be intimately related to these spin correlations.

The spin component of the Knight shift is a measure of the static spin susceptibility (χ_0) which is the real part of the spin-spin correlation function $\chi(\underline{q},\omega)$ at $\underline{q}=0$ and $\omega=0$ (or ω is small, as is the case of NMR experiments). The MMP theory models the susceptibility when influenced by these antiferromagnetic correlations however, the theory is phenomenologically based on experimental results. A full description of the MMP model is given in references 1,54 and 55. Including the antiferromagnetic correlations the spin-spin correlation function is written as,

$$\chi(\underline{q},\omega) = \chi_F(\underline{q},\omega) + \chi_{AF}(\underline{q},\omega) \qquad (6.1)$$

Where χ_F and χ_{AF} describe the Fermi free electron and antiferromagnetic contributions respectively. The real part of χ_F at $\underline{q}=0$ and $\omega=0$ is denoted as χ_0. The MMP theory models the antiferromagnetic component χ_{AF} such that,

$$\chi_{AF}(\underline{q},\omega) = \frac{\chi_Q}{1+\xi^2(Q-q)^2 - i(\omega/\omega_{sf})} \qquad (6.2)$$

Where χ_Q is the static spin susceptibility at $q = Q = (\pi/a,\pi/a)$ which is the antiferromagnetic wave vector and is related to χ_0 by $\chi_Q = \chi_0(\xi/\xi_0)$ where ξ is the antiferromagnetic correlation length (which is temperature dependent) and $1/\xi_0$ is the wave vector at which the antiferromagnetic contribution starts to dominate the spin-spin correlation function. (Here it is assumed that the lattice spacing a and b are equal.) $\hbar\omega_{sf}$ is a characteristic energy describing the antiferromagnetic

spin dynamics. From this, the real part of the static spin susceptibility at χ_0 at $q=0$ and $\omega=0$ is given by,

$$\chi_0 = \chi_P(0,0)+\chi_{AF}(0,0)=\chi_0[1+\frac{1}{2\pi^2}[\frac{a}{\xi_0}]^2] \qquad (6.3)$$

For the n=1,2 and 3 phases of $Bi_2Sr_2Ca_{n-1}Cu_nO_{4+2n}$ antiferromagnetic fluctuations are observed for materials with sufficient doping if Sr, Ca or Bi are replaced by La, Y or Pb respectively[61]. It is not known whether the small amount of Pb in the material under investigation here is sufficient to produce AF fluctuations[61]. Comparison of ^{63}Cu and ^{205}Tl spin-lattice relaxation data suggest the existence of antiferromagnetic correlations in the n=2 and 3 phases of $Tl_2Ba_2Ca_{n-1}Cu_nO_{4+2n}$[62].

It seems likely that any antiferromagnetic correlations that exist in the n=1 and 2 phases of the Bismuth and Thallium materials must be weak since temperature dependent normal state shifts are not observed for the n=1 and 2 phases. Does this MMP model explain the ^{17}O Knight shift data observed for the $Bi_2Sr_2Ca_2Cu_3O_{10}$ and $Tl_2Ba_2Ca_2Cu_3O_{10}$ materials ?. The answer would appear to be no for three reasons. Firstly this model is a one component model with only one common static susceptibility that is seen by all nuclei. If this was the case then the two Cu-O plane resonances of the Bismuth sample would both show the same temperature dependence which they clearly do not. Secondly the ^{205}Tl resonance in the n=3 phase of the thallium material is independent of temperature in the normal state. Thirdly the shifts observed for both the Lanthanum superconductor and oxygen deficient Yttrium superconductor vary quite smoothly

whereas a more distinct drop is observed before the transition temperature for the $Bi_2Sr_2Ca_2Cu_3O_{10}$ and $Tl_2Ba_2Ca_2Cu_3O_{10}$ materials.

It is worth noting that although the ^{205}Tl resonance does not follow the ^{17}O it would be useful to know what happens at the copper sites. Experiments on $YBa_2Cu_3O_7$ and $La_{2-x}Sr_xCuO_4$ materials have shown that the suggestion that the holes preside mainly on the oxygen 2p orbitals is correct[16,36,63,64]. However it has been agreed[20,65] that hybridization strongly binds the O 2p holes to the nearest Cu^{2+} ion and makes no contribution to the spin susceptibility. The spin susceptibility at the oxygen site is therefore directly related to that of the copper site and should show the same dependence.

$^{63,65}Cu$ NMR and NQR also probes the susceptibility directly at the Cu-O plane site but because of its large quadrupole moment results in very broad lines. However some very useful work has been done using aligned powders and single crystals[18,23,25,41,66-69].

Using aligned platelets the Knight shift component of the ^{63}Cu NMR of $Bi_2Sr_2CaCu_2O_8$ has been seen to decrease by $-\frac{1}{2}$ of its room temperature value by T_c[69]. This is unlike the ^{17}O dependence (independent of temperature in normal state), however on annealing the sample only a slight deviation above T_c was observed for the ^{63}Cu resonance[69]. The anneal increases the carrier concentration (but interestingly decreases T_c). These effects are possibly explained by the formation of a spin gap unrelated to the superconductivity[69].

It is strange that the two distinct Cu-O planes of the Bismuth material show different temperature dependencies but the ones of Thallium do not. One difference of the two structures is that there is a lot more buckling of the Cu-O

planes in the Bismuth material whereas for the Thallium the copper and oxygens are sited on a geometric plane for each of the planes[70].

As yet there is no theory or model that would explain this strange temperature dependence. A simplistic explanation would suggest a mechanism where electrons are removed from contributing to the spin susceptibility (paired up?) whilst still in the normal state. This mechanism could be described as a 2-dimensional superconductivity in the Cu-O planes which is observed only in the highest T_c HiT_c materials and at a higher temperature than that for bulk superconductivity.

6.3 Spin-lattice relaxation.

It would appear from the results for the ^{17}O relaxation rates at the Cu-O planes in the normal state that the relaxation can be described by a single band of non-interacting electrons in the same way as elemental metals (i.e. Korringa like). There are two reasons for this, firstly the value obtained for $K_s^2T_1T$ is very close to the theoretical value in the normal state for all temperatures measured, and the corresponding orbital shift is a reasonable value (this will be discussed in the next section).

$K_s^2T_1T$ can show large deviations from its theoretical value due to electron-electron and antiferromagnetic interactions[1,54,55,71,72]. Since in the other HiT_c systems the Knight shift is not very temperature dependent it is hard to determine whether $K_s^2T_1T$ or K_sT_1T is constant with temperature. Even here the data both the n=3 phases of the Bismuth and Thallium superconductors give reasonable fits assuming either a $K_s^2T_1T$ or a K_sT_1T relationship, (apart from the value of the orbital contribution obtained if a K_sT_1T is assumed). Interestingly enough the ^{89}Y

and ^{17}O relaxation rate in oxygen deficient $YBa_2Cu_3O_{7-\delta}$ was thought to be Korringa like [16,21,73] before the MMP theory. Table 6.1 lists the shift and relaxation data for a number of different HiT_c systems. Generally the relaxation rates for the Cu-O plane oxygens is Korringa like for the highest T_c oxides but the copper relaxation rates may be influenced by electron-electron interactions[39].

^{205}Tl NMR shows no shift in the normal state. There are some reports of a slight decrease of position in superconducting state[48], but other reports mention no differences between the normal and superconducting states. It is thought that the shift is predominately due to the orbital contribution. Electron-electron or antiferromagnetic correlations have been suggested as reasons for the non-Korringa like behaviour of the ^{205}Tl relaxation[47]. However earlier investigations of ^{205}Tl in these systems suggested that the relaxation was Korringa like[51].

The value of the orbital contribution is important since it is one of the factors that controls whether a fit is reasonable or not. For instance the ^{17}O relaxation data from oxygen depleted $YBa_2Cu_3O_{7-\delta}$[20] is plotted in figure 6.3 assuming a $K_s^2T_1T$ fit and in figure 6.4 assuming a $K_s T_1 T$ fit. As can be seen both give reasonable fits but with peculiar orbital shifts of -270ppm and 420ppm respectively. Although both these values of K_{orb} seem rather strange, data for the relaxation rate of ^{89}Y in oxygen depleted $YBa_2Cu_3O_{7-\delta}$[16] can be plotted assuming a $K_s^2T_1T$ relationship with a K_{orb} value of 300ppm or assuming a $K_s T_1 T$ relationship a K_{orb} value of 200ppm, both of these values are reasonable.

As was shown in chapter 2, the spin-lattice relaxation rate is governed by how the sum over q space is performed (Equation 2.19). Antiferromagnetic correlations will control the form factors and how the summation is performed.

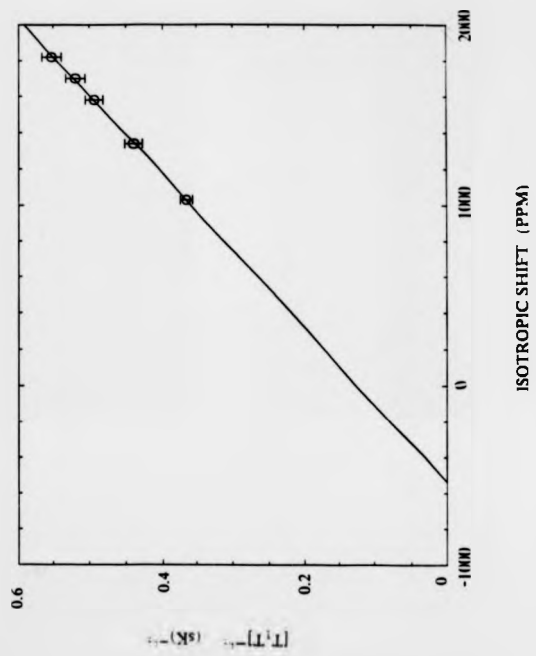

Figure 6.3. $[T_1T]^{-1/2}$ as a function of shift for the ^{17}O NMR data for $Y_1Ba_2Cu_3O_{7-\delta}$ ($\delta \sim 0.37$, 62K)[14].

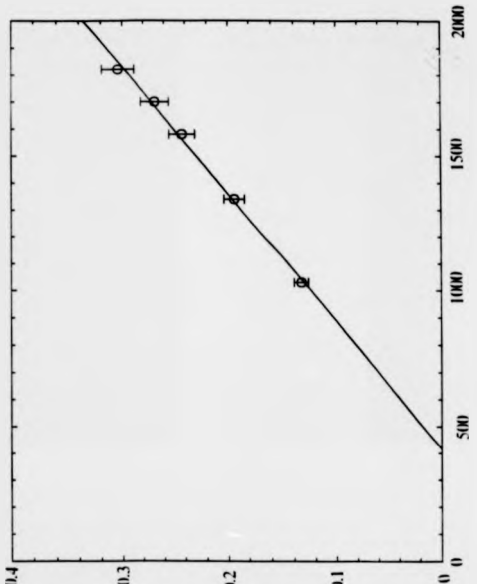

Figure 6.4. $[T_1T]^{-1}$ as a function of shift for the ^{17}O NMR data for $Y_1Ba_2Cu_3O_{7-\delta}$ ($\delta \sim 0.37$, 62K)[14].

Differences in the spin lattice relaxation rates in the $Y_1Ba_2Cu_3O_{7-\delta}$ and $La_{2-x}Sr_xCuO_4$ materials have been explained by the MMP theory[1,54,55]. It has been shown that for ^{63}Cu in oxygen deficient $Y_1Ba_2Cu_3O_{7-\delta}$ the relaxation rate is enhanced by these antiferromagnetic correlations[54] (whereas for the fully oxygenated $Y_1Ba_2Cu_3O_{7-\delta}$ the enhancement may be due to antiferromagnetic correlations or electron-electron interactions[18,39,74]).

Again the question arises, does the MMP theory explain the Korringa like behaviour of the two systems being studied here ?. The answer is possibly but not likely. The MMP model assumes a dynamical susceptibility in terms of the static susceptibility of the form,

$$\frac{\chi''(q,\omega_N)}{\omega_N} = \frac{\pi\chi(0)}{\Gamma} + \frac{\pi\chi(q)}{\Gamma_{AF,q}} \qquad (6.4)$$

Where $\Gamma_{AF,q}$ is the peak of the Lorenztian associated with the antiferromagnetic correlations and $\chi(q)$ has a peak at $q=Q_{AF}=(\pi/a,\pi/a)$.

It is possible that if the antiferromagnetic correlations are short range they will not be seen at the oxygen sites (as pointed out in Chapter 2). Therefore the oxygen relaxation is dominated by spin fluctuations near to $q=0$ and,

$$\frac{1}{T_1T} \propto \sum_{q=0} \frac{\chi''(q,\omega_N)}{\omega_N} = \frac{\pi\chi(0)}{\Gamma} \qquad (6.5)$$

Γ for a Fermi liquid is inversely proportional to the density of states (and therefore also $1/\chi(0)$) which leads to the Korringa relationship if there are no strong magnetic correlations. In $Y_1Ba_2Cu_3O_{7-\delta}$ the length scale of the antiferromagnetic

correlations increase with decreasing oxygen concentration. The above argument is used to explain the Korringa like behaviour of the fully oxygenated $Y_1Ba_2Cu_3O_{7-\delta}$[20,75] where any antiferromagnetic correlations should not influence the ^{17}O relaxation.

This argument is not convincing for the relaxation observed here. The antiferromagnetic correlations have to be strong enough to severely reduce the spin susceptibility in the normal state but weak enough not to interfere with the relaxation.

Despite this inconsistency with the lower T_c materials it is not inconsistent with the results for the relaxation rates of the Cu-O plane oxygens in the higher T_c materials (the n=2 phases of $Bi_2Sr_2Ca_{n-1}Cu_nO_{4+2n}$ and $Tl_2Ba_2Ca_{n-1}Cu_nO_{4+2n}$ and fully oxygenated $Y_1Ba_2Cu_3O_{7-\delta}$) which all give values of the Korringa constant $(K_s^2T_1T)$ close to the theoretical value expected if there is little electron-electron interaction at the oxygen sites[32,75]. This again supports the idea that electrons are somehow removed from contributing to the spin susceptibility as the temperature decreases but in the normal state, leaving those that remain to contribute to the relaxation. These remaining electrons behave in a similar manner to s-electrons in a simple metal and are Korringa like. If this is true it would appear that the change in shift observed above T_c is somehow related to the superconductivity.

Although the shift and relaxation data implies that the Korringa law is obeyed it does not rule out other behaviour, since the data cannot be uniquely fitted to just a Korringa like fit. Even in the MMP theory the energy Γ which is used to define the non-antiferromagnetic part of the spin dynamics is allowed to

be temperature dependent to completely fit the data for the oxygen deficient $Y_1Ba_2Cu_3O_{7-\delta}$[50] and so K_sT_1T is not completely independent of temperature.

For the Thallium sample no coherence peak was observed below T_c. This is in agreement with all other results of HiT$_c$ superconductors. A number of reasons have been proposed for this Hebel-Slichter enhancement not being seen. These include strong binding of the electron pairs, gap anisotropy or it is a consequence of the charge and spin separation[76-80].

6.4. The Orbital Contribution.

As stated before the orbital shift is independent of temperature but cannot be found directly by extrapolation to zero because of the induced supercurrents causing a shift observed NMR frequency (demagnetization). Estimates for K_{orb} of the ^{17}O resonances of the Cu-O planes vary and are sample dependent[41]. From measurements of the internal magnetic field in the $Y_1Ba_2Cu_3O_7$ using ^{89}Y NMR as a probe a value of 100 ± 100ppm was suggested[41], whereas estimates based on the shifts of the CuO_2 precursor materials are around -100ppm[32,81]. However a much higher value has been obtained for aligned $Y_1Ba_2Cu_3O_7$ where it is possible to determine the axial contribution to the shift which is independent of demagnetisation as the diamagnetic currents will cancel. By extrapolating to T=0K it is possible to estimate the isotropic value of K_{orb} as 240 ± 110ppm[20]. The values for K_{orb} obtained assuming a K_sT_1T fit are very much larger than this. In fact the observed shifts for the Cu-O planes in the Bismuth n=3 and Thallium n=3 phases drop to below the deduced values of K_{orb} from assuming a K_sT_1T relationship at ~90K for the Bismuth material and at ~110K for the Thallium material. These temperatures are higher than the temperatures at which the

insulating plane ^{17}O resonances (at $\sim$280ppm) of the two samples start to move (which is at $\sim$85K for Bismuth and $\sim$100K for Thallium). This implies that the decrease in shift occurs at a higher temperature than when demagnetization affects become important. The values of K_{orb} obtained assuming a Korringa relationship ($\sim$100ppm) are more reasonable, again suggesting that the system is Korringa like.

However, it would seem very strange indeed if these HiT_c materials behave in a similar manner to the free electron like metals. All other superconducting materials, such as the alloy materials (e.g. Nb_3Sn), the organic superconductors and $BaBiO_3$ cannot be described in the same manner as the simple metal superconductors.

Material (T_c)	Nuclei	Temp. dep or Indep. Normal Shift.	T_c seen by shift.	Relaxation Behaviour.
$La_{1.85}Ca_{0.15}CuO_{4-\delta}$	^{63}Cu	NA	NA	NA
(22K)	^{17}O	Dep.[26]	NO	NK_AF[26]
$La_{1.7}Sr_{0.3}CuO_{4-\delta}$	^{63}Cu	Dep.[56]	NO	NK(Q)_AF[56]
(38K)	^{17}O	Dep.[26]	NO	NK_AF[26]
$YBa_2Cu_3O_{7-\delta}$	^{89}Y	Indep.[27]	YES	K[27,29]
(90K)	^{17}O	Indep.[26,32]	YES	K[26,31,70]
	^{63}Cu	Indep.[34,35]	YES	NK(EE_AF)[12,61]
$YBa_2Cu_3O_{7-\delta}$	^{89}Y	Dep.[27]	NO	NK_AF[44]
(62K)	^{63}Cu	Dep.[33]	NO	NK_AF[33]
	^{17}O	Dep.[14,19]	NO	NK_AF[14,19]
$YBa_2Cu_4O_{10}$	^{89}Y	Dep.[20]	NO	NK_AF[20]
(100K)	^{63}Cu	Dep.[22]	NO	NK_(EE_AF)[22]
	^{17}O	NA	NA	NA
$Bi_2Sr_2CuO_6$	^{63}Cu	NA	NA	NA
(~6K)	^{17}O	Indep.[26]	YES	K[26]
$Bi_2Sr_2CaCu_2O_8$	^{63}Cu	Dep.[64]	NO	NK[64]
(85K)	^{17}O	Indep.[26,39]	YES	K[26]
$Bi_2Sr_2Ca_2Cu_3O_{10}$	^{63}Cu	NA	NA	NA
(110K)	^{17}O	Dep.[A]	NO	K[A]
$Tl_2Ba_2CuO_6$	^{205}Tl	Indep.[40,42]	YES	NK[40,42]
(80K)	^{63}Cu	NA	NA	NA
	^{17}O	NA	NA	NA
$Tl_2Ba_2CaCu_2O_8$	^{205}Tl	Indep.[41,42]	YES	NK[41,42]
(108K)	^{63}Cu	NA	NA	NK(Q)[42]
	^{17}O	Indep.[26]	YES	K[26]
$Tl_2Ba_2Ca_2Cu_3O_{10}$	^{205}Tl	Indep.[42,45]	YES	K[42,45]
(125K)	^{63}Cu	NA	NA	NK(Q)[42]
	^{17}O	Dep.[B]	NO	K[B]

Table 6.1 Summary of NMR shift and relaxation data for a number of HiT_c materials.

Notes for table 6.1.

K: Normal Korringa like relaxation.
NK: Not Korringa like relaxation.
EE: Relaxation enhanced by electron-electron interaction.
AF: Relaxation affected by antiferromagnetic correlations.
(Q): Zero field (Nuclear Quadrupole) data.
(A): See Chapter 4.
(B): See Chapter 5.

Chapter 6. References.

1. H. Monien, P. Monthoux and D. Pines: Phys. Rev. B 43 (1991) 275.
2. 'Solid State Physics', N. W. Ashcroft and N. D. Mermin (Saunders College 1987)
3. 'Superconductivity': ed. R. D. Parks, Vols 1 and 2 (Dekker 1969).
4. 'Introduction to superconductivity': A. C. Rose-Innes and E. H. Rhoderick' (2nd edition. Pergamon Press 1978).
5. J. Yu, K. T. Park and A. J. Freeman: Physica C 172 (1991) 467.
6. T. Oguchi, T. Sasaki and K. Terakura: Physica C 172 (1990) 277.
7. D. E. MacLaughin: Sol. State Phys. 31 (1976) 1.
8. F. Reif: Phys. Rev. 102 (1956) 1417.
9. W. D. Knight, G. M. Androes and R. H. Hammond, Phys. Rev. 104 (1956) 852.
10. 'Magnetic Resonance in Metals', J. Winter (OUP 1971).
11. Y. Kitaoka, S. Ohsugi, K. Ishida, K. Asayama: Physica C. 170 (1990) 189.
12. Y. Nakamura, K. Kumagai: Physica B. 165 (1990) 1303.
13. Y. Kitaoka, K. Ishida, F. Fijiwara, T. Kondo, K. Asayama, M. Horvatic, Y. Berthier, P. Butand, P. Sergransan, C. Berthier, H. Katayama-Yoshida, Y. Okabe and T. Takahashi in 'Strong Correlation and Superconductivity', (Springer 1989).
14. T. Imai, T. Shimizu, H. Yasuoka, Y. Ueda, K. Yoshimura and k. Kosuge: Physica C. 162 (1989) 169.
15. H. Lutgemeier and M. W. Pieper: Sol. State. Comm. 64 (1987) 267.
16. H. Alloul, T. Ohno, P. Mendels: Phys. Rev. Lett. 63 (1989) 1700.
17. G. J. Kramer, H. B. Brom, J. Van den Berg, P. H. Kes, D. J. W. Ijdo: Sol. State Comm 64 (1987) 705.
18. W. W. Warren, R. E. Walstedt, G. F. Brennert, G. P. Espinosa, J. P. Remeika: Phys. Rev. Lett. 59 (1987) 1860.
19. M. Mali, D. Brinkmann, I. Pauli, J. Roos, H. Zimmerman and J. Haliger: Phys. Lett A 124 (1987) 112.
20. M. Takigawa, A. P. Reyes, P. C. Hammel, J. D. Thompson, R. Heffner, Z. Fisk and K. C. Ott: Phys. Rev. B 43 (1991) 247.
21. E. Lippmaa, E. Joon, I. Heinmaa, A. Miller, V. Miidel, R. Stern and S, Vija: Physica C 162 (1989) 263.
22. P. Butaud, M. Horvatic, Y. Berthier, Segansan, Y. Kitaoka: Physica C 166 (1990) 301.
23. C. H. Pennington, D. J. Durand, D. B. Zax, C. P. Slichter, J. P. Rice and D. M. Ginsberg: Phys. Rev. B 37 (1988) 7944.
24. A. J. Vega, W. E. Gameth, E. M. McCarron and R. K. Bordia: Phys. Rev. B 39 (1989) 2322.
25. R. E. Walstedt, W. W. Warren, R. F. Bell, R. J. Cava, G. P. Schneemeyer, J. V. Waszczak: Phys. Rev.B. 41 (1990) 9574.
26. R. Dupree, Z. P. Han, D. McK. Paul, T. G. N. Babu and C. Greaves: Physica C 179 (1991) 311.
27. H. Zimmerman, M. Mali, D. Brinkman, J. Karpinski, E. Kaldis and S. Rusiecki: Physica C 159 (1989) 181.
28. H. Zimmerman, M. Mali, I. Mangelschots, J. Roos, L. Paul, D. Brinkman, J. Karpinski, S. Rusiecki and E. Kaldis: J. Less Comm. Metals 164-165 (1990)

138.
29. T. Machi, I. Tomeno, T. Miyatabe, N. KKoshizuka, S. Tanaka, T. Imai and H. Yasuoka: Physica C 173 (1990) 32.
30. R. E. Walstedt and R. F. Bell: Phys. Rev. B. 44 (1991) 7760.
31. A. Trokiner, R. Mellet, A-M. Pouguet, D. Movi, Y. M. Gao, J. Primot and J. Schneck: Phys. Rev. B. 41 (1990) 9570.
32. L. Reven, J. Shore, Y. Shengtian, T. Duncan, D. Schwartz, J. Chung and E. Oldfield: Phys. Rev. B. 43 (1991) 10466.
33. G. Balakrishan, R. Dupree, I. Farnan, D. McK. Paul and M. E. Smith: J. Phys. C 21 (1988) L847.
34. Y. Kitaoka, Y. Berthier, P. Butand, M. Horvatic, P. Segransan and C. Berthier: Physica C 162-164 (1989) 195.
35. J. T. Market, T. W. Noh, S. E. Russek, R. M. Cotts: Sol. State. Comm 63 (1987) 847.
36. M. Takigawa, P. C. Hammel, R. H. Heffner, Z. Fisk, K. C. Ott, J. D. Thompson: Phys. Rev. Lett. 63 (1989) 1865.
37. M. Horvatic, Y. Berthier, P. Butand, Y. Kitaoka, P. Segransan, H. Katayama-Yoshida, Y. Okabe, T. Takahahi: Physica C. 159 (1989) 689.
38. M. Takigawa, P. C. Hammel, R. H. Heffner, Z. Fisk, K. C. Ott and J. D. Thompson: Physica C. 162-164 (1989) 853.
39. R. E . Walstedt and W. W. Warren: Science 248 (1990) 1082.
40. C. H. Pennington, D. J. Durand, D. B. Zax, C. P. Slichter, J. P. Rice and D. M. Ginsberg: Phys. Rev. B 37 (1988) 7944.
41. C. H. Barrett, D. J. Durand, C. H. Pennington, C. P. Slichter, T. A. Freidman, J. P. Rice and D. M. Ginsberg: Phys. Rev. B. 41 (1990) 6283.
42. M. Takigawa, P. C. Hammel, R. Heffner, Z. Fisk: Phys. Rev. B 39 (1989) 7371.
43. P. Wzietek, D. Kongeter, P. Auban, D. Jerome, J. M. Bassat, J. P. Coutures, B. Dubois and P. Odier: Euro. Phys. Lett. 8 (1989) 363.
44. A. Trokiner, R. Mellet, A-M. Pougnet, D. Morin, Y. M. Gao, J. Primot and J. Schneck: Phys. Rev. B. 41 (1990) 9570.
45. Y. Kitaoka, Y. Bertier, P. Butaud, M. Horvatic, P. Segransan and C. Berthier: Physica C 162 (1989) 195.
46. D. M. Leeuw, W. A. Groen,J. C. Jol, H. B. Brom and H. W. Zandergen: Physica C 166 (1990) 349.
47. F. Hentsch, N. Winzek, M. Mehring, H. Mattausch and A. Simon: Physica C 158 (1989) 226.
48. S. V. Verkhovskii, Y. I. Zhdanov, K. N. Mikhalyov, B. A. Aleksashin, V. I. Ozhogin, A. Y. Yakubovskii and L. D. Shustov: Physica B 165 (1990) 1311.
49. R. J. Cava, B. Batlogg, K. M. Rabe, E. A. Rietman, P. Gallagher and L. W. Rupp: Physica C 156 (1988) 523.
50. T. Ohno, T. Kanashiro and K. Mizuno: J. Phys. Soc. Jpn 60 (1991) 2040.
51. A. K. Rajarajan, K. V. Gopalakrishnan, R. Vijayaraghavan and L. C. Gupta: Sol. State Comm. 69 (1989) 213.
52. F. Hentsch, N. Winzek, M. Mehring, H. Mattausch, A. Simon and R. Kremer: Physica C 165 (1990) 485.
53. M. Mehring, 467,in 'Earlier and Recent Aspects of Superconductivity' (Springer-Verlag 1989).

54. H. Monien, D. Pines and M. Takigawa: Phys. Rev. B 43 (1991) 258.
55. A. J. Millis, H. Monien and D. Pines: Phys. Rev. B 42 (1990) 167.
56. G. Shirane, Y. Endoh, R. J. Birgeneau, M. A. Kastner, Y. Hidaka, M. Oda, M. Susuki and T. Murakami: Phys. Rev. Lett. 59 (1987) 1613.
57. Y. Endoh, K. Yamada, R. J. Birgeneau, D. R. Gabbe, H. P. Jenssen, M. A. Kastner, C. J. Peters, P. J. Picone, T. R. Thurston, J. M. Tranquada, G. Shirane, Y. Hidaka, M. Oda, Y. Enomoto, M. Suzuki and T. Murakami: Phys. Rev. B 37 (1988) 7443.
58. J. M. Tranquada, D. E. Cox, W. Kunnmann, H. Moudden, G. Shirane, M. Suenaga, P. Zolliker, D. Vaknin, S. K. Shina, M. S. Alvarez, A. J. Jacobson and D. C. Johnston: Phys. Rev. Lett. 60 (1988) 156.
59. K. B. Lyons, P. A. Fleury, J. P. Remeika, A. S. Cooper and T. J. Negran: Phys. Rev B. 37 (1988) 2353.
60. K. B. Lyons, P. A. Fleury, L. F. Schneemeyer and J. V. Waszczak: Phys. Rev. Lett 60 (1988) 732.
61. A. Maeda, M. Hase, I. Tsukada, K. Noda, S. Takebayashi and K. Uchinokura: Phys. Rev. B 41 (1990) 6418.
62. I. I. Zhdanov, B. A. Aleksashin, K. N. Mikhalyov, V. V. Verkhovskii, A. Y. Yakubovskii, V. I. Ozhogin, L. D. Shustov and A. B. Maysoedov: Physica C 183 (1991) 247.
63. N. Nucker, J. Fink, J. C. Fuggle, P. J. Durham and W. M. Temmermann: Phys. Rev. B 37 (1988) 5158.
64. A. Bianconi, M. De Santis, A. Di Cicco, A. M. Flank, A. Fointaine, P. Lagarde, H. Katayama-Yosida, A. Kotani and A. Marcelli: Phys. Rev B 38 (1988) 7196.
65. F. C. Zhang and T. M. Rice: Phys. Rev. B 37 (1988) 3759.
66. R. E. Walstedt, W. W. Warren, R. F. Bell, G. F. Bennet, G. P. Espinoza, R. J. Cava, L. F. Schneemeyer and J. V. Waszczak: Phys. Rev. B 38 (1988) 9299.
67. C. H. Pennington, D. J. Durand, C. P. Slichter, J. P. Rice, E. D. Bukowski and D. M. Ginsberg: Phys. Rev. B 39 (1989) 2902.
68. R. E. Walstedt, W. W. Warren, R. F. Bell and G. P. Espinosa: Phys. Rev B 40 (1989) 2572.
69. R. E. Walstedt, R. F. Bell and D. B. Mitzi: Phys. Rev. B 44 (1991) 7760.
70. C. C. Torardi, M. A. Subramarian, J. C. Calabrese, J. Gopalakrihnan, K. J. Morriesey, T. R. Askew, R. B. Flippen, U. Chowdry and A. W. Sleight: Science 240 (1988) 631.
71. D. Pines in 'Solid State Physics', Vol.1 (Academic, New York 1955).
72. T. Moriya and K. Ueda: Solid State Comm. 15 (1974) 169.
73. H. Alloul, T. Ohno and P. Mendals: Physica C 162 (1989) 193.
74. T. Imai, T. Shimizu, T. Tsuda, H. Yasuoka, Y. Takabatake, Y. Nazazwa and M. Ishakawa: J. Phys. Soc. Jpn. 57 (1988) 1771.
75. P. C. Hammel, M. Takigawa, R. H. Heffner, Z. Fisk and K. C. Ott: Phys. Rev. Lett 63 (1989) 1992.
76. P. B. Allen and D. Rainer: Nature (1991) 396.
77. L. Coffey: Phys. Rev. Lett. 64 (1990) 1071.
78. H. Monien and D. Pines: Phys. Rev B 41 (1990) 6297.
79. D. van der Marel, M. Baurer, E. H. Habermeier, D. Heitmann, W. Kong and

A. Wittlin: Phys. Rev. B 43 (1991) 8606.
80. R. T. Collins, Z. Sclesinger, F. Holtzberg, C. Feild, U. Welp, G. W. Crabtree, J. Z. Liu and Y. Fang: Phys. Rev. B 43 (1991) 8701.
81. E. Oldfield, C. Coretsopoulos, S. Yang, L. Reven, H. C. Lee, J. Shore, O. H. Han and E. Ramli: Phys. Rev. B 40 (1989) 6832.

Chapter 7. Conclusions and Further Work.

7.1. Conclusions.

There appears to be no ambiguity in the site assignment for $Bi_2Sr_2CuO_6$, $Bi_2Sr_2Ca_2Cu_3O_{10}$ and $Tl_2Ba_2Ca_2Cu_3O_{10}$, with the resonances associated with the Cu-O planes of the materials all being found in the 1000-2000ppm region common to all the copper oxide superconductors.

The position of the ^{17}O NMR resonance associated with the Cu-O planes of $Bi_2Sr_2CuO_6$ (at -1300ppm) show no temperature dependence between 300K and 5K but the resonance does broaden with decreasing temperature. The mechanism for this is unknown.

For $Bi_2Sr_2Ca_2Cu_3O_{10}$ the resonances associated with the two distinct Cu-O planes of the unit cell are easily resolved from each other and have isotropic shifts of -1590ppm and -1285ppm for the outer and inner Cu-O planes at room temperature. Because of the axial shift the peak position of the outer Cu-O plane is at -1950ppm at room temperature. For both $Bi_2Sr_2CuO_6$ and $Bi_2Sr_2Ca_2Cu_3O_{10}$ the line at -275ppm is associated with the Sr-O plane. The ^{17}O resonance of the Bi-O plane is not observed due to incommensurate modulation of the Bi-O distance.

For $Tl_2Ba_2Ca_2Cu_3O_{10}$, which is structurally similar to $Bi_2Sr_2Ca_2Cu_3O_{10}$ the resonances associated with the two Cu-O planes are not easily resolved and both have shifts of -1400ppm. This difference between the two materials is probably due to the Cu-O planes of the Thallium material being a considerably less buckled than for the Bismuth material. This also explains the smaller axial

contribution to the shift and the smaller electric field gradient for the outer Cu-O plane of the Thallium sample compared with that for the Bismuth sample. Both the resonances associated with Tl-O and Ba-O planes are seen in the region expected (~ 280ppm).

The resonances for the Cu-O planes of both $Bi_2Sr_2Ca_2Cu_3O_{10}$ and $Tl_2Ba_2Ca_2Cu_3O_{10}$ show large temperature dependencies in the normal state, this is unlike conventional superconductors or the other higher T_c HiT_c materials. This temperature dependence could possibly be explained by antiferromagnetic correlations in a similar manner to that used to explain the temperature dependent normal state behaviour of the lower T_c HiT_c materials. However, this temperature dependence could also be explained by a 2-dimensional superconductivity in the Cu-O planes. In this mechanism pairing occurs in the Cu-O planes at a higher temperature than that of bulk superconductivity which is seen as a decrease in the spin-component of the Knight shift.

The resonances of the two planes of $Bi_2Sr_2Ca_2Cu_3O_{10}$ show different normal state temperature dependencies and cannot be described by a one component spin susceptibility model. However, the resonances of the two Cu-O planes of $Tl_2Ba_2Ca_2Cu_3O_{10}$ show the same temperature dependence as if they are coupled in some way and could therefore be described by a one component spin-susceptibility model.

The ^{17}O spin-lattice relaxation of the Cu-O planes of $Bi_2Sr_2Ca_2Cu_3O_{10}$ and $Tl_2Ba_2Ca_2Cu_3O_{10}$ appear to be Korringa like in the normal state despite the temperature dependent normal state shifts. The value of $K_s^2T_1T$ is very close to the theoretical value for s-type metals with no electron-electron or

antiferromagnetic interaction. The values obtained for the temperature independent orbital shift are -100ppm assuming a Korringa like relaxation. This value appears to be reasonable when compared to the value obtained for other systems.

If weak antiferromagnetic correlations are the cause of the normal state temperature dependence of the shift, they will not influence the ^{17}O relaxation because of the position of the oxygen sites in the unit cell. However, it seems very unlikely that the antiferromagnetic correlations are large enough to severely reduce the spin-component of the Knight shift but not affect the relaxation whilst in the normal state. This Korringa like behaviour is in agreement with the ^{17}O spin-lattice relaxation of the other higher T_c HiT_c materials which do not show temperature dependent shifts in the normal state. The relaxation for $Bi_2Sr_2Ca_2Cu_3O_{10}$ and $Tl_2Ba_2Ca_2Cu_3O_{10}$ is also suggestive of the pairing of electrons above T_c in the Cu-O planes which then make no contribution to the spin-susceptibility or the relaxation leaving the unpaired electrons unaffected.

7.2. Further Work.

Despite the large number of NMR groups working on HiT_c materials there are still a number of materials that have not been investigated by ^{17}O NMR or the investigation is incomplete. It would certainly be interesting to study the $n=4$ phase of $Tl_2Ba_2Ca_{n-1}Cu_nO_{4+2n}$ or all five phases of $TlBa_2Ca_{n-1}Cu_nO_{4+2n}$ ($n=1$ to 5) if they really are single phase.

The problem of broad lines associated with ^{63}Cu NMR for randomly orientated powdered samples would be removed if the materials could be aligned

or single crystals of sufficient size grown. It would certainly then be worth performing ^{63}Cu variable temperature shift and spin-lattice relaxation measurements on $Bi_2Sr_2Ca_2Cu_3O_{10}$ and $Tl_2Ba_2Ca_2Cu_3O_{10}$ and comparing this to the ^{17}O data.